Aus der Kinderchirurgischen Klinik und Poliklinik
im Dr. von Haunerschen Kinderspital
der Ludwig-Maximilians-Universität München
Direktor: Professor Dr. med. Dietrich von Schweinitz

Kinderchirurgische Forschung
Leiter: Prof. Dr. rer. nat. Roland Kappler

---

# "The role of NFE2L2 mutations and the epigenetic regulator UHRF1 in hepatoblastoma"

---

Dissertation
zum Erwerb des Doktorgrades der Naturwissenschaften
an der Medizinischen Fakultät der
Ludwig-Maximilians-Universität zu München
vorgelegt von

**Franziska Katharina Trippel**

aus

**Frankfurt am Main**

**2015**

**Mit Genehmigung der Medizinischen Fakultät**

**der Universität München**

| | |
|---|---|
| Betreuer: | Prof. Dr. Roland Kappler |
| Zweitgutachter: | Prof. Dr. Heiko Hermeking |
| Dekan: | Prof. Dr. med. dent. Reinhard Hickel |
| Tag der mündlichen Prüfung: | 13.01.2016 |

**Eidesstattliche Versicherung**

Trippel, Franziska Katharina

Ich erkläre hiermit an Eides statt,

dass ich die vorliegende Dissertation mit dem Thema,

# „The role of NFE2L2 mutations and the epigenetic regulator UHRF1 in hepatoblastoma“

Selbstständig verfasst, mich außer der angegebenen keiner weiteren Hilfsmittel bedient und alle Erkenntnisse, die aus dem Schrifttum ganz oder annähernd übernommen sind, als solche kenntlich gemacht und nach ihrer Herkunft unter Beziehung der Fundstelle einzeln nachgewiesen habe.

Ich erkläre des Weiteren, dass die hier vorliegende Dissertation nicht in gleicher oder in ähnlicher Form bei einer anderen Stelle zur Erlangung eines akademischen Grades eingereicht wurde.

München, 13.01.2016 Franziska Trippel

# Table of Content

# List of abbreviations

| | |
|---|---|
| ACTB | Beta-actin |
| AFP | Alpha-fetoprotein |
| AL | Amplicon length |
| ALAS1 | Delta-aminolevulinate synthase 1 |
| ALDH2 | Aldehyde dehydrogenase 2 |
| APC | Amyloid P component serum |
| APOC4 | Apolipoprotein C-IV |
| APC | Adenomatous polyposis coli |
| AQP9 | Aquaporin 9 |
| ARE | Antioxidant response element |
| AT | Annealing temperature |
| ATCC | American Type culture collection |
| β | Beta |
| bp | Base pair |
| BSA | Bovine Serum Albumin |
| BUB1 | Budding uninhibited by benzimidazoles 1 |
| BWS | Beckwith-Wiedemann syndrome |
| °C | Celsius degree |
| C1 | Cluster 1 |
| C2 | Cluster2 |
| ChIP | Chromatin Immunoprecipitation |
| CK1 | Casein kinase 1 |
| CNV | Copy number variations |
| CpG | cytosine-phospho-guanosine |
| $CO_2$ | Carbon dioxide |
| COG | Children´s Oncology Group |
| C1S | Complement component 1 |
| ct | Cycle of threshold |
| CT | Computed tomography |
| CTNNB1 | beta-catenin |
| CUL3 | Cullin 3 |
| CYP2E1 | Cytochrome p450 2E1 |
| d | Day |
| DAPI | 4',6-diamidino-2-phenylindole |
| DAVID | Database for Annotation, Visualization and Integrated Discovery |
| DHH | Desert hedgehog |
| DKK | Dickkopf |
| DLG7 | Discs large homolog 7 |
| DMSO | Dimethyl sulfoxide |
| DNMT | DNA methyltransferase |
| dNTPs | desoxynucleoside triphosphate |
| DTT | Dithiothreitol |
| DUSP9 | Dual specificity phosphatase 9 |
| DVL | Disheveled |
| E2F5 | E2F5 transcription factor ( |
| E.coli | lat: *Escherichia coli* |
| ECL | Electrochemiluminescence |
| EDTA | Ethylendiaminetetraacetic acid |
| EpCAM | Epithelial cell adhesion molecule |
| EtOH | Ethanol |

| | |
|---|---|
| Ex | Exon |
| FAP | Familial adenomatous polyposis |
| FCS | Fetal Calf Serum |
| fw | forward |
| FZD | Frizzled |
| GADPH | Glyceraldehyde-3-phosphate dehydrogenase |
| GCL | Glutamate-cysteine ligase |
| GPC3 | Glypican 3 gene |
| GHR | Growth hormone receptor |
| GSK3β | Glycogen synthase kinase 3 beta |
| GST | Glutathione S transferase |
| HP1 | Heterochromatin protein 1 |
| HPD | 4-hydroxyphenylpyruvase dioxygenase |
| H2AK5 | Lysine 5 of histone H2A |
| H3K9ac | Histone 3 lysine 9 acetylation |
| H3K4me2 | Histone 3 lysine 4 di-methylation |
| H3K4me3 | Histone 3 lysine 4 tri-methylation |
| H3K9me2 | Histone 3 lysine 9 di-methylation |
| H3K9me3 | Histone 3 lysine 9 tri-methylation |
| H3K27me2 | Histone 3 lysine 27 di-methylation |
| H3K27me3 | Histone 3 lysine 27 tri-methylation |
| h | Hour |
| HAT | Histone acetyltransferase |
| HCC | Hepatocellular carcinoma |
| HDAC | Histone deacetylase |
| HMOX1 | Heme oxygenase 1 |
| HHIP | Hedgehog-interacting protein |
| HMT | Histone methyltransferase |
| HP1 | Heterochromatin protein I |
| HR | High-risk |
| IGF | Insulin-like growth factor |
| IGFBP3 | Insulin-like growth factor binding protein 3 |
| IGFR | Insulin-like growth factor receptor |
| IgG | Immunoglobulin G |
| IHH | Indian hedgehog |
| IGSF1 | Immunoglobulin superfamily member 1 |
| indel | Insertion and deletion |
| IRS | Insulin receptor substrate |
| kDa | Kilo Dalton |
| KEAP1 | Kelch-like ECH-associated protein 1 |
| K19 | Keratin 19 |
| L | Liter |
| LB | Lysogeny Broth |
| Loc | Localization |
| LOH | Loss of heterozygosity |
| LOI | Loss of imprinting |
| LRP | Low density lipoprotein receptor-related protein |
| M | Mol |
| MeOH | Methanol |
| $MgCl_2$ | Magnesium chloride |
| min | Minute |
| mL | Milliliter |
| mM | Millimolar |

| | |
|---|---|
| MRI | Magnetic resonance imaging |
| MSP | Methylation-specific polymerase chain reaction |
| µg | Microgram |
| µL | Microliter |
| µM | Micromolar |
| n | Nano |
| NaCl | Sodium chloride |
| ng | Nanogram |
| NFE2L2 | Nuclear factor (erythroid-derived 2)-like 2 |
| NLE1 | Notchless homolog 1 |
| nm | Nanometer |
| N-myc | MYCN |
| NQO1 | NAD(P)H:quinone oxidoreductase 1 |
| $O_2$ | Oxygen |
| P | Pico |
| PBS | Phosphate buffered saline |
| PCR | Polymerase chain reaction |
| PHD | Plant Homeo domain |
| PRETEXT | Pre-treatment extend of disease |
| PTCH1 | Patched1 |
| PTEN | Phosphatase and tensin homolog |
| qRT-PCR | Quantitative real time polymerase chain reaction |
| rev | reverse |
| RING | Really Interesting New Gene |
| RNA | Ribonucleic acid |
| rpm | Rounds per minute |
| RPL10A | Ribosomal protein L10a |
| RPMI | Roswell Park Memorial Institute Medium |
| RT | Room temperature |
| SAM | S-adenosyl methionine |
| SD | Standard deviation |
| SDS | Sodium dodecyl sulfate |
| sec | Second |
| SEM | Standard error of the mean |
| SFRP1 | Secreted frizzled-related protein 1 |
| SHH | Sonic hedgehog |
| SIOPEL | International Childhood Liver Tumor Strategy Group |
| SMO | Smoothened |
| SR | Standard-risk |
| SRA | Set and Ring associated |
| STE | Sodium Chloride-Tris-EDTA |
| SUFU | Suppressor of Fused |
| TBE | Tris/Borate/EDTA |
| TBP | TATA-Box-binding-Protein |
| TE | Tris-EDTA Buffer |
| TFIID | Transcription factor II D |
| TIP60 | Tat-Interactive protein |
| TLCT | Transitional liver cell tumor |
| TSG | Tumor suppressor gene |
| TRIS | Tris (hydroxymethyl) amino methane |
| TTD | Tandem Tudor domain |
| U | Unit |
| UBL | Ubiquitin like |

| | |
|---|---|
| UDP | Uniparental isodisomy |
| UGT2B4 | UDP glucuronosyl- transferase 2 family, polypeptide B4 |
| UHRF1 | E3 Ubiquitin-like, containing PHD and RING finger domain 1 |
| USP7 | Ubiquitin-specific-processing protease 7 |
| UV | Ultraviolet |
| V | Volt |
| Vol | Volume |
| v/v | volume per volume |
| w/v | weight per volume |
| WIF | WNT inhibitory factor |

# 1 Introduction

Cancer in children and adolescents is an ever-present disease, and compared to adult cancer, a rare disease. In these days about one in every 600 children develop cancer before the age of 15, but still relatively little is known about disease causes [2]. Although improvement of treatment options and regimes have increased the overall 5-year survival rate up to approximately 80 % [3], cancer is still the leading cause of death by disease in children between 5 and 14 years [4].

Childhood cancer cannot be seen as a single disease – it has numerous subtypes and occurs at different sites of the body [5]. The types of cancer that preferably develop in children are different from those in adults. Whereas cancer types with high incidence in adult, such as lung, breast and colon cancer, are extremely rare among children, other cancer types like lymphoma, neuroblastoma and retinoblastoma are almost exclusively found in children [6]. Pediatric cancers are suggested to develop due to misregulation of differentiation during embryogenesis, while adult cancers are usually associated with mutations acquired over life. In addition, etiologic differences and genomic variations within even the same cancer type suggest that childhood and adult cancers may be discrete diseases. These observations elucidate the specific interest and focus on pediatric cancers, in this study hepatoblastoma.

## 1.1 Hepatoblastoma

Hepatoblastoma is a malignant disease of the liver. It accounts for about 1 % of all childhood cancers and is the most common malignant liver tumor in infancy with increasing incidence [7, 8]. Hepatoblastoma is assumed to arise from immature liver progenitor cells by aberrant activation of genes important in embryonic development. The annual incidence is 1.5 per million in children younger than 15 years. The median age of manifestation is 6 to 36 months, with 80 % of all cases diagnosed before three years of age [9]. The incidence of hepatoblastoma is higher in boys [10-12] and is increased in children with low-birth weight and prematurity [13, 14].

### 1.1.1 Histology

Hepatoblastoma exhibits heterogeneity and is characterized by a broad spectrum of disease characteristics, comprising the epithelial phenotype (56 %) as well as the mixed epithelial/ mesenchymal subtype (44 %) [15]. The epithelial hepatoblastoma type can further be divided into pure fetal (31 %), embryonal (19 %), macrotrabecular (3 %) and small-cell undifferentiated (3 %). The

most common mesenchymal tissue elements are immature fibrous tissue, spindle cells and osteoid. The presence of mesenchymal elements has been associated with improved prognosis in patients with advanced disease [16], whereas the pure fetal histology confers a better prognosis in completely resected tumors. Furthermore, it has been shown that the more primitive and undifferentiated the cells are, the more aggressive the tumors behave. Thus, tumors with a high amount of undifferentiated cells are associated with poor prognosis [16].

### 1.1.2 Symptoms and Diagnosis

Most children appear with a suspected abdominal mass or swollen abdomen, accompanied with abdominal pain, fever, nausea and weight loss. However, symptoms vary depending on the size of the tumor and the presence and location of metastasis.

For diagnosis, blood tests, including a complete blood count and liver- and kidney function tests are performed. Furthermore, alpha-fetoprotein (AFP) is routinely measured. At birth, infants still have relatively high levels of AFP, which decrease to normal adult levels within the first year of life. The normal level for AFP in children has been reported to be lower than 10 ng/mL [17, 18]. An AFP level higher than 500 ng/mL is a significant indicator of hepatoblastoma and hepatocellular carcinoma. However, liver tumor patients with low serum AFP (< 100 ng/mL) at diagnosis are classified as a high-risk subgroup with advanced state of disease at diagnosis, poor response to chemotherapy and a poor outcome [19]. Moreover, AFP can also be used as an indicator for treatment response and success. If treatment succeeds AFP levels will decrease to normal [20].

In addition to the physical examination and validation of laboratory parameters, imaging by ultrasound, computed tomography (CT) and by magnetic resonance imaging (MRI) is also an important diagnostic and prognostic tool and plays a central role in the staging of the tumor.

### 1.1.3 Staging

Staging of hepatoblastoma incorporates extend of liver involvement as well as tumor localization and the formation of metastasis. Currently, two main staging systems are used for hepatoblastoma. Firstly, the pre-treatment extend of disease (PRETEXT) staging system, which is based on imaging of the liver before surgery. Secondly, the “Children’s Oncology Group” (COG) staging, a system based on liver imaging and additional imaging of other parts of the body. The COG also integrates the results of surgery, if surgery was performed at diagnosis.

The PRETEXT staging was designed by the International Childhood Liver Tumor Strategy Group (SIOPEL). It rates disease progression according to the number of hepatic segments involved by imaging. The liver is divided into four segments, the right anterior and posterior segment, left medial and lateral segment. If one segment is involved, the hepatoblastoma is considered stage I. If all four lobes are involved, the disease is considered stage IV. In addition, PRETEXT includes the evaluation of cancer invasion of the portal (P) and hepatic veins (V) as well as the retro hepatic vena cava and hila nodal extension (E). It includes the presence of distant metastasis (M) and classifies its patients into high-risk (HR) or standard-risk (SR) patients. HR-patients show the presence of hepatoblastoma in all four sections and/or distant metastasis, venous involvement or other extra hepatic disease (30 % long-term survival), whereas SR-patients have a completely defined hepatoblastoma, involving at the most three sections (70 % - 100 % long term survival) [21-23].

In contrast to the PRETEXT, the COG staging reflects the degree of tumor removal and tumor expansion. The COG categorizes hepatoblastoma into four stages. Stage 1 is characterized by a localized tumor confined to the area of origin, which can be completely removed by surgery. After surgery no cancer cells remain on the edges or margins of the removed tissue and thus stage 1 has a very good prognosis with about 90 - 100 % long term survival. Hepatoblastoma of stage 2 is still localized, but microscopic residues of cancer cells can be observed after surgery. However, the prognosis of long-term survival in stage 2 is about 90 %. Stage 3, with a prognosis of 50 - 75 % long-term survival, is defined by a big tumor which has grown into or presses on vital tissues in the liver. Additionally, some, but not all lymph nodes connected to the tumor show signs of cancer infiltration. After surgery residuals of tumor cells remain present. Stage 4 describes dissemination of the tumor to abdominal lymph nodes, to the lung, or other organs and is associated with poor prognosis of about 30 % long-term survival [24, 25].

### 1.1.4 16-Gen signature

In 2008 colleagues of mine discovered a supportive classification system of hepatoblastoma based on two subgroups, named Cluster 1 (C1) and Cluster 2 (C2) [26]. The subclasses resemble distinct phases of liver development and are specified through a discriminating 16-gene signature which allows or at least contributes to differentiating liver tumors having a good prognosis from tumors with a bad prognosis. The 16-gene signature was identified by microarray analysis and consists of eight genes for each subgroup, by which it is possible to assign tumors to their corresponding subgroup, either C1 or C2 based on their gene expression [26].

The C1 set comprises aldehyde dehydrogenase 2 (ALDH2), amyloid P component serum (APCS), apolipoprotein C-IV (APOC4), aquaporin 9 (AQP9), complement component 1 (C1S), cytochrome p450 2E1 (CYP2E1), growth hormone receptor (GHR) and 4-hydroxyphenylpyruvase dioxygenase (HPD). However, the C2-group consists of alpha-fetoprotein (AFP), budding uninhibited by benzimidazoles 1 (BUB1), discs large homolog 7 (DLG7), dual specificity phosphatase 9 (DUSP9), E2F5 transcription factor (E2F5), immunoglobulin superfamily member 1 (IGSF1), Notchless homolog 1 (NLE1) and the ribosomal protein L10a (RPL10A) gene.

C1 tumors reflect the fetal phenotype of hepatoblastoma, while C2 tumors corresponded to the immature, embryonic type, which is highly associated with an advanced tumor stage, vascular invasion, extra hepatic metastasis and poor prognosis. This highly proliferating subgroup C2 is also typified by gains of chromosomes 8q and 2p [26]. In addition, increased expression levels of the Nmyc (MYCN) oncogene, intense nuclear accumulation and decreased membranous localization of beta-catenin (CTNNB1) have been observed to be frequent in C2 tumors [26]. Contrarily, C1 tumors show enhanced membranous staining and cytoplasmic accumulation of CTNNB1 with occasional nuclear localization. Markers for hepatic progenitor cells like AFP, epithelial cell adhesion molecule (EpCAM) and keratin 19 (K19), and the proliferation marker Ki67, MYCN and survivin were also significantly stronger expressed in the tumors of the C2-group than in the C1 tumors, which strongly contributes to the phenotype of poorly differentiated hepatoblastoma [27]. In contrast, markers of mature hepatocytes such as ALDH2, delta-aminolevulinate synthase 1 (ALAS1) and UDP glucuronosyl-transferase 2 family, polypeptide B4 (UGT2B4) are significantly less expressed in C2 tumors than C1 tumors. Hence, the expression signature using the 16-genes supports staging by recognizing the developmental stage of the liver, in predicting disease outcome and for conducting therapeutic regimes.

### 1.1.5 Treatment

A complete surgical removal of the tumor is the most important component of successful treatment for hepatoblastoma. However, about half of the patients with hepatoblastoma have an unresectable tumor at diagnosis. Therefore, chemotherapy is needed to shrink the tumor before surgery, to destroy remaining cancer cells after surgery and to exert an antitumor effect on overt or cryptic metastasis. The use of neoadjuvant and adjuvant chemotherapy has improved the survival chance, by leading to better resectability of hepatoblastoma and decreasing morbidity of surgery. Thus, chemotherapy is an essential part of treatment. Currently, SR-patients in countries using the SIOPEL protocol receive three courses of preoperative chemotherapy consisting of cisplatin and doxorubicin

(PLADO) and at least one additional course of PLADO postoperatively [28]. However, HR-patients do not respond to the PLADO treatment satisfactorily. Therefore, intensified chemotherapy is used. Cisplatin is given in combination with carboplatin or doxorubicin in a two week interval. Seven blocks of treatment are given neoadjuvant and three additional units postoperatively [29].

If classic chemotherapy is ineffective for patients, chemoembolization is performed. The chemotherapeutic agents are directly administered into the artery supplying the tumor, offering the advantage of higher local concentrations with lower systemic exposure. Chemoembolization has been explored in several small studies which show good results for hepatoblastoma patients [30-32]. Lastly, liver transplantation is a treatment option for patients with large solitary or multifocal PRETEXT4 tumors, or even metastatic disease, if the tumors could be cleared with chemotherapy [33].

### 1.1.6 Side effects and late effects of treatment

Chemotherapy, for both SR- and HR-hepatoblastoma patient groups, often causes immediate side effects such as nausea, hair loss, bruising and bleeding, tiredness, diarrhoea and an increased risk of infection. In addition, doxorubicin and cisplatin can also cause severe late side effects which affect patients for life. Doxorubicin is associated with cardiac toxicity, whereas cisplatin and carboplatin are associated with nephro- and ototoxicity [34]. Furthermore, children treated against childhood cancer display an increased risk for secondary cancers, lung damage, infertility, cognitive impairment and growth deficits [4], as the treatment may interfere with development. Several studies notice that childhood cancer survivors are more likely to have symptoms of depression, learning difficulties and problems with social interaction compared to children of the same age [35, 36].

Accordingly, an improvement in treatment, more effective diagnostic tools as well as therapies are required to reduce toxicity, long-term side effects and to increase cure rates.

## 1.2 Hepatocellular carcinoma

Hepatocellular carcinoma (HCC) is the second most common malignancy of the liver in children and is markedly distinct from hepatoblastoma. It mainly occurs in children older than six years of age and is predominantly found in male patients. Children with chronic hepatitis B virus (HBV) infection, cirrhosis and/or underlying metabolic diseases are the main high-risk groups for the development of HCC in childhood [37, 38]. However, the majority of HCC cases arise de novo without an antecedent history of liver disease [39]. Most current available treatment options for HCC are largely inefficient

due to extreme chemoresistance and advanced disease at time of diagnosis. Morbidity and mortality directly correlate with surgical resectability of the primary tumor. Therefore, the total resection of the tumor is, like in hepatoblastoma, the only chance for complete cure. Overall survival after three years remains below 25 %, comparable to stage IV hepatoblastoma [39].

## 1.3 Transitional liver cell tumors

There is a distinct group of malignant hepatocellular tumor that differs from both hepatoblastoma and HCC with respect to clinical presentation, morphology, immunophenotype and treatment response. These tumors are termed as transitional liver cell tumors (TLCT) and arise in an age group beyond the hepatoblastoma manifestation period. Thus, they occur in older children and adolescents. TLCTs emerge as large tumors with high AFP levels and high CTNNB1 expression. They represent an aggressive type of hepatic tumor and are considered a potential progeny of hepatoblastoma [40]. TLCT have been suggested to derive from neoplastic continuation along an ontogenetic differentiation pathway from hepatoblastoma to HCC. Hence, TLCTs exhibit clinical and histopathological features that are reminiscent of both hepatoblastoma and HCC [40].

## 1.4 Genetics and cytogenetics of hepatoblastoma

It is assumed that hepatoblastoma displays a relatively normal genomic background, based on its early manifestation and the low occurrence of obvious cytogenetic and genetic alterations [41]. Although most cases are sporadic, a highly elevated incidence of hepatoblastoma has been described in patients with genetic syndromes [41]. Familial adenomatous polyposis (FAP), an autosomal dominant disease, characterized by massive infestation of the colon with polyps [42] and the Beckwith-Wiedemann syndrome (BWS) [43], a genetic overgrowth syndrome are the two most common syndromes associated with hepatoblastoma. FAP patients carry germline mutations of the adenomatous polyposis coli (APC) tumor suppressor gene, leading to multiple colon polyps with universal progression to colon cancer. The risk of hepatoblastoma development in children in FAP kindreds is about 0.42 % [44]. BWS patients show at least two of five common features associated with abnormal growth including macroglossia, macrosomia, midline abdominal wall defects, ear creases/ear pits or neonatal hypoglycemia. All of these features are highly associated with variation within a defined region on the short arm of chromosome 11. Patients with chromosome 11p15.5 uniparental isodisomy (UPD) have an increased risk for developing embryonal tumors, including hepatoblastoma. UPD in these patients involves maternal loss of heterozygosity (LOH) and paternal

duplication [45]. The relative risk for hepatoblastoma in BWS patients is 2280-fold increased when compared to healthy children [46]. Other overgrowth syndromes described in association with the development of hepatoblastoma, even to a lesser extent, are the Simpson-Golabi-Behmel syndrome [47] and the Sotos syndrome [48, 49]. In Simpson-Golabi-Behmel patients alterations of the glypican 3 gene (GPC3) on chromosome Xq26 are observed, while in Sotos syndrome patients, deletions or mutations of the NDS1 gene could be detected.

The most common cytogenetic abnormality is trisomy, which can either occur alone or in conjunction with other structural changes in the genetic material. Common trisomies affect chromosomes 2, 8 or 20 [49-51]. Chromosome losses occur much less than chromosome gains. However, the most common chromosome loss is chromosome 18. In addition, unbalanced translocations involving a breakpoint on the proximal short arm of chromosome 1 are observed, which result in a duplication of the long arm of chromosome 1q. The most commonly involved reciprocal chromosomal arm is 4q [50]. The first initial recurring translocation described in three hepatoblastoma patients was der(4)t(1;4)(q12;q34) [52]. Moreover, it has been reported that hepatoblastoma is characterized by a family of chromosome translocations with similar breakpoints on either chromosome 1q12 or 1q21 [53].

Apart from chromosome anomalies, single hepatoblastoma cases are described that exhibit point mutations in the 110 kDa catalytic subunit of phosphatidylinositol-3-kinase (PIK3CA) [55], and amplifications in either PIK3C2B [56] or the pleomorphic adenoma gene (PLAG1) [57]. The only known recurrent alteration found in about two thirds of hepatoblastoma patients are mutations of the CTNNB1 gene. CTNNB1 is a key effector molecule of canonical WNT signaling and most mutations change exon 3 either by point mutation or deletion [58]. The CTNNB1 gene plays a decisive role in cell adhesion, by binding to E-cadherin, as well as cell proliferation, through its regulatory function within the WNT signaling pathway [59]. In quiescent cells, CTNNB1 is phosphorylated by glycogen synthase kinase 3 beta (GSK3β), which acts within a destruction complex consisting of APC, AXIN, GSK3ß and casein kinase 1 (CK1), leading to rapid degradation of CTNNB1 through the ubiquitin proteasome pathway [60-62]. However, alterations within the phosphorylation sites of the protein lead to the disruption of degradation. Consequently, CTNNB1 stabilizes and translocates into the nucleus, and activates transcription of target genes [63, 64] including MYC, cyclin D1 and PITX2 [65, 67]. Somatic mutations of genes participating in the degradation complex, such as APC, AXIN1 and AXIN2, have also been found in hepatoblastoma, although at a very low frequency [68-70]. Interestingly, the genetic lesions in CTNNB1, AXIN1, and AXIN2 described to be relevant for hepatoblastoma are also observed in adult HCC [69, 71]. This underlines the significance of activated WNT signaling in the genesis of liver cancer in all age groups [72]. Interestingly, it has been shown

that the introduction of activating mutations of CTNNB1 in a unique population of bipotential fetal liver cells is able to give rise to tumors [73]. Nonetheless, this observation is dependent on the cell type, as activation of CTNNB1 in hepatocytes is not sufficient to induce tumorigenesis, giving rise only to marked hepatomegaly [74, 75]. This suggests that for these cells additional mutations are needed for hepatoblastoma development.

Recently, our group has performed whole-exome sequencing of hepatoblastoma and TLCT samples in order to get more information about the genetic basis of childhood liver cancer [1]. We identified recurrent mutations in the already mentioned CTNNB1 gene as well as mutations within the transcription factor nuclear factor-erythroid-2-related-factor-2 (NFE2L2). Interestingly, whole-exome of pediatric HCC tissues also uncovered somatic mutations in these two genes [76], suggesting an import role of NFE2L2 in liver cancer development in addition to CTNNB1.

NFE2L2 belongs to the Cap 'N' Collar family that contains a conserved basic leucine zipper (bZIP) structure. It contains seven functional domains, known as Neh1–Neh7. Of these seven domains, the Neh2 domain, which is located in the N terminus of NFE2L2, is the major regulatory domain. Neh2 is responsible for ubiquitin conjugation [77] and contains two binding motifs named ETGE and DLG that are involved in the regulation of NFE2L2 stability. The main function of NFE2L2 is the activation of the cellular antioxidant response by inducing the transcription of several genes that are able to combat the harmful effects such as xenobiotics and oxidative stress. NFE2L2 has traditionally been regarded as the cell's main defense mechanism and as a major regulator of cell survival. However, recent studies have demonstrated that NFE2L2 promotes the survival not only of normal cells, but also of cancer cells. In tumor cells accumulated NFE2L2 creates an environment conducive for cell growth and protects against oxidative stress, chemotherapeutic agents [78] and radiotherapy [79].

NEF2L2 is primarily regulated by Kelch-like erythroid cell-derived protein 1 (KEAP1), a substrate adaptor Cullin 3 (CUL3)-dependent E3 ubiquitin ligase complex, that represses NFE2L2 by promoting its ubiquitination and subsequent proteasomal degradation. Under basal or unstressed conditions, NFE2L2 is primarily localized in a complex with KEAP1 via direct protein-protein interactions between the KEAP1-Kelch domain and the ETGE and DLG motifs of NFE2L2. KEAP1 binds CUL3 that represses NFE2L2 by promoting its ubiquitination and degradation. Under oxidative stress, NFE2L2 is not degraded and translocates to the nucleus. In the nucleus, NFE2L2 heterodimerises with small masculoaponeurotic fibro sarcoma (Maf) proteins and binds to the antioxidant response element (ARE), a cis-acting sequence found in the 5'-flanking region of many NFE2L2 target genes, involved in cytoprotection and metabolism [80-82]. Target genes of NFE2L2 comprise for example the NAD(P)H:quinone oxidoreductase 1 (NQO1), heme oxygenase 1 (HMOX1), glutamate-cysteine ligase (GCL) and glutathione S transferases (GSTs).

In cancer cells, several studies revealed the “dark” side of NFE2L2. It has been shown that NFE2L2 and its downstream target genes are overexpressed in cancer cell lines and human cancer tissues, giving cancer cells an advantage for survival and growth. Furthermore, it has been observed that NFE2L2 is upregulated in resistant cancer cells and is thought to be responsible for acquired chemoresistance [83, 84]. Interestingly, NFE2L2 mutations have been described to act as a driver in pediatric hepatocellular carcinogenesis [85]. Therefore, it is interesting to further study the role of NFE2L2 in hepatoblastoma.

## 1.5 Epigenetics

Epigenetics, epi- (Greek: επί- over, above, outer) – genetic (Greek: γενετικός genetikos, "genitive" and that from γένεσις genesis, "origin"), refers to mechanisms and consequences of heritable chromosomal modifications that are not based on changes in the DNA sequence. The main epigenetic modifications are DNA methylation and histone modifications (**Figure 1**). Both contribute to important processes during cell differentiation and development. Furthermore, they are involved in transcriptional regulation, protection of chromosomal stability; genomic imprinting, X chromosome inactivation as well as DNA repair [86, 87]. Thus, misregulation of DNA methylation and histone modifications are closely linked to carcinogenesis. Unlike the genetic abnormalities, which are irreversible, epigenetic alterations are relatively malleable and most likely reversible. Therefore, enzymes and genes involved in the establishment and maintenance of epigenetic marks have been considered as a new class of drug targets for cancer therapy.

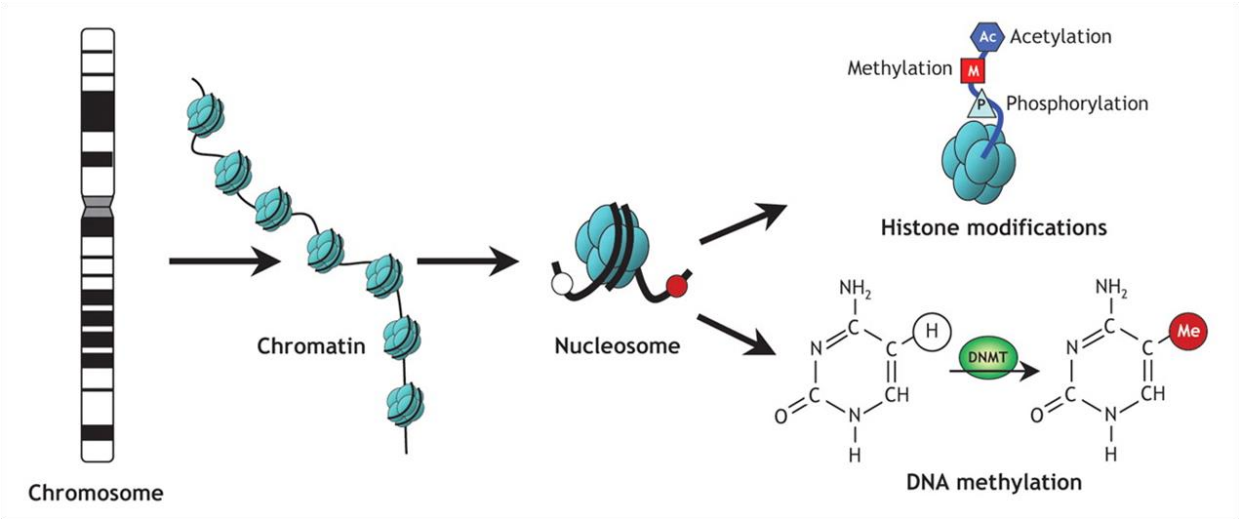


Figure 1: **Epigenetic modification of DNA and histones.** DNA is wrapped around octamers of histones thereby forming nucleosomes, the smallest units of chromatin. Histone modifications occur at multiple sites of the N-terminal tail through acetylation, methylation and phosphorylation. DNA methylation occurs at the 5-position of cytosine residues in a reaction catalyzed by DNA methyltransferases (DNMTs). Histone modifications as well as DNA methylation are the two central epigenetic mechanisms that play a role in gene regulation. Figure from [87]**.**

### 1.5.1 Histone modification

Post-translational modifications on histones offer a broad range of regulatory mechanisms, especially at the N-terminal tail regions. Possible modifications include acetylation, methylation, phosphorylation, ubiquitination, SUMOylation as well as poly-(ADP)-ribosylation, with the first three being best studied [89]. The constellation of these specific histone modifications form the so-called "histone code" and influence the interaction with the DNA backbone, neighboring nucleosomes and non-histone chromatin proteins, aiming to mediate a stable chromatin environment. Histone modifications influence the compaction of chromatin, affecting the ability of transcription factors, polymerases, repair enzymes, and the recombination machinery to access the substrate. More open and accessible chromatin is associated with transcriptional activity, while tightly folded, compact heterochromatin is associated with gene silencing. The exact effects on transcription and chromatin caused by the different modifications are dependent on the type of modification, its position as well as its extend.

For example, acetylation of lysine residues by histone acetyltransferases (HAT) neutralizes the lysine's positive charge and thereby reduces the packing tightness of DNA around the histone proteins. This, consequently, renders genes more accessible for transcription [90]. Accordingly, increased histone deacetylase (HDAC) activity at a certain locus results in deacetylation of histone proteins and tightening of the DNA around the histones, resulting in repression of transcription [91]. While histone acetylation activates transcription in most cases, the methylation of lysine and arginine residues leads, depending on the position in the histone tail and the number of methyl groups (mono-, di-, or tri-methyl), to activation or repression.

A classic example for activation by methylation is tri-methylation of histone 3 lysine 4 (H3K4me3). This modification leads to recruitment of the transcription factor II D (TFIID), and thereby contributes to the initiation of RNA polymerase II-dependent transcription [92]. Moreover, H3K4me3 is recognized by the chromatin remodelling complex nurf (ISWI family) and exerts an influence on the chromatin structure by opening up the chromatin [89]. A classic example of the repressing effect of histone methylation is the recruitment of the heterochromatin protein 1 (HP1) by H3K9me2/3. HP1 contributes to the deactivation of active genes by the establishment of condensed tightly packed chromatin (heterochromatin) [93]. As mentioned above, the number of attached methyl groups is an important factor for regulation. The mono-methylated forms of H3K9, H3K27 and H4K20 induce the activation of transcription, whereas the di- and tri-methylated forms lead to repression of transcription, due to binding of different effector proteins [94, 95]. The different degrees of methylation are generated by different histone methyltransferases (HMTs) and S-adenosyl methionine serves as the methyl group donor. Set7/9 for instance catalyzes mono-methylation,

whereas the MLL complexes tri-methylates H3K4. G9a is responsible for di-methylation of H3K9 and SUV39H1/2 tri-methylates H3K9 [96, 97].

The di-methylation of arginine is carried out by members of the PRMT family and can either occur symmetrical and asymmetrical. Symmetric methylation represses transcription, while asymmetric methylation activates transcription [98]. The recognition of methylated lysine and arginine residues is conducted by chromo domains [99], Tudor domains, MBT repeats [95], PHD finger motifs [100] and WD40-repeat proteins [101]. Demethylation of lysine and arginine residues is performed by different histone demethylases (HDMs). Lysine (K)-specific demethylase 1 (LSD1) for example removes the methyl groups of H3K4me1/2. Cleavage enzymes from the JHDM family are able to eliminate triple methylations, JMJD2A, demethylases H3K9me2/3 and H3K36me3. Jmjd6, for example, a homologue of the JHDM family specifically demethylates H3R2me2 and H4R3me2 [96].

### 1.5.2 DNA Methylation

In contrast to the epigenetic mechanism described above, methylation of DNA happens directly on the DNA. The marking of DNA by methyl groups is one of the most important regulatory mechanisms able to modify gene expression at the epigenetic level. DNA methylation is a post replicative modification that exclusively occurs at the C5 position of cytosine residues (5mC) and predominantly in the context of cytosine-phospho-guanosine (CpG) dinucleotide. The covalent addition of a methyl group to cytosine is mediated by DNA methyltransferases (DNMTs). DNMTs catalytically remove the methyl group (CH3) from the methyl doner S-adenosyl methionine (SAM) and transfer it to the carbon in the fifth position of the cytosine ring [102, 103], see **Figure 2**. CpG methylation is a relatively stable modification, which can maintain gene silencing over time, when methylation is conducted to the newly synthesized strand [104].

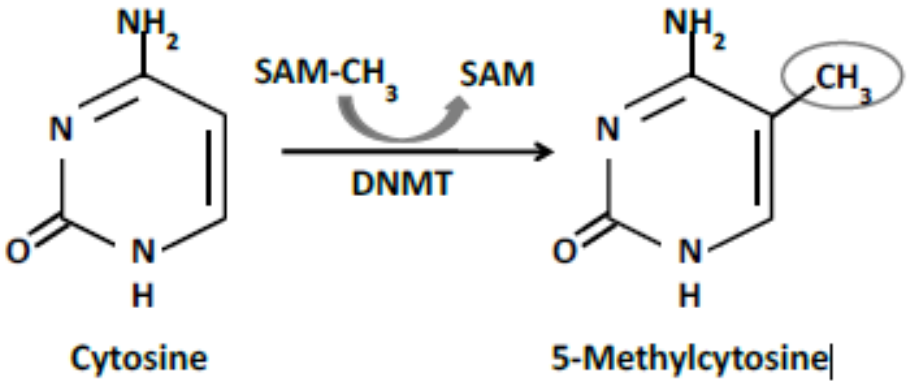


Figure 2: **Methylation of cytosine.** Methylation of cytosine through DNMT uses *S-adenosyl methionine* (*SAM*) as methyl donor.

Currently, there are three known catalytically active DNMTs within the DNMT family; the DNMT1, the DNMT3a and the DNMT3b, which play different roles in the methylation process. One the one hand, DNMT1, which interacts with the DNA replication clamp proliferating cell nuclear antigen (PCNA), has high affinity to hemi methylated DNA. It is responsible for maintaining DNA methylation following DNA replication or DNA repair. DNMT1 transmits the existing methylation pattern onto the newly replicated DNA strand and associates with replication foci throughout the S phase, whereas a diffuse nucleoplasmic distribution is observed during the G1 and G2 phase [105].

On the other hand, DNMT3a and DNMT3b share significant homology to DNMT1 and play a fundamental role in the de novo methylation of previously unmethylated CpGs [86, 93, 106]. In contrast to DNMT1, DNMT3a and DNMT3b are not associated with DNA synthesis. However, during replication of heterochromatic regions (late S phase), some of the DNMT3a-enriched foci appeared to overlap with replication foci [107]. DNMT3b remains diffuse in the nucleus at all cell cycle stages [107]. There is evidence for interaction and cooperation between DNMT1, DNMT3a and DNMT3b, reflecting a dependency of maintenance and de novo methylation. In addition, DNMT1, DNMT3a and DNMT3b interact with some chromatin-associated factors including, methyl-binding proteins (MBD2, MeCP2), HDACs, HMTs as well as transcriptional repressors [108, 109].

DNMT2 and DNMT3L are DNA methyltransferase homologues and are additional members of the DNMT family. Both, DNMT2 and DNMT3L show almost no methyl-transfer activity, thus play no further role in the methylation process of DNA [110].

The methylation pattern of CpGs through DNMTs is carefully adjusted, depending on the tissue specific differentiation state, through a complex arsenal of enzymes and methyl-DNA-binding proteins. About 80 % of the CpG sites within the genome are methylated [111], while the so called “CpG islands” usually appear in the unmethylated state. CpG islands are DNA fragments of 0.5-2 kb in length within the eukaryotic promoter having a high frequency of CpG sites (over 60 %) [86, 112]. X-chromosome inactivation as well as genomic imprinting are two known examples of naturally occurring CpG island methylation [86, 93, 113] in contrast to the usually unmodified state of CpG islands within the promoters. In cancer cells, a genome wide hypomethylation in combination with a site-specific CpG island promoter hypermethylation is observed [114]. Aberrant hypomethylation is associated with activation of proto-oncogenes, genomic instability and loss of imprinting (LOI), while promoter hypermethylation affects tumor suppressor genes (TSG). This epigenetic misregulation observed in cancer cells is associated with aberrant gene expression patterns, genomic instability and inactivating of TSG expression. Global DNA hypomethylation and promoter-specific hypermethylation are already observed in early stage tumors [114].

### 1.5.3 E3 Ubiquitin-like, containing PHD and RING finger domain, 1

The E3 Ubiquitin-like, containing PHD and RING finger domain 1 (UHRF1) also known as NP95 in mouse and ICBP90 in humans, is a 90 kDA nuclear protein that contains five distinct structural domains: the Ubiquitin-like (UBL) domain, a Tandem Tudor (TTD) domain, a Plant Homeo (PHD) domain, a Set and Ring associated (SRA) domain and the Really Interesting New Gene (RING) domain (**Figure 3**), which coordinate the inheritance of the epigenetic code

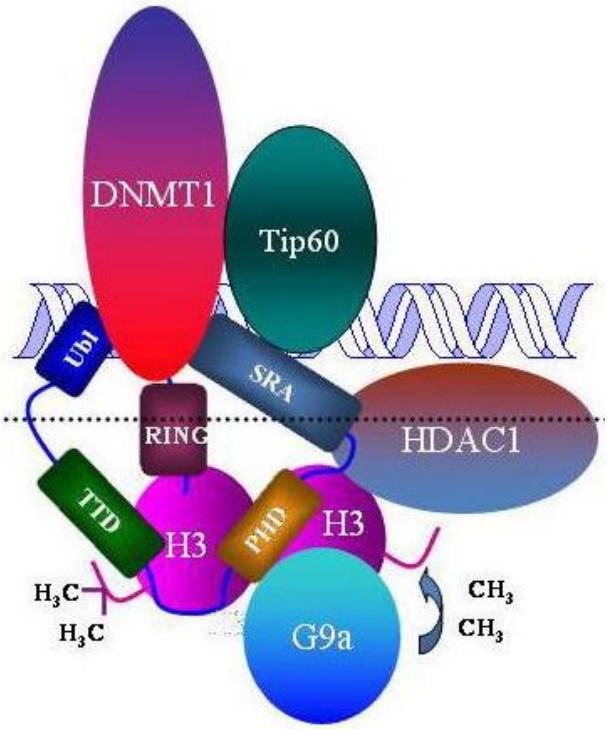


Figure 3**: Structural domains of UHRF1 interact with either DNA or histones.** UHRF1 contains five structural domains: the Ubiquitin-like (UBL) domain, a Tandem Tudor (TTD) domain, a Plant Homeo (PHD) domain, a Set and Ring associated (SRA) domain and the Really Interesting New Gene (RING) domain. UHRF1 interacts with DNMT1, Tip60 via its SRA, UBL and RING domain on DNA level, while interaction with histones is mediated via the TDD, PHD and Ring domain. UHRF1 interacts with HDAC1 and G9a. Figure from [114].

The essential function of UHRF1 in the maintenance of DNA methylation consists of substrate recognition and recruitment of DNMT1. The SRA domain of UHRF1 recognizes hemi-methylated DNA and recruits DNMT1 [116-119], while the TTD and PHD domain bind the tail of histone H3 in a highly methylation sensitive manner. TTD for example specifically binds H3K9me2 or H3K9me3 and likely signals to the methyltransferase G9a [117, 120], which methylates histones and induces heterochromatin formation, thereby contributing to gene silencing. UHRF1 also co-operates with histone deacetylase 1 (HDAC1) via the SRA domain [116, 121], leading to reduced acetylation which represses gene transcription. The UBL domain is thought to play a role in the recruitment of DNMT1, while the RING domain is responsible for the H3 ubiquitinylation [117]. The Tat-Interactive protein

(Tip60), a histone acetyltransferase with specificity towards lysine 5 of histone H2A (H2AK5), has also been reported to interact with UHRF1. Thus, UHRF1 guides important enzymes taking part in epigenetic programming.

Genetic ablation of UHRF1 leads to remarkable genomic hypomethylation, comparable to the genetic ablation of DNTM1 in ESCs [118, 122] and UHRF1-/- null mice already died in midgestation [123]. Further studies in tissue cultures cells demonstrate that UHRF1 depletion causes cell cycle arrest [124-126], hypersensitivity to DNA damage and chemotherapeutic agents [123, 127], or apoptosis [126, 128]. There is evidence that UHRF1 is an important factor in carcinogenesis and thereby might be a potential anti-cancer target. The expression of UHRF1 depends on tissue type. It is highly expressed in proliferating tissue, while in differentiated tissue no expression is observed [129]. In normal cells UHRF1 expression fluctuates with cell cycle [130]. Its expression peaks at late G1 phase and continues during G2 and M phases of the cell cycle. UHRF1 plays an important role in the G1/S transition during the cell cycle by regulating topoisomerase II alpha [129, 130] and retinoblastoma gene expression [131]. Moreover, UHRF1 functions in the p53-dependent DNA damage checkpoint. UHRF1 is overexpressed in various cancer types such as bladder [132], breast [116, 121], pancreatic [133], colon [134] and hepatocellular carcinoma [135]. Furthermore, it serves as a diagnostic marker for cancer state and aggressiveness [132, 136]. UHRF1 also has been suggested to be a biomarker for low-grade and high-grade cervical cancer lesions [137]. Previous studies demonstrated that elevated levels of UHRF1 keep cells in a proliferation state and prevent their differentiation [129, 138], which is also a common feature found in blastomas. Downregulation of UHRF1 in cancer cells leads to cell growth inhibition [139] and caspase 8 dependent apoptosis [118]. Furthermore, it was reported that UHRF1 binds, together with HDAC1 and DNMT1, to methylated promoters of a number of TSGs that play a role in cancer development. These include p16INK4A, p14ARF, BRCA1, CDKN2A and RASSF1 [116, 121, 140], suggesting that UHRF1 is involved in the gene silencing of tumor suppressor genes.

Recently, colleagues of mine identified a complex comprising DNMT1, Ubiquitin-specific-processing protease 7 (USP7) and UHRF1 [141], see **Figure 4**. The complex formation is mediated through protein domain interaction of the three involved proteins. UHRF1 associated via its SRA domain with the TRAF domain (amino acid 1-215, U-1) of USP7, whereas the TS domain of DNMT1 is bound by domain 3 of USP7 (amino acid 516-916, U3). The interaction between DNMT1 and UHRF1 takes place between the TS and SRA domain, respectively **(Figure 4).**

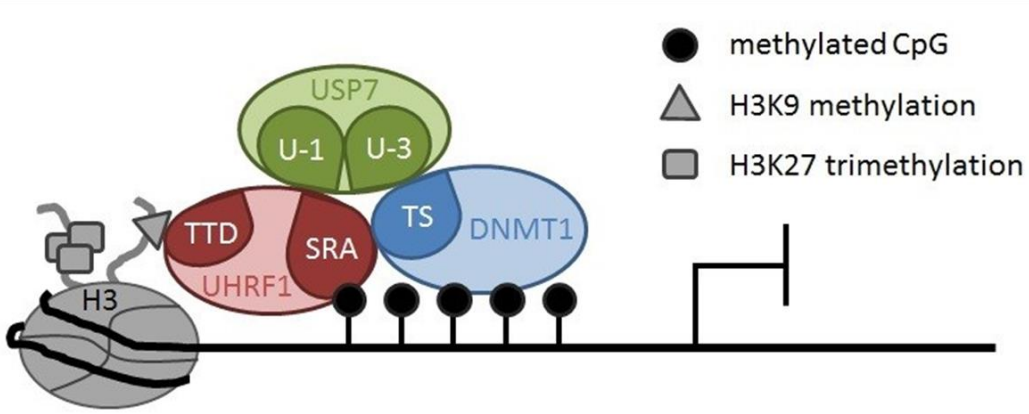


Figure 4: **Trimeric complex of DNMT1, USP7 and UHRF1.** USP7 and UHRF1 form a complex via interaction of corresponding protein domains. DNMT1 associates with USP7 via its TS domain. The TRAF domain of USP7 binds UHRF1 via the SRA domain. DNMT1 and UHRF1 interact through the TS and SRA domain. The complex binds on DNA during the methylation process and affects histone modifications.

While the main function of DNMT1 is methylation of hemi-methylated DNA to maintain methylation patterns [110, 142, 143] and USP7 stimulates DNMT1 activity and acts as a complex stabilizer [141, 144], UHRF1 acts as a key epigenetic regulator by controlling both, DNA methylation as well as histone modification through interaction with all three DNMTs, different HDACs and HMTs to mediate the chromatin state. However, binding of the trimeric complex at the Hedgehog-interacting protein (HHIP), Insulin-like growth factor-binding protein 3 (IGFBP3) and Secreted frizzled-related protein 1 (SFRP1) genes in HCT-116 cells was explored [141], TSGs that play an important role in embryogenesis and are relevant in hepatoblastoma. This finding directed us to the assumption that the complex might also be involved in hepatoblastoma development or progression.

## 1.6 Signaling pathways implicated in hepatoblastoma

Developmental disorders such as childhood tumors are known to be driven by proliferation and differentiation promoting pathways that govern normal development [145]. Misregulation or defects in relevant pathways that are involved in these processes may promote transformation and make these developing cells prone to tumorigenesis. For development of hepatoblastoma there are three main pathways described: the hedgehog, the IGF and the WNT signaling pathway. The three signaling pathways are inter alia regulated by their pathway inhibitors HHIP, IGFBP3 and SFRP1, respectively. *HHIP*, *IGFBP3* and *SFRP1* belong to the group of TSG, which have been described to protect cells from undergoing malignant transformation by regulation of the cell cycle, by induction of apoptosis, by inhibition of cellular migration and metastasis and by protection from mutagenic events [146]. A deregulation or complete silencing of TSG through deletions, loss of function mutations or promoter

hypermethylation is a common molecular mechanism that is observed in cancer cells. Since colleagues of mine have shown that the promoter regions of *HHIP*, *IGFBP3* and *SFRP1* are heavily methylated [147, 148], it is worth to speculate that this might be one of the reasons for misregulated pathway activation, leading to hepatoblastoma development.

### 1.6.1 Hedgehog signaling pathway

Hedgehog signaling plays a crucial role in the formation of the neural tube, the axial skeleton, limbs, the skin, hair and teeth during embryonic development [149-153]. Additionally, it has been shown that hedgehog signaling significantly contributes to embryonic liver development and liver regeneration after injury in adults [154-157].

So far, in vertebrates there are three homologues identified, Sonic- (SHH), Desert- (DHH) and Indian hedgehog (IHH), of which SHH is best studied. The different homologues are responsible for induction of signaling in different tissues and can act either in autocrine and paracrine fashion. SHH is involved in the development of large parts of the central nervous system, limbs, lung, intestines, liver, teeth and hair follicles [149-153, 158], whereas, DHH and IHH, are primarily involved in the development of the germ line and skeleton [159-161]. Hedgehog signaling is initiated by autocatalytic processing of the Hedgehog ligand [162], generating an N-terminal signaling domain which binds to the 12-transmembrane protein receptor Patched 1 (PTCH1) [163-165]. In the unactivated state, PTCH1 acts as an inhibitor of Smoothened (SMO), a 7-transmembrane protein related to the Frizzled family of WNT receptors. Once SHH, IHH or DHH form a complex with PTCH1, conformational changes abolish the inhibiting effect on SMO, leading to increased signaling [164, 166, 167]. Another theory suggests that PTCH1 acts as a sterol pump and regulates SMO activity by removing oxysterols either directly or indirectly from its environment [168, 169]. As a result the PTCH1/SMO interaction signal cascade gets activated and induces expression of target genes. This is mediated by transcription factors of the Glioblastoma (GLI) family. Target genes include genes that are associated with proliferation, like MYCN [170], IGF2 [171] and cyclin D1 [172]. Hedgehog signals are regulated through a positive feedback of the GLI1 expression or the ligand SHH, IHH and DHH, and negative feedback via PTCH1. HHIP is an additional regulator of the hedgehog pathway. It attenuates signaling by binding of all three family members, SHH, IHH and DHH [173] and thereby prevents complex formation with PTCH1.

During embryogenesis ligand expression and activation of the signaling pathway is strictly regulated in the liver. It has been shown that continuous activation of Hedgehog signaling is deleterious for differentiation of hepatoblasts to hepatocytes and consequently, needs to be shut off for proper

hepatic differentiation of hepatoblasts [174]. Deregulated and active signaling is often associated with formation of multiple types of solid tumors, including cholangiocarcinoma, hepatocellular carcinoma and hepatoblastoma [147, 175-177]. Mechanisms that have been described to be responsible for persistent hedgehog activation in hepatoblastoma are the overexpression of many signaling molecules such as SHH, PTCH1, SMO and GLI1 [147, 178] as well as the silencing of the pathway inhibitor HHIP by promoter hypermethylation [147]. These findings underscore the involvement of this pathway in the oncogenesis of hepatoblastoma and suggest the interference of signal transduction via, for instance, reactivation of gene expression of the pathway inhibitor HHIP as a promising approach for hepatoblastoma therapy.

### 1.6.2 IGF signaling

The insulin-like growth factor (IGF) signaling pathway is another important pathway involved in the regulation of normal development and growth in the liver. But, it is also described to play a role in tumor development, since increased expression of insulin-like growth factor 2 (IGF2) leads to constant activation of the IGF pathway [179], which then leads to activation of proliferation. IGF2 binds to the Insulin-like growth factor 1 receptor (IGF1R) receptor resulting in autophosphorylation of the tyrosine residues of the receptor. This leads to the recruitment of the adaptor proteins insulin receptor substrate (IRS) and Scr homology 2 domain containing (SHC) to the intracellular receptor βsubunits. This process activates signaling cascades through the PI3K-AKT and the RAS/RAF/MEK/ERK pathways, resulting in stimulation of transcription and cell cycle progression, increased proliferation and growth, as well as inhibition of apoptosis. IGFBP3 is multifunctional protein predominantly produced by the liver and inhibitor of the IGF signaling. IGFBP3 directly binds IGF2 and reduces its availability. Moreover, it has been shown that IGFBP3 is capable to induce an IGF-independent pathway of apoptosis and consequently prevents cell growth [180].

Recent studies suggested a critical role of the IGF axis in hepatoblastomagenesis, since it has been shown that the fetal growth factor IGF2 is transcriptionally upregulated in hepatoblastoma [181, 182]. Processes that may take part in IGF pathway activation include overexpression of IGF2, either as a consequence of LOH or loss of imprinting (LOI) at the IGF2/H19 locus [183] and/or amplification and subsequent upregulation of the transcriptional IGF2 activator pleomorphic adenoma gene 1 (PLAG1) [57], which are described for several hepatoblastoma cases. The activation of the downstream serine/threonine kinase and survival factor AKT by phosphorylation [55] and methylation of the IGFBP3 promoter is a phenomenon that is also described in hepatoblastoma cells [148]. Moreover, by studying the promoter hypermethylation of IGFBP3 in hepatocellular carcinoma,

Hanafusa and colleagues identified binding sites of the tumor suppressor p53. Consequently, methylation of this region within the IGFBP3 promoter also prevents the p53 mediated growth suppression of tumor cells [184], an additional mechanism that supports tumor formation. Thus, an active IGF pathway is characteristic for the molecular pathogenesis of liver cancer.

### 1.6.3 WNT signaling pathway

The WNT/β-catenin pathway is a pathway that has proven to be essential in organogenesis and normal cellular processes such as cell proliferation, differentiation, survival, apoptosis and cell motility [185]. It plays an important role in liver development and is also involved in liver regeneration, liver metabolism and the maintenance of normal function in the adult liver.

There are three WNT signaling pathways that have been characterized: the canonical WNT pathway, which is CTNNB1 dependent, the non-canonical planar cell polarity pathway and the non-canonical WNT/calcium pathway. The latter two pathways are CTNNB1 independent [185]. The canonical WNT pathway is involved in the regulation of gene transcription, whereas the non-canonical planar cell polarity pathway is responsible for the organization of the cytoskeleton of the cell and the non-canonical WNT/calcium pathway regulates the calcium homeostasis within the cell. Of these three pathways, the canonical, CTNNB1 dependent pathway is most interesting for hepatoblastoma development. CTNNB1 is a crucial effector of WNT signaling that plays important roles in intercellular adhesion and in cell growth, survival and differentiation. In normal epithelial cells, CTNNB1 is localized at the plasma membrane and forms a complex with E-cadherin and α-catenin at the sites of adherent junctions. Excess of CTNNB1 is phosphorylated at four N-terminal serine-threonine residues by GSK3β and CK1 which act within a cytoplasmic destruction complex including APC and AXIN. The phosphorylation of CTNNB1 leads to rapid degradation of CTNNB1 by the ubiquitin-proteasome pathway. WNT signaling gets activated through WNT binding to the 7 transmembrane receptor Frizzled (FZD). This induces association with a co-receptor, either LRP5 or LRP6 (low density lipoprotein receptor-related protein), and leads to activation of Disheveled (DVL) [186]. DVL inhibits the ability of GSK3β to phosphorylate CTNNB1 and thereby prevents its proteasomal degradation. Subsequently, CTNNB1 accumulates in the cytoplasm, translocates into nucleus, binds the TCF/LEF family and induces transcription of specific target genes of the WNT signaling pathway such as c-Myc and cyclin D1 [63, 64, 186]. Inhibitors of the WNT pathway are secreted frizzled related proteins (SFRP), the WNT inhibitory factor 1 (WIF1) and the Dickkopf protein (DKK). While SFRP1 and WIF1 directly bind to WNT or form a non-active complex with the receptor FZD, DKK mediates the inactivation of the WNT signaling pathway by binding to LRP [187].

Aberrant activation of CTNNB1 has also been implicated in the pathogenesis of hepatobiliary neoplasia, ranging from benign lesions to liver cancer. As already mentioned in section 1.4 abnormal WNT signaling plays a key role in hepatoblastoma development. In particular, the finding of high-rate mutations in the CTNNB1 gene has implicated aberrant activation of WNT signaling as a hallmark of hepatoblastoma. Besides mutations in key players of the WNT pathway such as CTNNB1, APC and AXIN, a variety of mechanisms, including microRNAs and epigenetic events have been reported to modulate WNT signal activity. It already has been described that DNA methylation within the promoter region is responsible for the reduced expression of the WNT pathway inhibitors SFRP1, WIF1 and DKK1 in cancerous cells, resulting in active signaling [188-190]. Since the deregulation of this pathway is common in hepatic cancers, the restoration of functional regulatory components might therefore be an attractive target for potential therapies.

## 1.7 Aim of the study

The cause of hepatoblastoma is still largely unknown. However, the development and progression of hepatoblastoma is associated with CTNNB1 mutations, genetic syndromes and/or deregulation of embryonic pathways such as the WNT, the IGF or hedgehog signaling pathway through inhibition of their regulatory components via DNA methylation. We therefore set out to expand the knowledge on the genetic basis of hepatoblastoma development and progression. Based on the whole-exome sequencing data, recently acquired in our laboratory [1], we first aimed to perform targeted sequencing of additional hepatoblastoma samples, cell lines and TLCTs referring to CTNNB1 and NFE2L2. Furthermore, we wanted to perform functional analysis of NFE2L2-mutations regarding KEAP1-mediated degradation and target gene activation. Additionally, we wanted to study the role of NFE2L2 in cell proliferation. This included the depletion of NFE2L2 via siRNA and analysis of target gene expression and hepatoblastoma cell viability. Moreover, we wanted to define the clinical relevance NFE2L2 activity concerning prognosis and outcome.

Furthermore, we wanted to investigate the mechanisms of hypermethylation of TSGs in reference to UHRF1, since it cooperates with two key regulatory modules of the epigenetic machinery and since it has been shown to bind to HHIP, IGFBP3 and SFRP1, three TSGs hypermethylated in cancer cells. We therefore wanted to determine the consequences of a UHRF1 knockdown on demethylation of the HHIP, IGFBP3 and SFRP1 promoter regions, on re-expression of these TSGs and on cell proliferation. Additionally, we wanted to examine the role for UHRF1 as a prognostic marker in hepatoblastoma.

# 2 Material

## 2.1 Cell culture

### 2.1.1 Cell lines

| | |
|---|---|
| HepT1 *Homo sapiens* (human), liver, hepatoblastoma | (Pietsch et al., 1996, [191]) |
| HepG2 *Homo sapiens* (human), liver, hepatoblastoma, [192] (Product number: ATCC-HB6065) | (ATCC, Manassas, USA) |
| HUH6 *Homo sapiens* (human), liver, hepatoblastoma (Product number: JCRB0401) | (JCRB, Osaka, Japan) |
| HEK293T Homo sapiens (human), embryonic kidney (Product number: ATCC-CRL-3216) | (ATCC, Manassas, USA) |

### 2.1.2 Cell Culture Reagents

| | |
|---|---|
| Dimethyl sulfoxide (DMSO), sterile | Merck, Darmstadt, Germany |
| Dulbecco`s Modified Eagle Medium (DMEM) | Invitrogen, Karlsruhe, Germany |
| Dulbecco's Phosphate-Buffered Saline (DPBS) | Invitrogen, Karlsruhe, Germany |
| Fetal Calf Serum (FCS), sterile | Sigma- Aldrich, Taufkirchen, Germany |
| Penicillin-Streptomycin (10 x) (10.000 U/mL Penicillin; 10.000 µg/mL Streptomycin) | Invitrogen, Karlsruhe, Germany |
| Roswell Park Memorial Institute Medium (RPMI) | Invitrogen, Karlsruhe, Germany |
| Trypsin - EDTA 0.05 % | Invitrogen, Karlsruhe, Germany |

### 2.1.3 Cell Culture Transfection Reagents

| | |
|---|---|
| HiPerFECT, 1 mL | Qiagen, Hilden, Germany |
| X-tremeGENE HP Transfection Reagent | Roche Diagnostic, Penzberg, Germany |

### 2.1.4 Cell Culture Material

| | |
|---|---|
| Biosphere® Filtertips 1-10 µL, sterile | Sarstedt AG & Co., Nümbrecht, Germany |
| Biosphere® Filtertips 1-100 µL, sterile | Sarstedt AG & Co., Nümbrecht, Germany |
| Biosphere® Filtertips 100-1000 µL, sterile | Sarstedt AG & Co., Nümbrecht, Germany |
| Cell scraper | Sarstedt AG & Co., Nümbrecht, Germany |

| | |
|---|---|
| Costar® Stripette® Serologic Pipettes 5 mL, sterile | Corning GmbH, Wiesbaden, Germany |
| Costar® Stripette® Serologic Pipettes 10 mL, sterile | Corning GmbH, Wiesbaden, Germany |
| Costar® Stripette® Serologic Pipettes 25mL, sterile | Corning GmbH, Wiesbaden, Germany |
| EasyFlasksTM, Cell culture flasks, 25 $cm^2$, Non-pyrogenic DNase und RNase free | NUNC, Langenselbold, Germany |
| EasyFlasksTM, Cell culture flasks, 75 $cm^2$, Non-pyrogenic, DNase und RNase free | NUNC, Langenselbold, Germany |
| Plastic tubes, 15 mL, sterile | greiner bio-one, Frickenhausen, Germany |
| Plastic tubes, 50 mL, sterile | greiner bio-one, Frickenhausen, Germany |
| Petri dishes 100 x 20 mm, non-pyrogenic, sterile | NUNC, Langenselbold, Germany |
| 6-Well Plates, non-pyrogenic, sterile BD | NUNC, Langenselbold, Germany |
| 12-Well Plates, non-pyrogenic, sterile BD | NUNC, Langenselbold, Germany |
| 24-Well Plates, non-pyrogenic, sterile BD | NUNC, Langenselbold, Germany |
| 96-Well Plates, non-pyrogenic, sterile BD | NUNC, Langenselbold, Germany |

### 2.1.5 siRNAs

| | |
|---|---|
| siGENOME Non-Targeting siRNA #1 (D-001210-01-20; Sequence N/A) | Thermo Scientific, Schwerte, Germany |
| Pre-designed Silencer Select_UHRF1 siRNA (s26553; 5´-ACAGTCTTGTGATCAGAAA-3´) | Applied Biosystems, Carlsbad, USA |
| Flexi tube siRNA Hs_NFE2L2_7 (SI03246950, 5´-CCCATTGATGTTTCTGATCTA-3´) | Qiagen, Hilden, Germany |

## 2.2 Prokaryotic cultures

### 2.2.1 Bacteria

| | |
|---|---|
| One Shot® TOP10 Chemically Competent *E. coli* | Invitrogen, Karlsruhe, Germany |
| Genotyp:F-mcrA Δ(mrr-hsdRMS-mcrBC) ϕ80lac | |
| ZΔM15 ΔlacX74 recA1 araD139 Δ(ara-leu) 7697 | |
| galU galK rpsL (StrR) endA1 nupG λ- | |

| | |
|---|---|
| *Escherichia coli* DH5α | Invitrogen, Karlsruhe, Germany |
| Genotype: F- ϕ80*lac*ZΔM15 Δ(*lac*ZYA-*arg*F)U169 *rec*A1 *end*A1 *hsd*R17(rk-,mk+) *pho*A*sup*E44 *thi*-1 *gyr*A96 *rel*A1 λ- | |

### 2.2.2 Culture media

| | |
|---|---|
| Lysogeny Broth (LB) Medium: (V = 1 L); pH: 7.0<br>• 10 g/L Tryptone<br>• 5 g/L Yeast extract<br>• 10 g/L NaCl | Roth, Karlsruhe, Germany |
| LB-Agar for plates: (V = 1 L); pH: 7.0<br>• 10 g/L Tryptone<br>• 5 g/L Yeast extract<br>• 10 g/L NaCl<br>• 15 g Agar | Roth, Karlsruhe, Germany |
| Super Optimal Broth Medium with glucose (S.O.C) | Invitrogen, Karlsruhe, Germany |

### 2.2.3 Antibiotics

| | |
|---|---|
| Kanamycin (50 µg /mL) | Sigma, Steinheim, Germany |
| Ampicillin (100 µg /mL) | Sigma, Steinheim, Germany |

### 2.2.4 Plasmids

| | |
|---|---|
| pEGFP-N1<br>(Kanamycin Resistance) | ClonTech, Mountain View, CA, USA |
| pRL-CMV Dual-Glo® Luciferase Assay System<br>(Ampicillin Resistance) | Promega, Mannheim, Germany goat |
| pKEAP1<br>(Ampicillin Resistance) | provided by Dr. Ben Major (University of North Carolina, USA) |
| pNQO1-ARE luciferase reporter<br>(Ampicillin-Resistance) | provided by Dr. Masayuki Yamamoto (Tohoku University, Japan) |

| | |
|---|---|
| pUC19 control DNA (Ampicillin-Resistance) | Invitrogen, Karlsruhe, Germany |

### 2.2.5 Antibodies

| | |
|---|---|
| Mouse anti-human UHRF1 | kindly provided by C. Bronner (Strasbourg University France, [128]) |
| Rabbit anti-human β-actin, (# 4970) | Cell signaling technology, Danvers, USA |
| Horseradish peroxidise-conjugated goat anti-mouse immunoglobulin G,(P0260) | DakoCytomotion, Hamburg, Germany |
| Horseradish peroxidise-conjugated goat anti-rabbit immunoglobulin G (P0488) | DakoCytomotion, Hamburg, Germany |
| Rabbit anti-human NFE2L2, (sc-722) | Santa Cruz Technology, Heidelberg, Germany |
| Goat anti-rabbit-Alexa 488, (A-11034) | Invitrogen, Karlsruhe, Germany |
| Histone H3 dimethyl Lys 4 antibody (39679) | Active Motif, La Hulpe, Belgium |
| Histone H3 dimethyl Lys 9 antibody (39683) | Active Motif, La Hulpe, Belgium |
| Histone H3 trimethyl Lys27 antibody (61017) | Active Motif, La Hulpe, Belgium |
| RNA pol II antibody (39097) | Active Motif, La Hulpe, Belgium |
| Normal mouse IgG antibody (sc-2025) | Santa Cruz Technology, Heidelberg, Germany |

### 2.2.6 Pyrosequencing Assay

| | |
|---|---|
| PyroMark® Q24 CpG LINE-1 (accession no. X58075) | QIAGEN GmbH, Hilden, Germany |

## 2.3 Chemicals / Reagents

| | |
|---|---|
| 6x DNA Loading Dye | Fermentas GmbH, St. Leon-Rot, Germany |
| Acetic Acid | Carl Roth, Karlsruhe, Germany |
| Agaroses | PeQLab, Erlangen, Germany |
| Albumin Fraction V (BSA) | Carl Roth, Karlsruhe, Germany |
| β-Mercaptoethanol | Sigma-Aldrich, Steinheim, Germany |
| Bio Rad Protein Assay | Bio-Rad, Munich, Germany |
| Boric acid | Carl Roth, Karlsruhe, Germany |
| Bovine Serum Albumin (BSA) (100 X) | Fermentas GmbH, St. Leon-Rot, Germany |
| Bromophenolblue | SERVA, Heidelberg, Germany |

| | |
|---|---|
| Chloroform | Carl Roth, Karlsruhe, Germany |
| cOmplete Protease Inhibitor Cocktail Tablets (PI) | Roche, Mannheim, Germany |
| $ddH_20$ | Invitrogen, Karlsruhe, Germany |
| dNTPs | Roche, Mannheim, Germany |
| Dimethyl sulfoxide (DMSO) | Merck, Darmstadt, Germany |
| Disodium hydrogen phosphate | Merck, Darmstadt, Germany |
| Dithiothreitol (DTT) (0.1 M) | Invitrogen, Karlsruhe, Germany |
| Ethylenediaminetetraacetic acid (EDTA) | Carl Roth, Karlsruhe, Germany |
| Ethanol, absolut | Merck, Darmstadt, Germany |
| Ethidium bromide (EtBr), 10 mg /mL | Sigma, Steinheim, Germany |
| Formaldehyde 37 % | Merck, Darmstadt, Germany |
| Glycerol | Applichem, Darmstadt, Germany |
| Glycine | GERBU Biotechnik, Gaiberg, Germany |
| Isopropyl alcohol | Sigma-Aldrich, Steinheim, Germany |
| Igepal CA-630 | Sigma-Aldrich, Steinheim, Germany |
| Loading Dye Solution (6 x) | MBI Fermentas, St. Leon-Rot, Germany |
| Magnesium chloride | Carl Roth, Karlsruhe, Germany |
| Methanol | Merck, Darmstadt, Germany |
| NEB Cut Smart Buffer | New England Biolabs, Frankfurt, Germany |
| NuPAGE® MOPS SDS Running Buffer (20X) | Invitrogen, Karlsruhe, Germany |
| Paraformaldehyde | Carl Roth, Karlsruhe, Germany |
| Phenol | Carl Roth, Karlsruhe, Germany |
| Phosphate buffered saline (PBS) (-$CaCl_2$ und $MgCl_2$, 1 x) | Invitrogen, Karlsruhe, Germany |
| Potassium chloride | Merck, Darmstadt, Germany |
| Potassium dihydrogen orthophosphate | Merck, Darmstadt, Germany |
| Powdered milk | Carl Roth, Karlsruhe, Germany |
| Propidium iodide | Sigma-Aldrich, Steinheim, Germany |
| PyroMark Annealing Buffer | QIAGEN GmbH, Hilden, Germany |
| PyroMark Binding Buffer | QIAGEN GmbH, Hilden, Germany |
| PyroMark Denaturation Buffer | QIAGEN GmbH, Hilden, Germany |

| | |
|---|---|
| PyroMark Wash Buffer | QIAGEN GmbH, Hilden, Germany |
| PyroMark Gold Q24 Reagents | QIAGEN GmbH, Hilden, Germany |
| Sodium acetat | Carl Roth, Karlsruhe, Germany |
| Sodium chloride, | Carl Roth, Karlsruhe, Germany |
| Sodium dodecyl sulfat (SDS) | Biomedicals, Eschwege, Germany |
| Streptavidin coated sepharose beads | GE Healthcare, Frankfurt, Germany |
| TE-Buffer | Upstate, Billerica, USA |
| TRI Reagent® RNA Isolation Reagent | Sigma-Aldrich, Steinheim, Germany |
| Tris (hydroxymethyl)-aminomethane (TRIS) | Carl Roth, Karlsruhe, Germany |
| Triton X-100 | Sigma-Aldrich, Steinheim, Germany |
| Tween 20 | Sigma-Aldrich, Steinheim, Germany |
| Ultra Pure TM DNase/RNase-Free Distilled water | Invitrogen, Karlsruhe, Germany |
| Vectashield® Mounting Medium with DAPI | Vector Laboratories Inc., Burlingame, USA |
| X-Ray Roentoroll solution | Tetental AG, Schützenwall, Germany |
| X-Ray Superfix 25 Solution | Tetental AG, Schützenwall, Germany |

## 2.4 Buffer and Solutions

Buffers and Solutions were prepared in $dH_20$ and autoclaved if needed and pH adjusted with NaOH or HCl.

Cell lysis Buffer:

- 0.5 % (v/v) Triton X-100
- 1 mM Sodium orthovanadate in PBS
- Protease inhibitor (1 x)

Cell fraction lysis Buffer

- 10 mM Hepes; pH 7.9
- 10 mM KCl
- 1 mM DTT
- 0.1 mM EDTA
- 1 x PI

Extraction Buffer

- 20 mM Hepes; pH 7.9
- 420 mM NaCl
- 1.5 mM $MgCl_2$
- 0.1 mM EDTA
- 25 % (v/v) Glycerol
- 1 mM DTT
- 1 x PI

PBST

- 1 X PBS, 500 mL
- Tween 20, 500 µL

Running Buffer

- 50 mL 10 X MOPS-SDS-Running Buffer
- 450 mL $dH_20$

5 x SDS-Buffer:

- 2 % (w/v) SDS
- 5 % (v/v) β-Mercaptoethanol
- 10 % (w/v) Glycerine
- 1 mM EDTA
- 0.005 % Bromphenolblue
- 62.5 mM TRIS-HCl (pH 6.8)

STE-Buffer, pH 8.0:

- 10 mM Tris base
- 0.1 M NaCl
- 1 mM EDTA
- 1 % (w/v) SDS

Stripping-Buffer, pH 2.0:

- 25 mM Glycine-HCl
- 1 % (w/v) SDS

TAE, pH 8.0

- Tris base
- 0.5 M $Na_2EDTA$
- Acetic acid

TBE-Buffer, pH 8.0:

- 89 mM Tris base
- 2 mM EDTA
- 89 mM Boric acid

TE-Buffer, pH 8.0:

- 10 mM TRIS-HCl
- 1 M EDTA

Transfer-Buffer

- 48 mM Tris base
- 39 mM Glycine

Wash-Buffer:

- 0.1 % (v/v) Tween 20 in PBS

## 2.5 Molecular Size Markers

| | |
|---|---|
| Gene Ruler™ 100 bp DNA Ladder | Fermentas GmbH, St. Leon-Rot, Germany |
| Gene Ruler™ 1 kb DNA Ladder | Fermentas GmbH, St. Leon-Rot, Germany |

## 2.6 Enzymes

| | |
|---|---|
| High Fidelity *Taq* polymerase | Thermo Scientific, Schwerte, Germany |
| Maxima Hot Start *Taq* DNA - Polymerase | Fermentas, St. Leon-Rot, Germany |
| Q5 Hot Start High-Fidelity DNA - Polymerase | New England BioLabs, Frankfurt, Germany |
| Proteinase K, 10 mg/mL | Sigma-Aldrich, Steinheim, Germany |
| RNase H | Roche Diagnostics, Penzberg, Germany |
| Super Script™ II Reverse Transcriptase | Invitrogen, Karlsruhe, Germany |
| T4 DNA Ligase | Fermentas, St. Leon-Rot, Germany |
| iTaq SYBR Green Supermix with ROX | Bio-Rad, Munich, Germany |

### 2.6.1 Restriction enzymes

| | |
|---|---|
| SacI-HF 2000 Units | New England BioLabs, Frankfurt, Germany |
| NheI-HF 2000 Units | New England BioLabs, Frankfurt, Germany |

## 2.7 Kits

| | |
|---|---|
| ChiP-IT Express Enzymatic | Active Motif, La Hulpe, Belgium |
| DNeasy blood and tissue Kit | QIAGEN GmbH, Hilden, Germany |

| | |
|---|---|
| Dual-Glo Luciferase Assay System | Promega, Mannheim, Germany |
| EpiTect Bisulfite Kit | QIAGEN GmbH, Hilden, Germany |
| ECL Plus Western Blotting Detection Reagents | Amersham, Buckinghamshire, UK |
| Mycoplasma PCR ELISA | Roche Diagnostics, Penzberg, Germany |
| PureLink™ Genomic DNA Purification Kit | Invitrogen, Karlsruhe, Germany |
| QIAquick PCR Purification Kit | QIAGEN GmbH, Hilden, Germany |
| QIAquick Gel Extraction Kit | QIAGEN GmbH, Hilden, Germany |
| QIAprep Spin Miniprep Kit | QIAGEN GmbH, Hilden, Germany |
| QIAGEN Plasmid Midi Kit | QIAGEN GmbH, Hilden, Germany |
| RNase-Free DNase Set | QIAGEN GmbH, Hilden, Germany |
| RNeasy Mini Kit | QIAGEN GmbH, Hilden, Germany |

## 2.8 Consumables

| | |
|---|---|
| BD Falcon™ Round-Bottom Tubes | BD, Heidelberg, Germany |
| Biosphere® Filtertips | Sarstedt AG & Co., Nümbrecht, Germany |
| Coverglas | Menzel-Gläser, Braunschweig, Germany |
| Electroporation cuvettes | PeQLab, Erlangen, Germany |
| Hybond-C extra Nitrocellulose membran | Amersham, Buckinghamshire, UK |
| Hyperfilm™MP | Amersham, Buckinghamshire, UK |
| Microwell Plates | NUNC, Langenselbold, Germany |
| Multidishes NunclonTM | NUNC, Langenselbold, Germany |
| Nalgene® Cyrotube | Schubert&Weiss, Iphofen, Germany |
| Nunc™ F96 MicroWell™ White Polystyrene Plate | NUNC, Langenselbold, Germany |
| Object slide | Menzel-Gläser, Braunschweig, Germany |
| Pipette tips (10 µL, 100 µL, 1000 µL) | Sarstedt, Nümbrecht, Germany |
| PyroMark Q24 Plate | QIAGEN GmbH, Hilden, Germany |
| 8-Well PCR stripes | Eppendorf, Hamburg, Germany |
| PCR 96 Well Plates | PeQLab, Erlangen, Germany |
| Quarz cuvette QS 10.00 mm | Hellma, Müllheim, Germany |
| 8 - 12 % Tris-Glycine Gels | Invitrogen, Karlsruhe, Germany |

| | |
|---|---|
| Whatman paper | Whatman, Maidstone, UK |
| Safe-lock Eppendorf tube (1.5 mL, 2 mL) | Eppendorf, Hamburg, Germany |

## 2.9 Equipment

| | |
|---|---|
| Agarose gel electrophoreses apparatus | Bio-Rad, Munich, Germany |
| Biofuge fresco, Heraeus | Kendro, Langenselbold, Germany |
| Biofuge pico, Heraeus | Kendro, Langenselbold, Germany |
| Bio Photometer | Eppendorf, Hamburg, Germany |
| Camera AxioCam MRm | Zeiss, Jena, Germany |
| Camera Power Shot G6 | Canon, Krefeld, Germany |
| Cell screen Olympus IX50 | Innovatis, Bielefeld, Germany |
| Centrifuge 5702 | Eppendorf, Hamburg, Germany |
| Centrifuge J2-21 | Beckman Coulter, Krefeld, Germany |
| Centrifuge LMC-3000 | G. Kisker, Steinfurt, Germany |
| CO2-Incubator MCO-20AIC | Sanyo, Tokio, Japan |
| Dounce homogenizer | Kimble, Meinigen, Germany |
| Excella E24 Incubator Shaker Series | New Brunswick Scientific, Enfield, USA |
| Heat block MR 3001 | Heidolph, Kehlheim, Germany |
| Heatblock „Thermomixer comfort“ | Eppendorf, Hamburg, Germany |
| GelJet Imager Version 2004 | Intas, Göttigen, Germany |
| GENios Microplatereader | Tecan, Crailsheim, Germany |
| Mastercycler RealPlex2 | Eppendorf, Hamburg, Germany |
| Mastercycler personal | Eppendorf, Hamburg, Germany |
| Microlitercentrifuge MZ014 | G. Kisker, Steinfurt, Germany |
| Microscope Axiovert 40 CFL | Zeiss, Jena, Germany |
| Microscope Axiovert 135 | Zeiss, Jena, Germany |
| Microtom Leica SM 2000R | Leica, Solms, Germany |
| Micro scales Te1245 | Sartorius, Göttingen, Germany |
| Microwave | Panasonic, Hamburg, Germany |
| Mini®-Sub Cell GT | Biorad, Munich, Germany |

| | |
|---|---|
| NanoDrop 1000 instrument | Thermo Scientific, Wilmington, USA |
| Incubator | Memmert, Schwabach, Germany |
| pH-Meter inoLab pH720 | WTW, Weilheim, Germany |
| Pipette Accu-Jet | Brand, Wertheim, Germany |
| PowerPac Basic™ | Bio-Rad, Munich, Germany |
| Pulse Generator EPI 2500 | Dr. L. Fischer, Heidelberg |
| PyroMark Q24 system | QIAGEN GmbH, Hilden, Germany |
| PyroMark Q24 Vacuum Workstation | QIAGEN GmbH, Hilden, Germany |
| Scales Vic-5101 | Acculab, Edgewood, USA |
| Shaker, Rock-N-Roller | G. Kisker, Steinfurt, Germany |
| Shaker, Unimax 1010 | Heidolph, Schwabach, Germany |
| Suctionsystem „EcoVac“ | Schütt, Labortechnik, Göttingen, Germany |
| Thermal Printer DPU-414 | Seiko Instruments, Neu-Isenburg, Germany |
| Thermomixer Compact | Eppendorf, Hamburg, Germany |
| Vortexer „Genie2“ | Scientific Industries, NY, USA |
| Water bath GFL 1083 | GFL, Wien, Austria |
| Western-Blot Detectionsystem „CP1000“ | AGFA, Köln, Germany |
| Work flow, Hera Safe | Kendro, Hanau, Germany |
| XCell II™ Blot Module | Invitrogen, Karlsruhe, Germany |
| XCell SureLock™ Electrophoresis Cell | Invitrogen, Karlsruhe, Germany |

## 2.10 Software

| | |
|---|---|
| CHROMAS v1.45 software | Griffith University, Queensland, Australia |
| GraphPad Prism 5.0 | GraphPad Software, La Jolla, USA |
| Methyl Primer Express® Software v1.0 | Applied Biosystems, Darmstadt, Germany |
| PyroMark Q24 Advanced Software | QIAGEN GmbH, Hilden, Germany |
| Realplex | Eppendorf, Hamburg, Germany |

# 3 Methods

## 3.1 Patients

Hepatoblastoma specimens as well as corresponding normal liver tissue were obtained from pediatric patients undergoing surgical resection in the department of pediatric surgery of the Dr. von Hauner Children´s Hospital in Munich. Written informed consent was obtained from each patient and the study protocol was approved by the Committee of Ethics of the Ludwig-Maximilian-University of Munich (Approval number: 431-11).

## 3.2 Sanger sequencing

Sequence verification was carried out by PCR amplification of candidate exons using High Fidelity Taq polymerase (Thermo Scientific) and subsequent Sanger sequencing of ExoSap-IT (Affymetrix) purified amplicons. PCR conditions for detecting mutations in exon 2 of the *NFE2L2* gene (primers NRF2-EX2-F and NRF2-EX2-R), mutations (primers BCAT-1 and BCAT-2) or deletions (primers BCAT-3 and BCAT-4) in exon 3 of the *CTNNB1* gene have been described previously [57, 193]. Sequencing was done with primers (see, Table 1) on an ABI 3730 capillary sequencer in the LMU Sequencing Facility using the ABI BigDye Terminator kit. Sequence analysis was performed using the CHROMAS v1.45 software.

Table 1: **List of primers used for Sanger Sequencing:**

| Primer | Sequence 5´→3´ |
|---|---|
| NRF2-EX2_F | ACCATCAACAGTGGCATAATGTG |
| NRF2-EX2_R | GGCAAAGCTGGAACTCAAATCCAG |
| BCAT-1 | GATTTGATGGAGTTGGACATGG |
| BCAT-2 | TGTTCTTGAGTGAAGGACTGAG |
| BCAT-3 | AAAATCCAGCGTGGACAATGG |
| BCAT-4 | TGTGGCAAGTTCTGCATCATC |

## 3.3 Generation of NFE2L2 Plasmids

Human *NFE2L2* cDNAs (wild-type and mutant forms) were sub-cloned into the pEGFP-N1 vector. To amplify the *NEFEL2* coding DNA sequence, PCR reaction was performed with Q5 Hot Start High-Fidelity DNA Polymerase at the Mastercycler personal using the following conditions:

| | | |
|---|---|---|
| Hot start | 3 min at 98 °C | |
| Denaturation | 10 sec at 98 °C | 35 cycles |
| Annealing | 30 sec at 66 °C | |
| Extension | 30 sec at 72 °C | |
| Final Extension | 5 min at 72 °C | |
| Hold | 4 °C | |

PCR product was subjected to a restrictions enzyme digest using the enzymes NehI-HF and Sac1-HF (for detailed protocol see below) to create sticky ends. 1 % agarose gel electrophoresis was performed for separation and visualization of fragments. Bands of right size were cut and subjected to a DNA clean-up step using the QIAquick Gel Extraction Kit according to the manufacturer´s protocol. Ligation reaction was performed using a total volume of 20 µL including 2 µL 10 X T4 DNA Ligase Buffer, a molar ratio of 1:3 vector to insert, X µL $dH_20$ and lastly 1 µL of T4 ligase. The reaction was mixed, spun down and incubation for 16 h at 4 °C.

## 3.4 Transformation

For transformation 1 µL of the ligation reaction was added to One Shot TOP10 or DH5 alpha chemically competent E.coli cells and incubated for 30 min on ice. Bacteria were heat shocked for 45 sec at 42 °C in a water bath and immediately transferred back on ice for about 2 min. 250 µL S.O.C medium was added and cells were incubated for 1 h at 37 °C while shaking horizontally. Aliquots of transformation reactions (50 - 150 µL) were platted on pre-warmed selective LB-agar plates containing the appropriate antibiotic ampicillin (100 µg/mL) or kanamycin (50 µg/mL). Plates were incubated top down over night at 37 °C. For further investigation five to eight antibiotic-resistant colonies were picked and cultured overnight in 5 mL LB-medium containing the appropriate antibiotic ampicillin (100 µg/mL) or kanamycin (50 µg/mL).

## 3.5 DNA Purification with Mini/ Midi preparation

To isolate plasmid DNA the QIAprep MINIprep Kit protocol (Qiagen) and QIAprep MIDIprep Kit protocol were used. For elution of plasmid DNA 50 µL $H_2O$ for the MINIPrep and 250 µL $H_20$ for the MIDIprep were used.

## 3.6 Restriction enzyme digestion

Plasmid DNA from clones of transformed cells was digested using the enzymes Neh1-HF and Sac1-HF. To prepare digestion reactions, DNA, 1/10 volume 10 x buffer, 1/10 volume BSA (10 x) were mixed with 1 µL of the restriction enzymes Neh1-HF and Sac1-HF. Reactions were incubated at 37 °C for at least 1 h followed by 20 min at 65 °C for enzyme inactivation. Afterwards, DNA samples were mixed with 6 x loading buffer and resolved on a 0.8 % - 1.5 % agarose gel at 100 V. Bands were subjected to a DNA clean-up step using the QIAquick Gel Extraction Kit. Positive plasmid clones were mixed with specific sequencing primers to check for correctness of sequence and insertion (**Table 2**). Samples were sent to the LMU Sequencing Facility and sequencing was performed on the ABI 3730 capillary sequencer using the ABI BigDye Terminator kit. Sequence analysis was performed using the CHROMAS v1.45 software.

Table 2: **List of primers used for sequence validation of constructed plasmids:**

| Primer | Sequence 5´→3´ |
|---|---|
| **NRF2_Seq_1** | **CAAAATCAACGGGACTTTCC** |
| **NRF2_Seq_1** | **CCCTGTTGATTTAGACGG** |
| **EGFP-rev** | **TGCCGGTGGTGCAGATG** |

## 3.7 Eukaryotic cell culture

The human hepatoblastoma cell lines HepT1, HepG2 and HUH6 as well as the human embryonic kidney cell line HEK293T were cultured under standard conditions, in Roswell Park Memorial Institute Medium (RPMI 1640) Medium (1 x), liquid - with GlutaMAX$^{TM}$ I containing 10 % (v/v) fetal calf serum (FCS) and 1 % Penicillin/Strepomycin at 37 °C in a 5 % $CO_2$ incubator. Every 2-3 days cells (80 % confluence) were split using Trypsin-EDTA-Solution (0.05 %). Mycoplasma contamination tests were performed every now and then and results have always been negative.

## 3.8 Plasmid Transfection

Plasmid transfection was performed using X-tremeGENE HP DNA Transfection Reagent; following the manufactures instructions applying a 3:1 (HEK293T) or 1:1 (HepT1, HepG2 and HUH6) ratio of microliter (µL) X-tremeGENE HP DNA Transfection Reagent to microgram (µg) of DNA. Reagent was warmed to room temperature (RT) and vortexed before use. 500 ng to 2 µg of DNA were incubated in serum-free medium. 0.5 µL to 6 µL of X-tremeGENE HP was added and incubated for 30 min at RT to allow complex formation. X-tremeGENE HP Reagent: DNA-complex was added drop-wise and incubated until the time point of interest.

## 3.9 NQO1-ARE reporter assay

5 x $10^5$ cells were seeded in 12-well plates the day before transfection, respectively. Cells were then transfected with 300 ng of the reporter plasmid pNQO1-ARE-Luc, 300 ng of expression constructs (pEGFP-N1, pEGFP-WT, pEGFP-L30P, pEGFP-R34P, pEGFP-R34G, or pEGFP-T80A), 300 ng of pFLAG-KEAP1, and 10 ng of the reference plasmid pRL-CMV using XtremeGENE HP transfection reagent described above. 48 h after transfection reporter gene activity was determined using the Dual-Glo Luciferase Reporter Assay System. Cell culture medium was removed and 100 µL of fresh medium was applied. 100 µL of *Dual-Glo™ Luciferase Reagent* equal to the volume of culture medium was added. Reaction was mixed and incubated for 10 min at RT to allow cell lysis. After incubation 180 µL of cell suspension was transferred into a white 96-well plate and measurement for firefly luminescence was performed using the GENios microplate reader. 100 µL of Dual-Glo™ Stop & Glo® Reagent was added to inhibit the Firefly-Luciferase and incubated for additional 10 min to measure *Renilla* luminescence using the GENios microplate reader. Firefly luciferase activity was normalized to *Renilla* luciferase activity.

## 3.10 NFE2L2 localization analyses

Cells were seeded onto 18 mm Ø cover slips the day before transfection. Cells were then transfected with 1 µg of the expression constructs (pEGFP-N1, pEGFP-WT, pEGFP-L30P, pEGFP-R34P, pEGFP-R34G, or pEGFP-T80A) using XtremeGENE HP transfection reagent as recommended. After 48 h, cells were washed with PBS and fixed with 3 % paraformaldehyde for 15 min. Nuclei were stained with Vectashield® containing 4, 6-diamidino-2-pheylindole (DAPI) and mounted onto glass slides. Images were acquired using the Zeiss Axiovert 135 Microscope.

## 3.11 Electroporation of hepatoblastoma cell lines

Cells were passaged one day before electroporation so that they were in their logarithmic growth phase on the day of electroporation. Prior to electroporation, cells were washed with PBS, counted, and resuspended in normal growth media to a cell density of $1 \times 10^7$ cells/ mL. 200 µL of cell suspension was gently mixed and transferred into electroporation cuvettes. SiRNA targeting UHRF1 (siUHRF1), siRNA targeting NFE2L2 (siNEFEL2) or appropriate non-targeting control siRNA (siGENOMEN Non-targeting siRNA #1, siNTC) were added to the cell suspension to a final concentration of 80 pmol. The cuvette was connected to the PowerPac Basic™ and cells subjected to an electric pulse of 350 V (HepT1, HUH6) or 250 V (HepG2) for 10 ms. Cells were allowed to recover briefly before placement in normal growth media. RNA, DNA and protein were isolated at time points of interest.

## 3.12 RNA Isolation

Total RNA was isolated from HEK293T, HUH6, HepT1 and HepG2 cells and tumor or normal liver tissue. Tumor and normal liver tissue were homogenized with 1,000 µL TriReagent and incubated for 5 min at RT. For cells, medium was discarded and cells washed with PBS. 1,000 µL TriReagent was added directly onto the cells. The Cell/TriReagent mix was transferred into Eppendorf tubes and incubated for 5 min at RT. After addition of 200 µL chloroform tissue and cell samples were vortexed for 15 sec and centrifuged for 15 min at 12,000 rpm (4 °C) for phase separation. The upper, aqueous phase was transferred into a new Eppendorf tube, mixed with 1 Vol. isopropanol and incubated for 10 min at RT. The incubated mixture was centrifuged for 15 min at 12,000 rpm (4 °C). The supernatant was discarded and the RNA pellet washed twice with 1.5 mL 70 % ice cold ethanol and centrifuged at 7500 rpm for an additional 15 min (4 °C). The pellet was air dried for 10-15 min at RT, dissolved in 20-50 µL DNase/RNase free water and incubated for 15 min at 55 °C. RNA concentration was measured using the NanoDrop 1000 instrument.

## 3.13 DNase Digestion for RNA cleanup

Sample volume of RNA was adjusted to a volume of 100 µL with RNase-free water. 350 µL RLT Buffer supplemented with β-mercaptoethanol was added to RNA and mixed. Total RNA was purified using the Qiagen RNeasy Mini Kit protocol with an additional DNase on column digestion step (RNase-Free DNase Set) and stored at -80 °C. RNA concentration was quantitatively measured using the NanoDrop 1000 instrument.

## 3.14 Reverse Transcription

500 ng to 2 µg of RNA was transcribed to cDNA using SuperScriptII RT reagents. RNA, 5 µL random hexamer primer and DNase/RNase free water (total volume 12 µL) were mixed and incubated at 70 °C for 10 min. Reaction mix containing 4 µL 5 x reaction buffer, 2 µL 0.1 M Dithiothreitol (DTT, Invitrogen) and 1 µL 10 mM dNTP mix, (total volume 7µL) was added to the RNA-Primer mix, incubated for 10 min at RT and for 2 min at 42 °C. 1 µL SuperScriptII (reverse transcriptase) was added and incubated for 1 h at 42 °C. Afterwards, samples were incubated at 70 °C for 10 min. 1 µL RNase H (1 U/ µL) was added to cleave remaining RNA and samples were incubated at 37 °C for 20 min. cDNA was stored at -20 °C.

## 3.15 Quantitative real time polymerase chain reaction (qRT-PCR)

A SYBR Green-based protocol, the Master cycler RealPlex2 and the software "realplex" were used for detecting mRNA abundance. For reaction iTaq-SYBR Green-Supermix, 500 nM forward primer, 500 nM reverse primer, DNase/RNase free water ($dH_20$) and cDNA corresponding to 40 µg RNA of sample (20 µL in total) were used. The following protocol was run at the Mastercycler personal:

| | | |
|---|---|---|
| Initial Denaturation | 2 min at 95 °C | |
| Denaturation | 15 sec at 95 °C | 40 cycles |
| Annealing | 15 sec at 55 °C | |
| Extension | 20 sec at 68 °C | |
| Melting curve | 15 sec at 60 °C | |
| | 20 min from 60 °C – 95 °C | |
| | 15 sec at 95 °C | |
| Hold | 4 °C | |

Primers, which were used for qRT-PCR are shown in **Table 3**. Melting curve analysis was performed to assess primer specificity. Data were normalized to the expression level of the TATA-Box-binding-Protein (*TBP*, housekeeping gene). For calculation of the relative mRNA expression level the ΔΔCT method [194] was used and expressed as fold change relative to the corresponding control sample.

Table 3: **List of qRT-PCR primers used in this study:**

| Gene | Primer fw 5´→3´ | Primer rev 5´→3´ | AL | AT | Loc |
|---|---|---|---|---|---|
| HHIP | TGTACATCATTCTTGGTGATGGG | AGCCGTAGCACTGAGCCTGT | 91 | 55 | Ex6/7 |
| IGFBP3 | GTCCAAGCGGGAGACAGAATAT | CCTGGGACTCAGCACATTGA | 91 | 55 | Ex2/3 |
| SFRP1 | CATGACGCCGCCCAAT | GATGGCCTCAGATTTCAACTCG | 91 | 55 | Ex1/2 |
| GAPDH | GGCACCGTCAAGGCTGAG | CCCACTTGATTTTGGAGGGAT | 91 | 55 | Ex4/5 |
| ACTB | CCTGAACCCCAAGGCCA | CACAGCCTGGATAGCAACGTAC | 91 | 55 | Ex3/4 |
| NFE2L2 | CGGTATGCAACAGGACATTGAG | GGCTTCTGGACTTGGAACCAT | 101 | 55 | Ex4/5 |
| NQO1 | GCTGCCATGTATGACAAAGGAC | CCGGTGGATCCCTTGCAGA | 101 | 55 | Ex4/5 |
| KEAP1 | ATTGGCTGTGTGGAGTTGCA | TGGCAGTGGGACAGGTTGA | 101 | 55 | Ex2/3 |
| TBP | GCCCGAAACGCCGAATAT | CCGTGGTTCGTGGCTCTCT | 72 | 55 | Ex4/5 |

Amplicon length in base pairs (AL), annealing temperature in °C (AT) and primer localization (Loc) , indicating the exons (Ex) covered by PCR assay.

## 3.16 Whole cell protein lysates for Western Blot analysis

Cells were seeded at a density of 1 x $10^6$ / 10 cm dish and cultured for 48 h, and then harvested. The medium was completely removed and cells were washed with 1 mL ice cold PBS. 200 µL of lysis-buffer, containing proteinase inhibitor cocktail, was added. Cell lysates were collected with a cell scraper and transferred into a reaction tube. The cell lysate was incubated on ice for 30 min and centrifuged at 13,000 rpm (4 °C) for 30 min. Supernatant was transferred in a new reaction tube and stored at -20 °C (long term storage -80 °C).

## 3.17 Cell fractions for Western Blot analysis

Nuclear protein extracts were prepared from transfected cells cultured for 48 h in 10 cm dishes. All nuclear extraction procedures were performed on ice with ice cold reagents. Cells were washed with phosphate-buffered saline (PBS) and harvested by scraping with 400 µL of lysis buffer and incubated for 25 min. Then, 25 µL of 20 % Igepal (Sigma) was added and vortexed for 15 sec. After centrifugation at 13,000 rpm for 1 min at 4 °C the supernatant, containing the cytoplasm, was collected (cell lysate). Nuclei pellets were resuspended in 75 µL of extraction buffer and incubated on ice for 15 min with occasional vortexing. Debris was pelleted by centrifugation at 13,000 rpm for 10

min at 4 °C. The supernatant was collected (= nuclear extract) and the protein concentration of cell lysates and nuclear extracts were determined using the Bradford Protein Assay Kit.

## 3.18 Determination of protein concentration

To determine the protein concentration the 1x Bradford Protein Assay solution was used. To establish a standard curve the bovine serum albumin (BSA) standard was diluted in concentrations of 1,200 µg/mL to 0 µg/mL. The standard dilutions as well as the undiluted samples and sample dilutions of 1:2 and 1:10 in PBS were transferred in a 96 well plate (duplicates). The final volume of the samples was 10 µL. 200 µL of the 1 X Bradford reagent (1:5 diluted) was pipetted to each well and the plate was incubated for 15 min at RT. After measuring absorbance at 595 nm, concentrations were calculated and volume of protein lysate needed for Western Blot analysis was determined.

## 3.19 Sodium dodecyl sulfate (SDS)-polyacrylamide-gel electrophoresis

SDS-Polyacrylamide gel electrophoresis was carried out using the commercially available NuPAGE electrophoresis system. 10-40 µg protein lysate diluted to a volume of 20 µL with PBS was mixed with 5 µL of 5 x SDS-sample buffer (see section 2.4), incubated at 99 °C for 10 min and centrifuged for 10 min at 13,000 rpm. Pre-stained protein ladder and protein samples were loaded onto 8-12 % gradient Tris-Glycine SDS gels and run in MOPS SDS-running buffer (see section: 2.4) at a constant voltage of 100 V for 60 min.

## 3.20 Transfer to membrane

After separation of proteins by SDS-PAGE and in order to make the proteins accessible to antibody detection, proteins were transferred using the X-Cell II Blot System onto a nitrocellulose membrane. The transfer was carried out at a voltage of 25 V for 1.5 h in transfer buffer (see section 2.4). Afterwards, membranes were placed into 5 % non-fat dry milk to block non-specific binding for at least 2 h at RT. Membranes were incubated overnight with the primary antibodies mouse anti-human UHRF1 (1:1,000 or rabbit anti-human ß-actin (1:2,000) at 4 °C. Before and after incubation with the corresponding secondary antibodies membranes were washed three times for 10 min with PBS containing 0.1 % Tween 20 (PBST). Incubation with secondary antibodies was performed at RT for 1 h using horseradish peroxidiase-conjugated goat anti-mouse or goat anti-rabbit immunoglobulin G secondary antibodies (1:2,000). For chemiluminescent detection of specific

protein bands, the ECL Plus Western detection kit was used. 1 mL of solutions A and 25 µL of solution B were mixed together, applied directly to the membranes, and incubated for 1 min to fully percolate the membranes. Signals were detected by autoradiography using high performance autoradiography films, Hyperfilm$^{TM}$MP.

## 3.21 DNA Extraction from cell culture and tissue

Genomic DNA was extracted by phenol/chloroform after proteinase K treatment. Therefore, 1000 µL STE Buffer (see section 2.4) and 50 µL Proteinase A were added to the cell pellet and placed at 55 °C overnight. 1 Vol. Phenol was added to the cells and mixed by inversion for 5 min. The mixture was centrifuged for 10 min at 8,000 rpm (4 °C). The upper phase was transferred into a new Eppendorf tube, 1 Vol. chloroform was added, again mixed by inversion for 5 min and centrifuged for 10 min at 8,000 rpm (4 °C). The upper aqueous phase, containing nucleic acids, was transferred to a new tube, and DNA precipitated by addition of 2.5 Vol. of 100 % ethanol. The threadlike precipitate was collected and transferred into a new tube. Precipitate was washed twice with 70 % ethanol and centrifuged at 12,000 rpm for 5 min. The resulting DNA pellet was dried, dissolved in 30-100 µL DNase/RNase free water and incubated for 10 min at 60 °C. DNA concentration was measured using the NanoDrop 1000 instrument.

## 3.22 DNA Extraction from human blood

Genomic DNA was extracted from 14 mL blood from a healthy control subjects using the Flexi gene DNA isolation kit according to the manufacturer's protocol. DNA concentration was measured using the NanoDrop 1000 instrument.

## 3.23 In vitro *de novo* methylation for positive control DNA

Complete methylation of all CpG dinucleotides was ensured by treatment of the genomic DNA with CpG methyltransferase (M. SssI) to produce a reference for complete DNA methylation.

10 µg DNA in DNase/RNase free water
1/10 Vol. NEB Buffer 2 (10x)
1/10 Vol. SAM (1:20)
40 U M.SssI (4 U/µl)

Components were added in the listed order, mixed gently and incubated for 4 h at 37 °C, followed by incubation for 20 min at 65 °C for inactivation of the enzyme. DNA was precipitated at -20 °C with 50 µL of 3 M sodium acetate and 750 mL 100 % ethanol, overnight. At the next day the DNA was centrifuged for 10 min at 13,000 rpm. The pellet was washed with 500 µL 70 % ethanol, centrifuged for 10 min at 13,000 rpm, and air dried for 5 - 10 min. The DNA pellet was resuspended in 20 µL of DNase/RNase free water and used immediately or stored at -20 °C.

## 3.24 Bisulfite conversion after DNA Extraction

DNA was used for bisulfite-mediated conversion of unmethylated cytosine by using the Epitec Bisulfite Kit as recommended by the manufacturer.

## 3.25 Methylation-specific polymerase chain reaction (MSP)

For methylation-specific polymerase chain reaction (MSP), bisulfite-treated DNA was amplified with primers specific for the methylated and unmethylated promoter region of the *HHIP*, *IGFBP3*, *SFRP1* or *ACTB* gene. Therefore, 500 nM reverse primer (methylated (M) or unmethylated (U)), 500 nM forward primer (methylated (M) or unmethylated (U)), 1 x Hot start Taq-Buffer, 2 mM dNTPs, 1.5 mM $MgCl_2$, Hot start Taq Polymerase (1 U), $dH_20$ and 1 µL bisulfite DNA were mixed. MSP primer design was accomplished using Methyl Primer Express using the following criteria: CpG percentage > 55 %; observed/expected CpG > 65 %; CpG length > 300 bp. Reaction was carried out at the Mastercycler personal using the following conditions:

| | | |
|---|---|---|
| Hot start | 4 min at 95 °C | |
| Denaturation | 30 sec at 95 °C | 38 cycles |
| Annealing | 30 sec at X °C | |
| Extension | 45 sec at 72 °C | |
| Final Extension | 10 min at 72 °C | |
| Hold | 4 °C | |

20 µL of MSP reaction were mixed with 6 x loading buffer and resolved on an 1.0 % - 1.5 % agarose gel containing ethidium bromide at 110 V. Bands were detected by ethidium bromide fluorescence and their size was estimated by comparison with a DNA size standard (100 bp ladder). Primer sequences and annealing temperatures for PCR are listed in **Table 4**.

Table 4: **List of MSP-primers:**

| Gene | | Primer fw 5´→3´ | Primer rev 5´→3´ | AL | AT | Loc |
|---|---|---|---|---|---|---|
| **HHIP** | **U** | **TTGTAGTAGTTGGGTAGTTTTGGAATTTTT** | **AAACCTTAAAACCAACCTCAAAA** | **144** | **53.5** | **+230** |
| | **M** | **AGTAGTCGGGTATGTTCGGAATTTTC** | **GAACCTTCGAAACCAACCTCG** | **143** | **53.5** | **+231** |
| **IGFBP3** | **U** | **TTGGGTGAGTTTTGAGTTGTATGTTTTT** | **AAACACACCAACCACTATATAAAAACCAAA** | **167** | **61** | **+180** |
| | **M** | **GCGAGTTTCGAGTTGTACGTTTTC** | **GCCGACCGCTATATAAAAACCG** | **167** | **61** | **+180** |
| **SFRP1** | **U** | **TTTTGTAGTTTTTGGAGTTAGTGTTGTGTG** | **CAATAACAACCCTCAACCTACAATCAA** | **145** | **58** | **-36** |
| | **M** | **TTTGTAGTTTTCGGAGTTAGTGTCGC** | **CGACCCTCGACCTACGATCG** | **138** | **58** | **-36** |
| **ACTB** | **U** | **GGGTTGAATTGGGTATTGTTTAGT** | **AAACAACTTTCAAAACAACACACAC** | **243** | **55** | **+195** |
| | **M** | **TCGAATCGGGTATTGTTTAGC** | **ACAACTTTCGAAACGACGC** | **243** | **55** | **+195** |

Methylated (M), unmethylated (U) primer set, amplicon length in base pairs (AL), annealing temperature in °C (AT), primer localization (Loc), (+) base pairs upstream and (-) and base pairs downstream of transcriptional start site.

## 3.26 Pyrosequencing

For pyrosequencing, the region of interest was amplified from 1 µL bisulfite treated DNA, using primer sets for *HHIP*, *IGFBP3*, *SFRP1* and *LINE1* (see, **Table 5**). PCR reactions containing 500 nM reverse primer, 500 nM forward primer, 1 x Hot start Taq-Buffer, 2 mM dNTPs, 1.5 mM $MgCl_{2,}$, Hot start Taq Polymerase (1U), DNase/RNase free water (total 20 µL) were run at the following temperatures at the Mastercycler personal:

| | | |
|---|---|---|
| Hot start | 4 min at 95 °C | |
| Denaturation | 20 sec at 95 °C | 40 cycles |
| Annealing | 20 sec at x °C | |
| Extension | 30 sec at 72 °C | |
| Final Extension | 5 min at 72 °C | |
| Hold | 4 °C | |

3 µL of PCR product were used for 0.8 % agarose gel electrophoresis to check for presence and size of the amplified product. The remaining 17 µL of PCR product were mixed with 4 µL streptavidin coated sepharose beads, 40 µL binding buffer and 19 µL DNase/RNase free water (total volume 80 µL). Prepared mixture was added to a 24-well PCR plate. PCR plate was constantly agitated for at least 5 min. While shaking the 24-well plate, sequencing primer was diluted to 0.3 µM in Annealing Buffer. 25 µL of the solution was added to each well of the PyroMark Q24 Plate. After 5 min the PCR product mix was applied to the PyroMark Q24 Vacuum Workstation including a denaturation step using

Denaturation Buffer. The resulting biotinylated single strand was added to the PyroMark Q24 Plate containing the corresponding sequencing primers HHIP_Seq, IGFBP3_Seq, SFRP1_Seq and LINE1. PyroMark Q24 Plate and PyroMark Gold Q24 Reagents were prepared as recommended by the manufacturer and subjected to pyrosequencing in the PyroMark Q24 system.

Table 5: **Primers used for pyrosequencing:**

| Gene | | Primer fw 5´→3´ | Primer rev 5´→3´ | AL | AT |
|---|---|---|---|---|---|
| **HHIP** | **PCR** | **GGGAGGAGAGAGGAGTTT** | **BIO-AACCAACCTCCAAAATACTAAACC** | **169** | **55** |
| | **Seq** | **TTTAGGATTGAGTTTTTGTTTTAAG** | | | |
| **IGFBP3** | **PCR** | **TGGTTTTTTGAGATTTAAATGTAAGTTAGA** | **BIO-ATCACCCCAATCACTCCTA** | **229** | **57.4** |
| | **Seq** | **TTGGGTTATTTAGGTTTTATATAG** | | | |
| **SFRP1** | **PCR** | **GGAGTTAGAGATTAGTTTGGTTAATATGG** | **BIO-AAAAACCTAAATCATACTTACAAACC** | **264** | **54.6** |
| | **Seq** | **GGTAAGAGGTTGTAATTTTAGTTAT** | | | |
| **LINE1** | **PCR** | **accession no. X58075** | **accession no. X58075** | **146** | **55** |
| | **Seq** | **accession no. X58075** | | | |

Forward primer (primer fw), 5'-biotinylated (BIO) reverse primer (primer rev) for PCR reaction (PCR), specific primer for pyrosequencing (Seq), amplicon lengths in base pairs (AL) as well as annealing temperatures in °C (AT).

## 3.27 Chromatin immunoprecipitation (ChIP)

2.5 x $10^7$ HUH6 cells were transfected with siUHRF1 or siNTC. After 48 h, the protein-DNA complexes were crosslinked with 1 % formaldehyde for 10 min at RT. The crosslinking reaction was quenched with 10 mL Glycine Stop-Fix Solution (ChIP-IT Kit) for 5 min and cells were washed twice for 5 min with ice cold 1 X PBS. Cell lysis, enzymatic digest and chromatin immunoprecipitation for tri-methylated H3K27 (H3K27me3), di-methylated H3K4 (H3K4me2), di-methylated H3K9 (H3Kme2), RNA polymerase II (RNA Pol II) and normal control IgG were performed according to the manufacturer`s protocol. 2 µg of antibody against H3K27me3, H3K4me2, H3K9me2, RNA Pol II and IgG, were mixed with sheared chromatin and magnetic beads and incubated for 4 h at 4 °C. Following the final eluation, crosslink reversal and proteinase K digestion of the immunoprecipitated chromatin was carried out. Chromatin samples were subjected to a DNA clean-up step using the QIAquick PCR Purification KIT. qRT-PCR was performed on purified DNA from each of the ChIP reactions using primer pairs (see, **Table 6**) for loci within promoter region of the *HHIP*, *IGFBP3*, the *SFRP1*, *GAPDH* and *ACTB* gene.

Table 6: **Primers used for chromatin immunoprecipitation:**

| Gene | Primer fw 5´→3´ | Primer rev 5´→3´ | AL | AT |
|---|---|---|---|---|
| **HHIP** | **TTCCCACCTCCTACGGCC** | **TCCTCTCTCCTCCCCGCTT** | **101** | **55** |
| **IGFBP3** | **GCTCCCTGAGACCCAAATGTAA** | **GCTCGGCATTCGTGTGTACC** | **101** | **55** |
| **SFRP1** | **ACGCCGTGATCCATTCCC** | **CGGCTCAACACCCCTTAAAAA** | **101** | **55** |
| **GAPDH** | **GAGAGAGCCGCTGGTGCAC** | **GAGGTTTCTGCACGGAAGGTC** | **101** | **55** |
| **ACTB** | **GCCAACGCCAAAACTCTCC** | **CAGTGCAGCATTTTTTTACCCC** | **101** | **55** |

Forward primer (primer fw), reverse primer (primer rev), amplicon length in base pairs (AL) and annealing temperature in °C (AT).

## 3.28 Cell Viability Assay

To asses cell proliferation, a cell viability assay was performed. Directly after electroporation, cells were seeded at a density of 5000 cells per well in a 96 well format (NUNC) in 100 µL RPMI medium. 10 µL of the MTT labeling agent (5mg/mL in PBS) was added to each well and incubated at 37 °C for 4 h. Media-containing wells without cells were used for background estimation. For cell lysis, 100 µL of the SDS-HCl solution (10 % SDS / 0.01M HCl) was added to each well and mix thoroughly using the pipette. The plate was incubated over night at 37 °C. The absorbance of the colored solution was quantified on the GENios reader by measuring at a wavelength of 595 nm.

## 3.29 Statistical analyses

Data were expressed as means + standard deviation (SD) or standard error of the mean (SEM) and statistically subjected to Student's unpaired *t*-test and Spearman rank correlation test. Kaplan-Meier estimates of overall survival time in the various groups were compared using the log-rank Mantel-Cox test. A level of $P<0.05$ was considered to be significant, $P < 0.01$ highly significant. Functional annotation of mutated genes was performed using the DAVID Bioinformatics Resources v6.7 (National Cancer Institute, Frederick, MD) by computing gene-ontology statistics against the whole human genome database.

# 4 Results

## 4.1 Genetic investigation

### 4.1.1 Hepatoblastoma harbors only few somatic mutations

To better understand the genetic basis of childhood liver cancer, our group has performed whole exome sequencing of 15 hepatoblastoma and three transitional liver cell tumor (TLCT) samples, along with corresponding normal liver tissues, in cooperation with PD Dr. Tim Strom of the Institute of Human Genetics of the Technical University of Munich [1]. Collectively, a total of 125 somatic mutations were identified (Figure. 5). However, the over-all frequency mutation rate in hepatoblastoma was low, with 2.9 variants per tumor genome (range 1 to 7), while in TLCTs, the mean sequence variation rate was 27.3 (range 11 to 48) per tumor genome. Recurrent mutations within the beta-catenin (CTNNB1) gene were found in about 80 % of the sequenced samples, a frequency which has also been described earlier [58]. Besides the CTNNB1 mutations, we identified missense mutations in the nuclear factor (erythroid-derived 2)-like 2 (NFE2L2) gene as another recurrent event, which was affected in two hepatoblastoma cases (**Figure 5**).

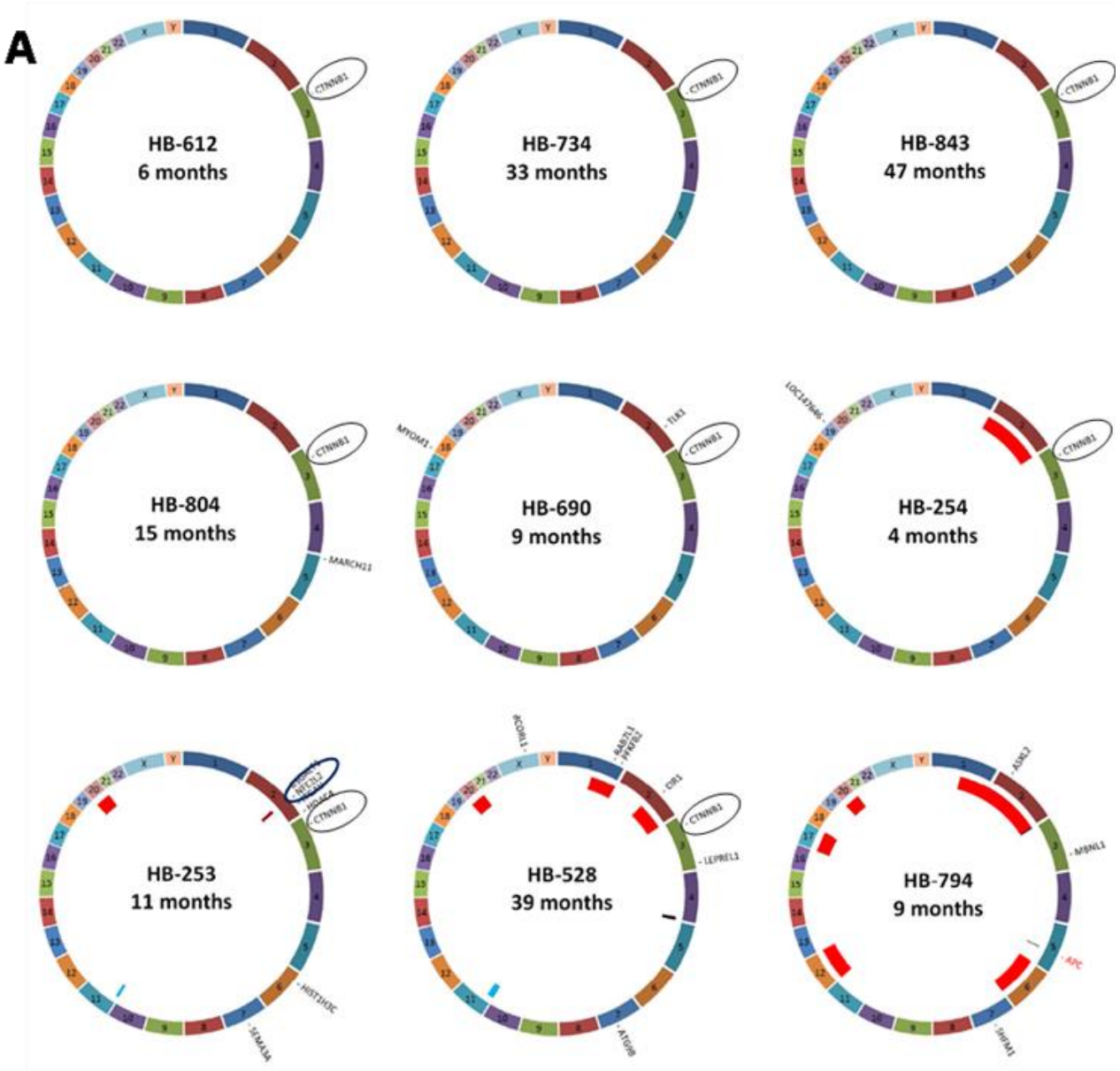
A
HB-612
6 months
CTNNB1
HB-734
33 months
CTNNB1
HB-843
47 months
CTNNB1
HB-804
15 months
CTNNB1
MARCH11
HB-690
9 months
MYOM1
TLK1
CTNNB1
HB-254
4 months
LOC147646
CTNNB1
HB-253
11 months
CTNNB1
HIST1H3C
SEMA3A
HB-528
39 months
ACOXL
BARD1
PAFAH1B2
CIB1
CTNNB1
LEPREL1
ATG5B
HB-794
9 months
ASXL2
MBNL1
APC
SMYM1

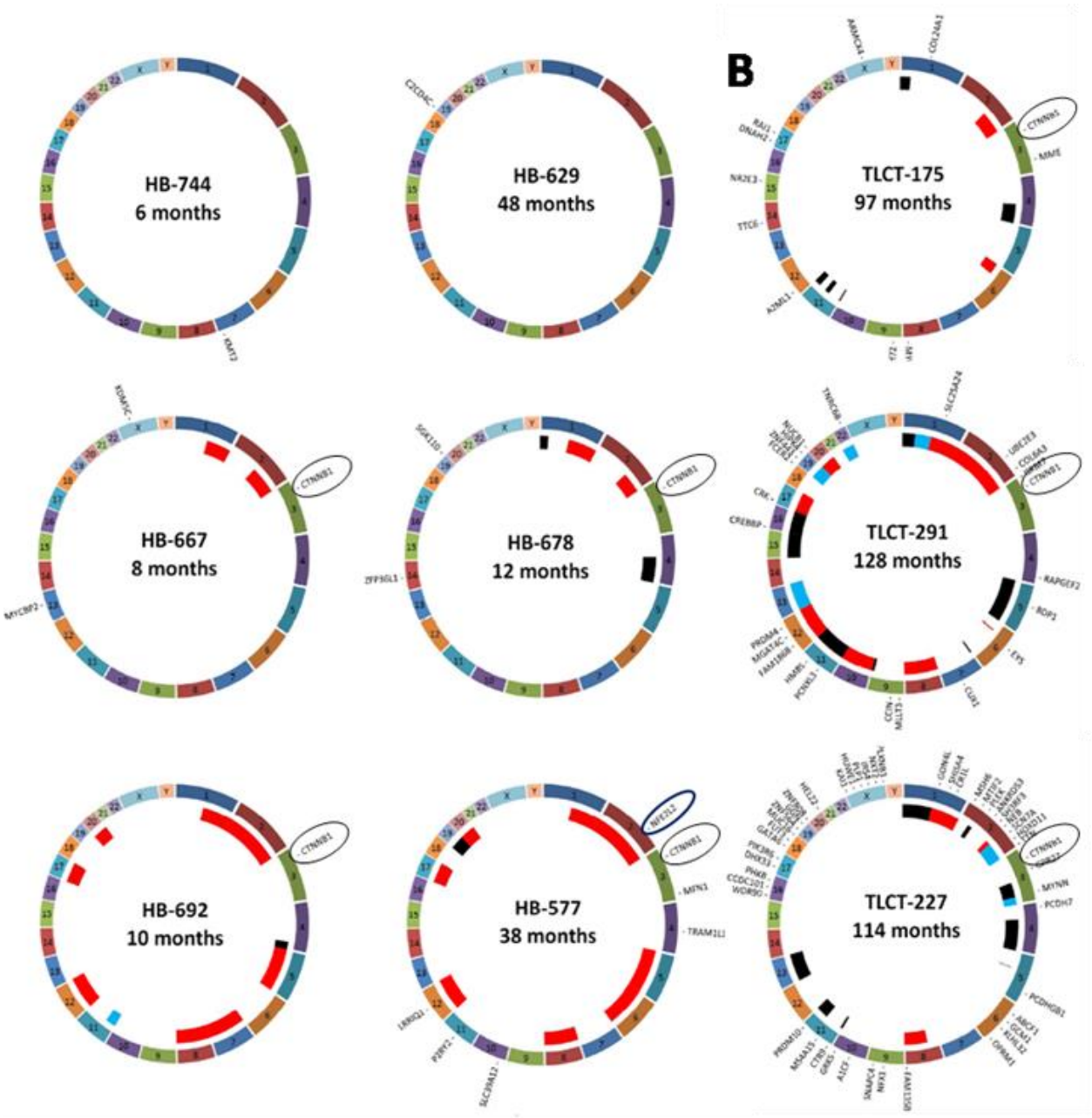


Figure 5: **Mutations and copy number variations in pediatric liver tumors.** Ring plots of **(A)** hepatoblastoma and **(B)** TLCT cases with chromosomes arranged end to end in the outer-most ring and mutated genes depicted outside of each diagram (recurrent mutations are highlighted through circles, the known germ line *APC* mutation in hepatoblastoma-794 in red font). The inside ring shows somatic copy number gains (red), losses (black), and copy-neutral allelic imbalances (blue). Data from Eichenmüller et al. 2014 [190].

### 4.1.2 Gene regulation is frequently impeded in childhood liver cancer

In order to identify functional pathways that are frequently hit by mutation in childhood liver cancer, we performed functional annotation of mutated genes using the Database for Annotation, Visualization and Integrated Discovery (DAVID). The main biological processes, which were associated with the 30 different detected mutated genes identified in our hepatoblastoma samples were transcription (30 % of mutated genes), chromatin organization (20 %), chromosome organization (20 %) as well as chromatin modification (16.6 %), (**Table 7**). Accordingly, the top scoring cellular component with 13.3 % was the nucleoplasm (**Table 8**).

The most prominent candidate genes which were found to be mutated in hepatoblastoma were CTNNB1, NFE2L2, histone H3.1 (HIST1H3C), the histone deacetylase 4 (HDAC4), the lysine-specific demethylase 5C (KDM5C) and the lysine-specific methyltransferase 2C (KMT2C). Moreover, two corepressors interacting with histone deacetylases, the CBF1 Interacting Co-repressor (CIR1) and the BCL6 Co-repressor-Like 1 (BCORL1) and one co-repressor binding to the polycomb repressive complex 2 (PRC2), ASXL2 (additional sex combs like transcriptional regulator 2) were identified. Additionally, the E3 ubiquitin protein ligase (MYCBP2) was detected. Interestingly, most of these genes code for epigenetic modifiers, playing an important role in the regulation of different epigenetic processes. HDAC4, KDM5C and KMT2C for instance are directly responsible for the deacetylation and (de)methylation of histones, respectively, while CIR1 and BCORL1 indirectly regulate the deacetylation of histones. However, ASXL2 is involved in the regulation and recruitment of the PRC2 and trithorax-group (trxG) activator complex and thereby indirectly regulates in histone methylation. Hence, our findings support the assumption that not only genetic changes, but also misregulation of epigenetic processes, through different mechanisms, contribute to the development of hepatoblastoma.

Table 7: **Functional annotation of mutated genes in hepatoblastomas for relevant biological processes:**

| GO-ID | Biological Processes | Count | % | P-value | Genes |
|---|---|---|---|---|---|
| GO:0006350 | transcription | 9 | 30.0 | 3,80E-02 | ASXL2, HDAC4, CIR1, BCORL1, NFE2L2, KMT2C, KDM5CCTNNB1, MCYBP2 |
| GO:0006325 | chromatin organization | 6 | 20.0 | 6,70E-04 | HDAC4, BCORL1, HIST1H3C, TLK1, KMT2C, KDM5C |
| GO:0051276 | chromosome organization | 6 | 20.0 | 2,00E-03 | HDAC4, BCORL1, HIST1H3C, TLK1, KMT2C, KDM5C |
| GO:0016568 | chromatin modification | 5 | 16.7 | 1,70E-03 | HDAC4, BCORL1, TLK1, KMT2C, KDM5C |
| GO:0045596 | negative regulation of cell differentiation | 4 | 13.3 | 8,00E-03 | HDAC4, CIR1, ITGAV, CTNNB1 |
| GO:0032989 | cellular component morphogenesis | 4 | 13.3 | 4,00E-02 | MFN1, SEMA3A, CTNNB1, MCYBP2 |
| GO:0010558 | negative regulation of macromolecule biosynthetic process | 4 | 13.3 | 8,60E-02 | HDAC4, CIR1, ITGAV, CTNNB1 |
| GO:0033554 | cellular response to stress | 4 | 13.3 | 9,30E-02 | ATG9B, SHFM1, TLK1, NFE2L2 |
| GO:0009890 | negative regulation of biosynthetic process | 4 | 13.3 | 9,60E-02 | HDAC4, CIR1, ITGAV, CTNNB1 |
| GO:0033043 | regulation of organelle organization | 3 | 10.0 | 6,50E-02 | TLK1, CTNNB1, MCYBP2 |
| GO:0000904 | cell morphogenesis involved in differentiation | 3 | 10.0 | 7,90E-02 | SEMA3A, CTNNB1, MCYBP2 |
| GO:0001568 | blood vessel development | 3 | 10.0 | 8,00E-02 | ZFP36L1, ITGAV, CTNNB1 |
| GO:0001944 | vasculare development | 3 | 10.0 | 8,30E-02 | ZFP36L1, ITGAV, CTNNB1 |
| GO:0032990 | cell part morphogenesis | 3 | 10.0 | 8,60E-02 | MFN1, SEMA3A, MCYBP2 |
| GO:0045445 | myoblast differentiation | 2 | 6.7 | 3,60E-02 | MBNL1, CTNNB1 |
| GO:0010906 | regulation of glucose metabolic process | 2 | 6.7 | 6,50E-02 | HDAC4, PFKFB2 |
| GO:0010675 | regulation of cellular carbohydrate process | 2 | 6.7 | 7,10E-02 | HDAC4, PFKFB2 |
| GO:0006109 | regulation of carbohydrate metabolic process | 2 | 6.7 | 7,20E-02 | HDAC4, PFKFB2 |

Mutated genes were sorted by their putative biological function using DAVID. Only groups with a frequency of > 5 % of all genes are presented.

Table 8: **Functional annotation of mutated genes in hepatoblastomas for relevant cellular components:**

| GO-ID | Cellular Component | Count | % | P-value | Genes |
|---|---|---|---|---|---|
| GO:0044451 | nucleoplasm part | 4 | 13.3 | 5,40E-02 | HDAC4, CIR1, SHFM1, CTNNB1, |
| GO:0030017 | sacromere | 3 | 10.0 | 1,00E-02 | HDAC4, MYOM1, CTNNB1 |
| GO:0030016 | myofibril | 3 | 10.0 | 1,30E-02 | HDAC4, MYOM1, CTNNB1 |
| GO:0044449 | contractile fiber part | 3 | 10.0 | 1,30E-02 | HDAC4, MYOM1, CTNNB1 |
| GO:0043292 | contractile fiber | 3 | 10.0 | 1,50E-02 | HDAC4, MYOM1, CTNNB1 |
| GO:0043005 | neuron projection | 3 | 10.0 | 9,90E-02 | SEMA3A, CTNNB1, MCYBP2 |
| GO:0000118 | histone deacetylase complex | 2 | 6.7 | 6,20E-02 | HDAC4, CIR1 |

Mutated genes were sorted by their putative biological function using DAVID. Only groups with a frequency of > 5 % of all genes are presented.

By examining the TLCT candidate genes using DAVID, we detected transcription and its regulation being the main biological processes impaired by mutations (**Table 9**). The top-scoring cellular component in TLCTs was the nuclear lumen (14.3 %) followed by the nucleoplasm (10 %), (**Table 10**). Noteworthy, mutated genes code for the co-repressor GON4L, two co-activators (PRIC285, CCDC101), another E3 ubiquitin protein ligase (HUWE1), as well as several transcription factors (MYC, GATA6, HOXD11, PRDM10, NFX1). Hence, the hepatoblastoma and TLCT data suggest that deregulation of the transcription regulatory machinery is an important step in liver cancer development.

Table 9: **Functional annotation of mutated genes in TLCTs for biological processes:**

| GO-ID | Biological Processes | Count | % | P-value | Genes |
|---|---|---|---|---|---|
| GO:0045449 | regulation of transcription | 20 | 28.6 | 3,30E-03 | ZNF564, ZNF808, BDP1, CREBBP, GONAL, NR2E3, CTNNB1, HOXD11, GCM1, PRDM4, GATA6, PRDM10, ZNF443, PRIC285, CUX1, CRK, MYC, MYNN, MLLT3, NFX1 |
| GO:0006350 | transcription | 18 | 25.7 | 2,00E-03 | ZNF564, ZNF808, BDP1, CREBBP, NR2E3, CTNNB1, HOXD11, GCM1, PRDM4, GATA6, PRDM10, ZNF443, PRIC285, CUX1, MYC, MYNN, MLLT3, NFX1 |
| GO:0006355 | regulation of transcription, DNA-dependent | 15 | 21.4 | 7,00E-03 | ZNF564, ZNF808, CREBBP, GON4L, NR2E3, HOXD11, CTNNB1, GCM1, GATA6, ZNF443, CUX1, CRK, MYC, NFX1, MLLT3 |
| GO:0051252 | regulation of RNA metabolic process | 15 | 21.4 | 8,5 0E-03 | ZNF564, ZNF808, CREBBP, GON4L, NR2E3, HOXD11, CTNNB1, GCM1, GATA6, ZNF443, CUX1, CRK, MYC, NFX1, MLLT3 |
| GO:0007155 | cell adhesion | 8 | 11.4 | 1,90E-02 | PCDHGB1, PLEK, KAL1, COL6A3, PCDH7, COL24A1, CTNNB1, MUC16 |
| GO:0022610 | biological adhesion | 8 | 11.4 | 1,90E-02 | PCDHGB1, PLEK, KAL1, COL6A3, PCDH7, COL24A1, CTNNB1, MUC16 |
| GO:0006357 | regulation of transcription from RNA polymerase II promoter | 8 | 11.4 | 2,30E-02 | GATA6, CREBBP, NR2E3, CUX1, CRK, MYC, CTNNB1, NFX1 |
| GO:0045934 | negative regulation of nucleobase, nucleoside, nucleotide and nucleic acid metabolic process | 6 | 8.6 | 4,90E-02 | MSH6, GRM7, NR2E2, CUX1, CTNNB1, NFX1 |
| GO:0051172 | negative regulation of nitrogen compound metabolic process | 6 | 8.6 | 5,20E-02 | MSH6, GRM7, NR2E2, CUX1, CTNNB1, NFX1 |
| GO:0031327 | negative regulation of cellular biosynthetic process | 6 | 8.6 | 6,80E-02 | PLEK, GRM7, NR2E2, CUX1, CTNNB1, NFX1 |
| GO:0009890 | negative regulation of biosynthetic process | 6 | 8.6 | 7,30E-02 | PLEK, GRM7, NR2E2, CUX1, CTNNB1, NFX1 |
| GO:0006351 | transcription, DNA-dependent | 5 | 7.1 | 2,70E-02 | PRDM4, NR2E3, MYNN, MYC, NFX1 |
| GO:0032774 | RNA biosynthetic process | 5 | 7.1 | 2,80E-02 | PRDM4, NR2E3, MYNN, MYC, NFX1 |
| GO:0045944 | positive regulation of transcription from RNA polymerase II promoter | 5 | 7.1 | 5,70E-02 | GATA6, CREBBP, NR2E3, MYC, CTNNB1 |

Mutated genes were sorted by their putative biological function using DAVID. Only groups with a frequency of > 5 % of all genes are presented.

Table 10: **Functional annotation of mutated genes in TLCTs for cellular components:**

| GO-ID | Cellular Component | Count | % | P-value | Genes |
|---|---|---|---|---|---|
| GO:0031981 | nuclear lumen | 10 | 14.3 | 7,90E-02 | GCM1, HUWE1, GATA6, CREBBP, DHX33, NR2E3, MYC, GGN, CTNNB1, CTR9 |
| GO:0044451 | nucleoplasm part | 7 | 10.0 | 1,50E-02 | GCM1, GATA6, CREBBP, NR2E3, MYC, CTNNB1, CTR9 |
| GO:0005667 | transcription factor complex | 5 | 7.1 | 7,30E-03 | GCM1, GATA6, CREBBP, NR2E3, CTNNB1 |
| GO:0005694 | chromosome | 5 | 7.1 | 8,80E-02 | MSH6, A1CF, HMBS, CREBBP, TTN |

Mutated genes were sorted by their putative biological function using DAVID. Only groups with a frequency of > 5 % of all genes are presented.

### 4.1.3 Activation of Wnt signaling is the key event in liver tumorigenesis

Sequencing tumor samples revealed that mutations within the CTNNB1 gene were the main recurrent mutations [1], which has also been described earlier [58]. Based on this finding, we further investigated additional hepatoblastoma samples, one TLCT and four hepatoblastoma cell lines and reanalyzed the three TLCTs and the 15 hepatoblastoma samples out of the sequencing cohort using Sanger sequencing, in order to determine the status of the *CTNNB1* gene. For CTNNB1 we detected 29 out of 43 hepatoblastoma samples to be mutated within the CTNNB1 gene, including the sequenced samples (**Figure 6**). All of the four hepatoblastoma cell lines showed mutated CTNNB1 (**Figure 6**). We also detected a mutation of CTNNB1 in the TLCT sample, which was not analyzed earlier, and confirmed the mutations in the three TLCTs, already detected via whole exome-sequencing (**Figure 6**). Additionally, we confirmed the inherited c.3809_3810insC frame-shift mutation in the APC gene in the one hepatoblastoma sample which was already known from [1] (**Figure 6**). APC mutations are described to increased CTNNB1 activity and have also been detected in some hepatoblastomas [68]. Moreover, an increased risk for hepatoblastoma is associated with Familial adenomatous polyposis (FAP) which is characterized by defects in the APC gene [195]. These data clearly indicate that activation of the WNT pathway is the key driver of tumorigenesis in the liver. However, since there are hepatoblastoma samples that do not show mutations in any of the WNT-associated genes (**Figure 6**), other molecular mechanism must exist. Since, it has been shown that epigenetic deregulation has an impact on activated WNT signaling, epigenetic changes within the WNT pathway may also be of great relevance in hepatoblastoma development.

### 4.1.4 Recurrent *NFE2L2* mutations in hepatoblastoma

Besides the CTNNB1 mutations, missense mutations in the NFE2L2 gene was another recurrent event detected using the whole-exome sequencing technology [1]. In this study, we therefore performed

targeted sequencing of our validation cohort (43 hepatoblastoma cases, four TLCT tumors and four hepatoblastoma cell lines) for NFE2L2 mutations using conventional Sanger sequencing, also including the sequenced hepatoblastoma samples (**Figure 6**). In addition to the two already detected NFE2L2 mutations we identified missense mutations in two other hepatoblastoma cases and the hepatoblastoma cell line HepT1 cell line (**Figure 6**), altogether in 9.8 % of all cases.

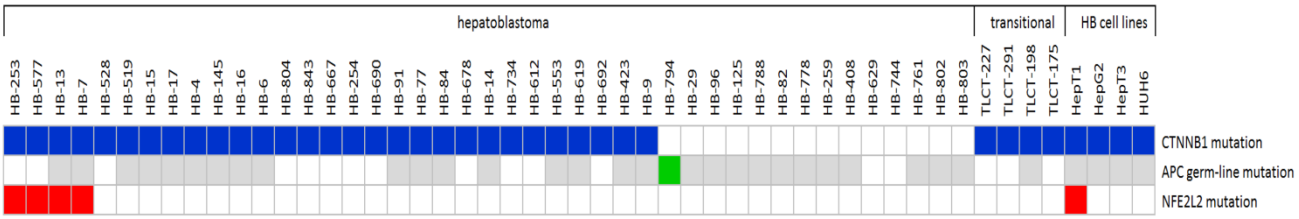


Figure 6: **Sanger sequencing of pediatric liver tumors**. A cohort of 43 hepatoblastoma samples (HB), four TLCT tumors and four hepatoblastoma cell lines was investigated for genetic alterations in the candidate genes *CTNNB1, NFE2L2* and *APC* by Sanger sequencing. Blue quarters represent tumors carrying missense mutation within the *CTNNB1* gene; green quarters indicate mutations within the *APC* gene and red quarters represent tumors carrying missense mutations within *NFE2L2*. Grey quarters show the tumor samples not analyzed for *APC* germ line mutations.

Interestingly, all mutations lead to amino acid substitutions at the N-terminus of the NFE2L2 protein, with missense mutations at base position 89, 100, 101, and two cases at 138 (**Figure 7**).

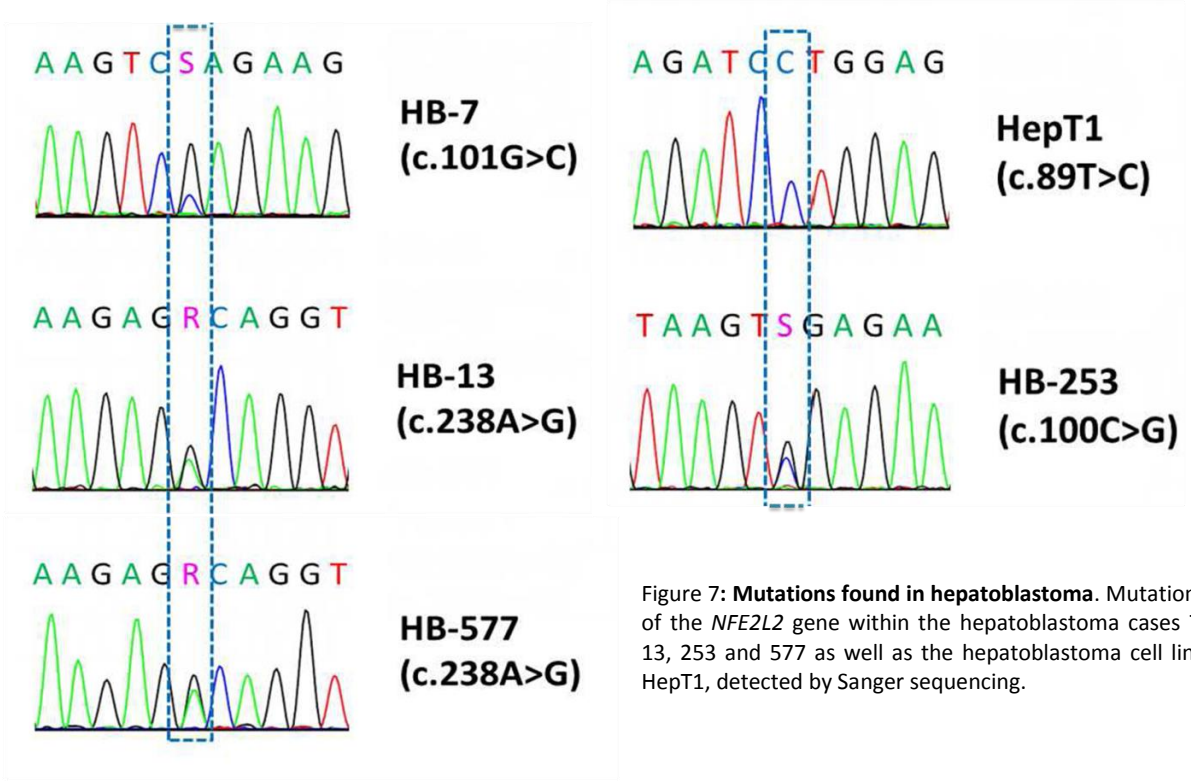


Figure 7**: Mutations found in hepatoblastoma**. Mutations of the *NFE2L2* gene within the hepatoblastoma cases 7, 13, 253 and 577 as well as the hepatoblastoma cell line HepT1, detected by Sanger sequencing.

### 4.1.5 Mutations impede KEAP1-mediated degradation of NFE2L2

NFE2L2 is known to not only play a role in the cellular defense against oxidative stress, but also in tumorigenesis, by the induction of anti-apoptotic and detoxification processes [196]. The five detected NFE2L2 mutations were found in cases harboring CTNNB1 mutations (72.5 % of all cases), a coincidence already described for adult [197, 198] and pediatric HCC [76]. Interestingly, the five NFE2L2 mutations found in hepatoblastoma are located either in or adjacent to the DLG and ETGE motifs (**Figure 8**), which have been described to be essential for binding of the KEAP1/CUL3 complex that mediates ubiquitination and proteasomal degradation of NFE2L2 [193].

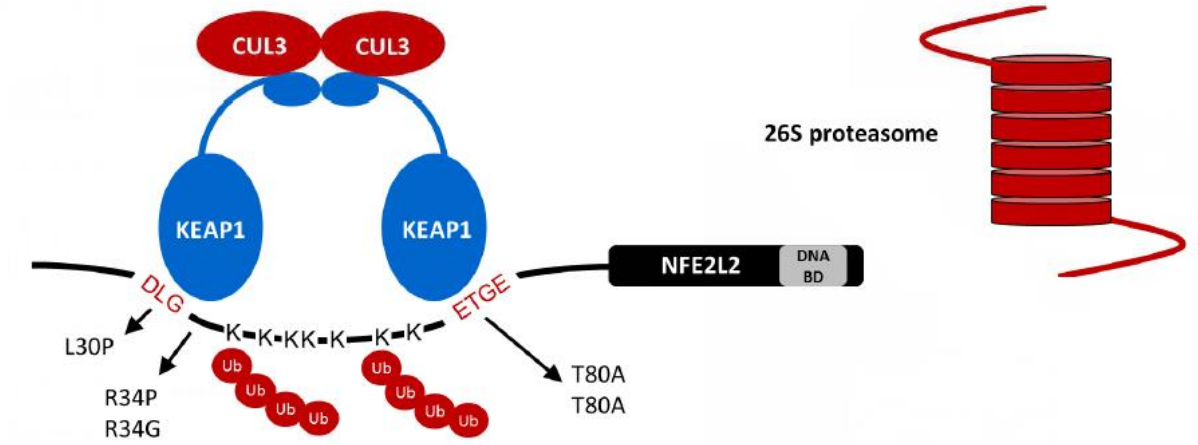


Figure 8: **Mutational variations of *NFE2L2* in hepatoblastoma.** Schematic illustration of the NFE2L2 degradation complex, consisting out of two KEAP1 and two CUL3 subunits. The complex binds to the DLG and ETGE motifs of the NFE2L2 protein thereby inducing ubiquitination of lysine residues (K) and proteasomal degradation. The location of *NFE2L2* mutations are indicated by arrows.

In order to determine whether the identified NFE2L2 mutations lead to NFE2L2 transcriptional activity that is insensitive to KEAP1-mediated degradation, we fused the wild-type and the four mutated forms of NFE2L2 (L30P, R34P, R34G, and T80A) to GFP. GFP constructs were ectopically expressed in the presence or absence of KEAP1 in HEK293T cells known to exhibit low basal levels of NFE2L2-dependent transactivation [199] and (**Figure 9**), along with a firefly luciferase reporter plasmid containing NFE2L2-responsive ARE binding sites and pRL-CMV as a control.

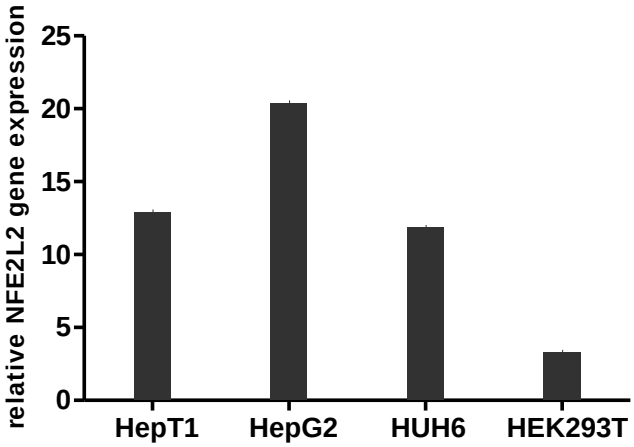


Figure 9: **Relative gene expression of *NFE2L2* in HepT1, HepG2, HUH6 and HEK293T.** The mRNA abundance of NFE2L2 was revealed using qRT-PCR.

Using the dual-luciferase assay, we were able to monitor the activity of our NFE2L2 mutants. We found that both wild-type and mutant NFE2L2 strongly increased reporter activity, which was more pronounced for the mutant forms (**Figure 10A**). Co-transfection of KEAP1 resulted in a significant decrease in reporter activity in wild-type NFE2L2 and R34P transfected cells, whereas in cells transfected with the mutated forms L30P, R34G, and T80A, this reduction was completely prevented. In line with this, the latter three accumulated exclusively in the nucleus, which is indicative for transcriptional activity, while the R34P mutant was found in the cytoplasm and the nucleus, comparable to wild-type NFE2L2 (**Figure 10A**). Strikingly, the same set of experiments performed in the hepatoblastoma cell line HUH6, showed identical results (**Figure 10B**). Measurements in HepG2 cells, which already have a high relative gene expression NFE2L2 (Figure 9), followed the same trend, but without reaching statistical significance (**Figure 10C**). These data clearly demonstrate that NFE2L2 mutations found in hepatoblastoma result in a high NFE2L2 transcriptional activity by interfering with KEAP1-mediated degradation.

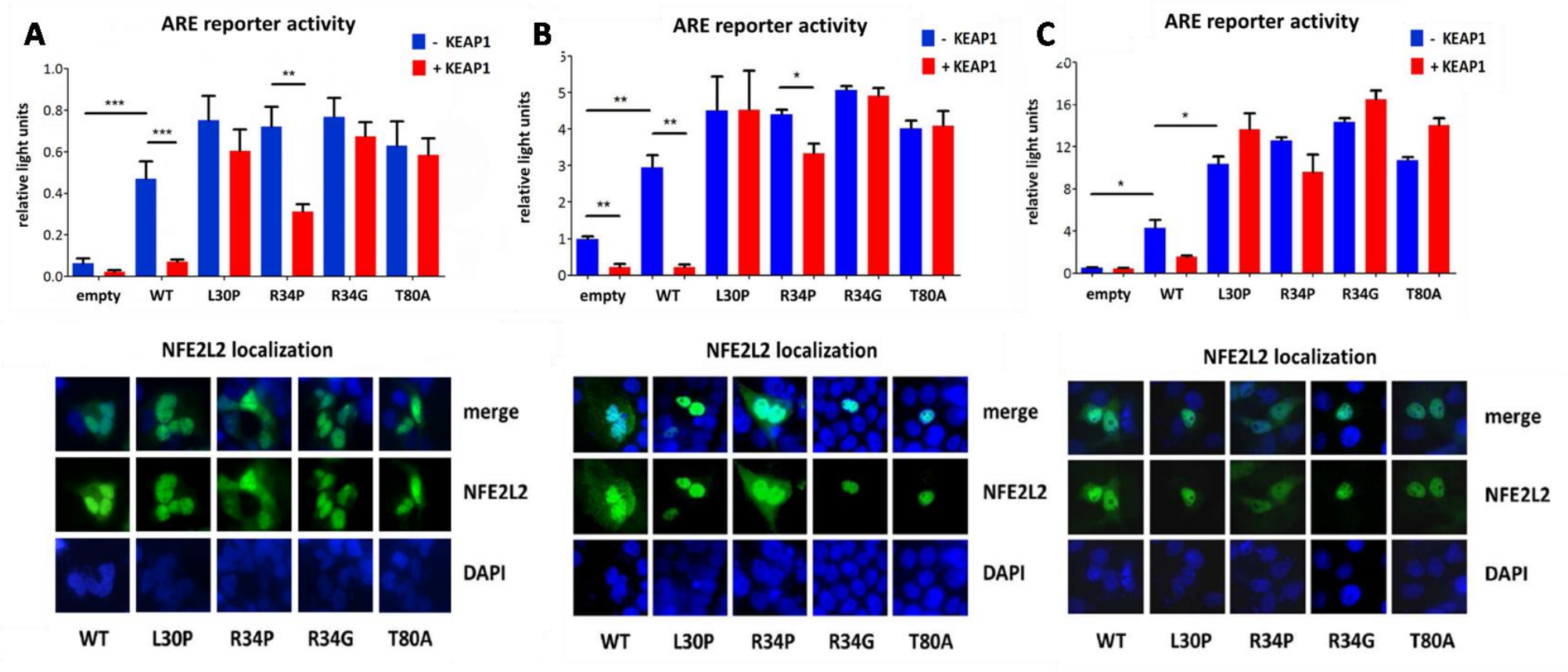


Figure 10**: Functional relevance of *NFE2L2* in hepatoblastoma.** Reporter assay experiments of HEK293T **(A)**, HUH6 **(B)** and HepG2 **(C)** cells transiently transfected with the pEGFP vector (empty), pEGFP containing wild-type (WT) or the four mutated forms of *NFE2L2* in the presence or absence of *KEAP1*. The activity of the NFE2L2-responsive ARE luciferase reporter was measured after 48 h and normalized to the activity of *Renilla* luciferase. Mean ± SEM of our reporter assay experiments in duplicates are shown. Exclusive nuclear accumulation of the GFP-tagged mutant NFE2L2 proteins L30P, R34G, and T80A (green) after transfection into cells, counterstained with DAPI (blue). The R34P mutant as well as the wild-type NFE2L2 were located both in the cytoplasm and the nucleus.

### 4.1.6 Knockdown of the *NFE2L2* downregulates *NQO1* and inhibits proliferation

To better understand the role of NFE2L2 in proliferation of hepatoblastoma, we employed transient siRNA knockdown of NFE2L2 in hepatoblastoma cells (HepT1, HepG2 and HUH6) to specifically modulate this pathway. As shown in **Figure 11A-C**, significant knockdown (> 80 %) of NFE2L2 mRNA was achieved in all three hepatoblastoma cell lines, as measured by qRT-PCR. To ensure that knockdown of NFE2L2 resulted in a significant modulation of NFE2L2 regulated target genes we analyzed the transcript level of the classical ARE-regulated NFE2L2 target gene NQO1, 48 h post transfection by qRT-PCR. NFE2L2 knockdown resulted in a significant decrease in the basal expression of NQO1 (**Figure 11A-C**) showing that basal activity of NFE2L2 is required for the expression of this gene. To assess whether reduced levels of NFE2L2 would impact cell proliferation, we generated cell growth curves over a time course of 96 h for NFE2L2 diminished and control cells using the MTT proliferation assay. Knockdown of NFE2L2 resulted in decreased cell proliferation, being significant for HepG2 (**Figure 11B**) and partly for HUH6 (**Figure 11C**). NFE2L2 suppressed HepT1 cells led to a slightly impaired growth rate compared to control transfected cell lines (**Figure 11A**).

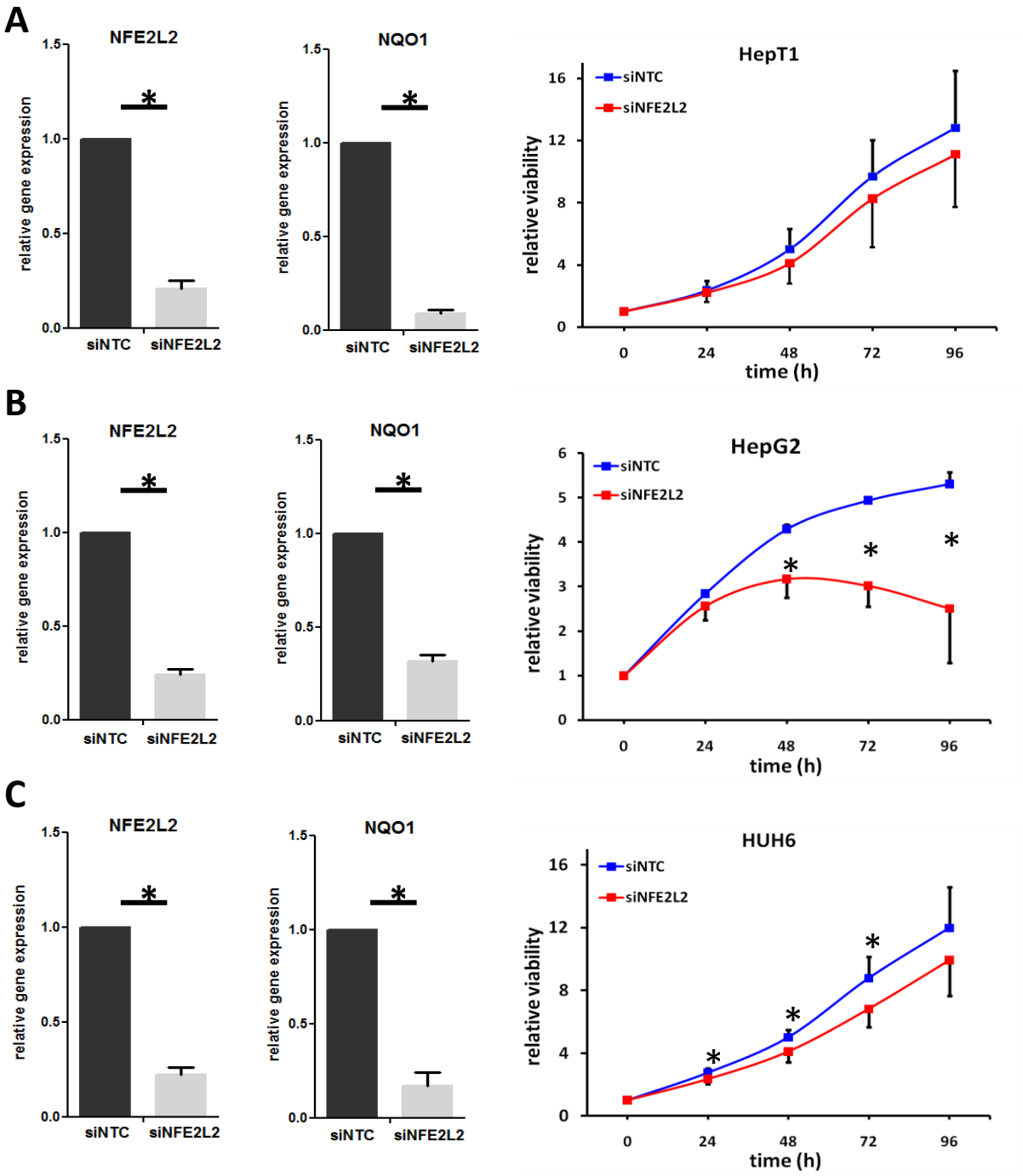


Figure 11: **Knockdown of *NFE2L2* decreases target gene expression and inhibits cell proliferation**. HepT1 **(A)**, HepG2 **(B)** and HUH6 **(C)** were transfected using siRNA against *NFE2L2* or non-targeting siRNA. 48 h after transfection, cells were harvested. *NFE2L2* and *NQO1* mRNA levels were quantified by quantitative real-time PCR analysis. mRNA abundance of siNTC was set to 1. The values illustrate gene expression in relation to the house-keeping gene TATA-Box-binding-Protein *(TBP).* The viability of HepT1 **(A)**, HepG2 **(B)** and HUH6 **(C)** cells after transfection with siRNA against *NFE2L2* or non-targeting siRNA was assessed at the time points indicated using MTT assays and optical density (OD) measurements. The values given represent the mean ratio of control siRNA transfected vs. siRNA against *NFE2L2* transfected cells from triplicate measurements ±SD. *P < 0.05 vs. control siRNA, (unpaired Student's *t*-test).

### 4.1.7 Upregulation of the NFE2L2 target gene *NQO1* is associated with poor outcome

In order to see whether transcriptional deregulation of genes involved in NFE2L2 signaling is a common phenomenon in pediatric liver cancers, we determined the mRNA abundance of NFE2L2, KEAP1, and the NFE2L2 prototypical target gene NQO1 in our cohort of 43 hepatoblastomas and four TLCT primary tumors. NQO1 catalyzes the reduction and detoxification of highly reactive quinones that can cause redox cycling and oxidative stress [200]. We found a highly significant downregulation of NFE2L2 and a striking upregulation of NQO1 in the tumor tissues compared to normal livers. In contrast, KEAP1 expression was unchanged between both tissues (**Figure 12A-C**). Interestingly, the three tumors with the highest NQO1 expression harbored NFE2L2 mutations. In order to identify the reason for the high NQO1 expression of two other tumors that lack NFE2L2 mutation, we performed Sanger sequencing of the genes KEAP1 and CUL3, which have been described to be alternatively mutated in NFE2L2-activated cancers [199, 201]. Both genes were wild-type in both cases (data not shown), thereby suggesting alternative genetic and/or epigenetic mechanisms that drive activation of NFE2L2 signaling in pediatric liver cancers.

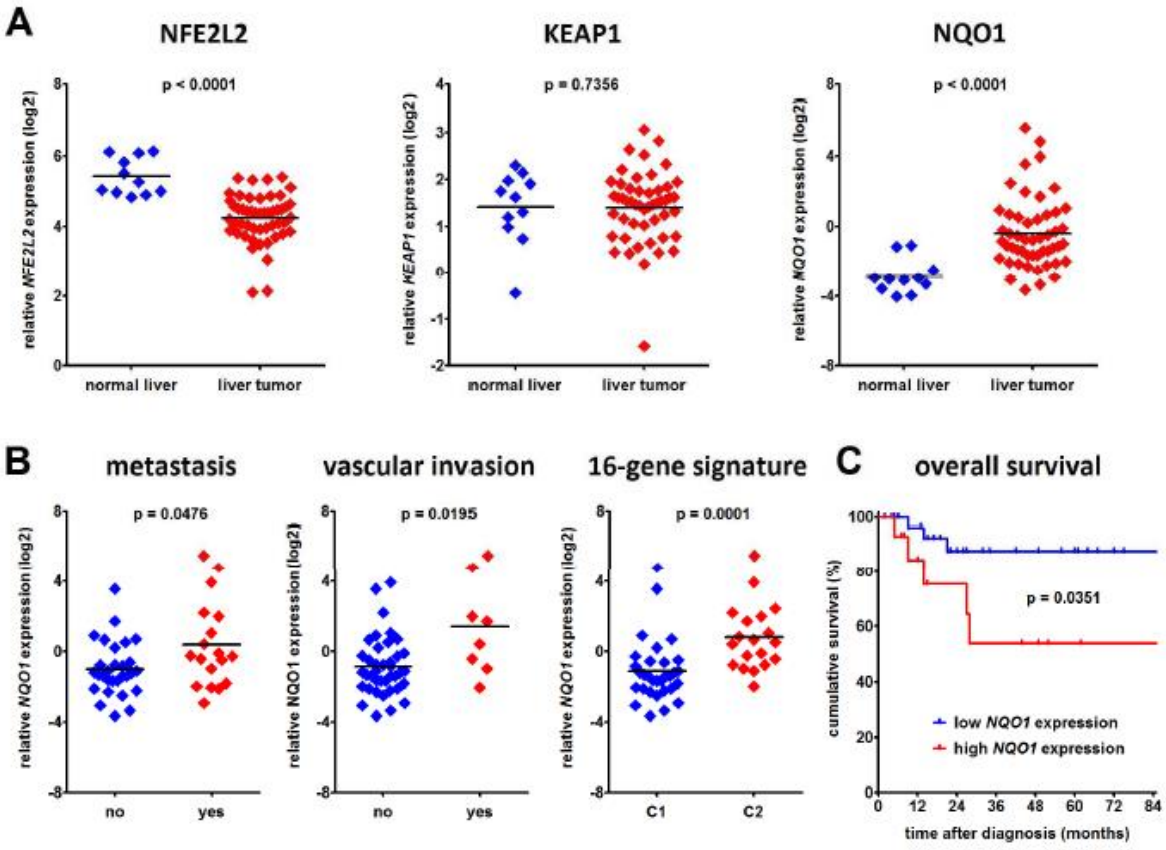


Figure 12: **Clinical relevance of NFE2L2 activity in pediatric liver tumors. (A)** mRNA abundance of the genes *NFE2L2*, *KEAP1*, and *NQO1* relative to levels of the housekeeping gene *TBP* in 11 normal liver (blue diamonds), 43 hepatoblastoma and four TLCT tissues (red diamonds). **(B)** Correlation of the relative *NQO1* expression of the tumor samples with the clinical parameters metastasis, vascular invasion, and the 16-gene signature [10]. **(A+B)** The mean expression values (black lines) and statistical significances from the unpaired Student's *t*-test are given. **(C)** Overall survival was calculated as time from diagnosis to death of disease and is plotted for 32 hepatoblastoma/TLCT patients with low (blue line) and 15 with high (red

line) *NQO1* expression (defined as >5-fold increased expression than the mean of 11 normal liver tissues) over a period of 84 months. Statistical significance was calculated using Mantel-Cox test.

In a next step we analyzed whether NFE2L2 activation in tumors predominantly occurs in a defined subset of pediatric liver tumors. We summarized all clinical data of each patient (**Figure 13**) and correlated the NQO1 expression with clinicopathological features such as age, gender, onset of disease, histology, multifocal growth, outcome, and the high-risk characteristics vascular invasion (portal vein or three hepatic veins), intra-abdominal extra hepatic extension, high PRETEXT stage, metastatic disease, alpha-fetoprotein at diagnosis less than 100 ng/mL, or tumor in all liver sections [29]. We found that NQO1 was significantly increased in metastatic tumors and tumors with vascular invasion (**Figure 12B**). Interestingly, the C2 subtype of the 16-gene signature, predicting poor prognosis in hepatoblastoma [26], was also significantly associated with high NQO1 expression (**Figure 12B**). In line with this, overall survival of patients with high NQO1 expression was significantly worse compared to low expressers (**Figure 12C**). These data suggest that NFE2L2 activation, especially increased NQO1 expression might be of prognostic significance for hepatoblastoma patients.

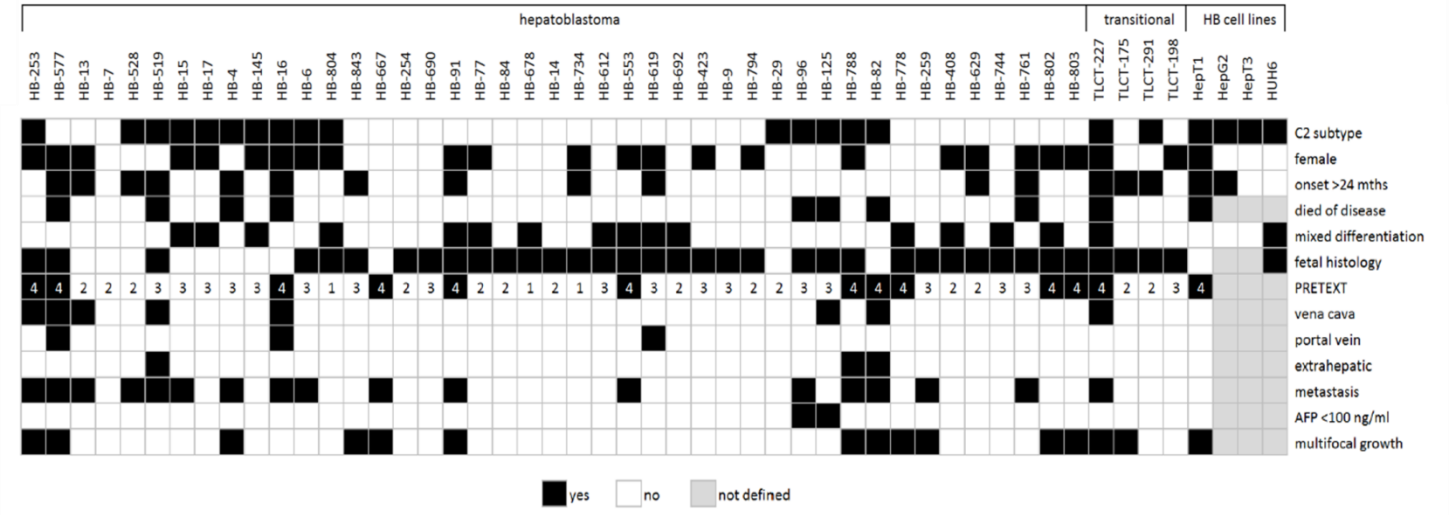


Figure 13: **Summary of clinical characteristics in pediatric liver tumors**. Clinicopathological characteristics are color-coded and depicted in rows for each tumor (in columns) of our cohort of 43 hepatoblastoma and four TLCT patients as well as four hepatoblastoma cell lines.

## 4.2 Epigenetic investigations

### 4.2.1 UHRF1 binds to promoter regions of *HHIP, IGFBP3*, and *SFRP1*

As shown in section 4.1, the development of childhood liver cancers cannot be explained by genetic alterations alone. Instead, aberrant epigenetic modifications seem to play a prominent role at a very early stage in neoplastic development. In hepatoblastoma, sustained activation of three main pathways of embryogenesis, including the hedgehog signaling pathway, the IGF signaling pathway and the WNT signaling pathway, through heavy promoter methylation of their inhibitors *HHIP, IGFBP3* and *SFRP1* have been reported [146, 147]. Since *UHRF1* plays a key role in the regulation of DNA methylation, we wanted to investigate the role of *UHFR1* in methylation of the three tumor suppressor genes (TSGs) *HHIP, IGFBP3* and *SFRP1* in hepatoblastoma.

In 2011, Felle and colleagues [140] reported that UHRF1 binds together with DNMT1 and USP7 on the promoter regions of *HHIP*, *IGFBP3* and *SFRP1* in HCT 116 cells. On this basis we wanted to verify the binding of the complex in the hepatoblastoma cell line HUH6. We observed an enrichment of UHRF1 at the *HHIP, IGFBP3, SFRP1* loci together with DNMT1 and USP7, whereas the presence of RNA Polymerase II was hardly detectable (**Figure 14**). Relative enrichment of the trimeric complex was highest on the *SFRP1* locus, followed by *IGFBP3* and *HHIP*, respectively. An enrichment of RNA Polymerase II was detected at the *ACTB* locus, while weak binding of UHRF1 was observed. The DNMT1 binding level was low in *ACTB* and USP7 showed a comparable binding level to *HHIP, IGFBP3, SFRP1*. This suggests that the trimeric complex might also be of relevance for TSG gene silencing in hepatoblastoma.

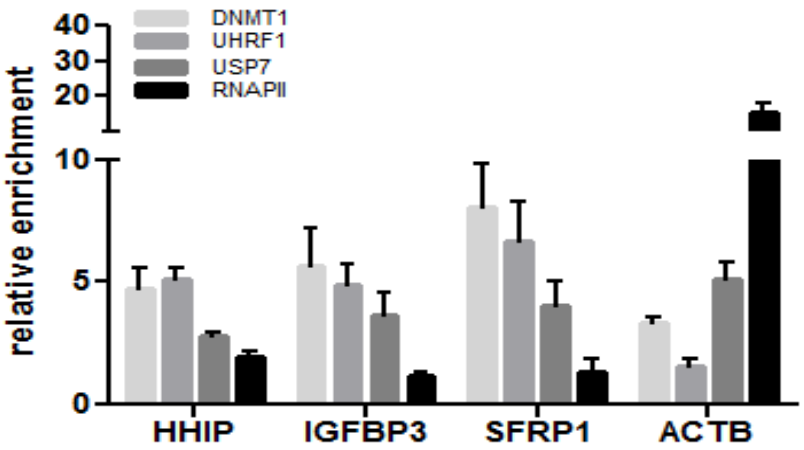


Figure 14: **UHRF1 complex binds on the promoter regions of *HHIP, IGFBP3*, and *SFRP1*.** Chromatin immunoprecipitation (ChIP) was performed with HUH6 cells and antibodies for DNTM1, UHRF1, USP7 and RNAP II. The mean +/- standard deviation of three independent ChIP experiments is shown. Genes of interest and used antibodies for ChIP are indicated.

The enrichment of specific binding versus IgG background is plotted. The active *ACTB* gene shows high levels of RNAP II and low binding levels of UHRF1 complex members. Experiments were performed and kindly provided by Max Felle.

### 4.2.2 *UHRF1* is overexpressed in hepatoblastoma

Expression profile analysis of the complex partners was carried out in our hepatoblastoma samples using qRT-PCR, in order to examine differences of gene expression between tumor and normal liver samples for *DNMT1*, *USP7* as well as *UHRF1*. We demonstrated increased abundance of *UHRF1* transcripts in the tumor samples in comparison to the mean of seven normal liver tissue samples (**Figure 15**). The established hepatoblastoma cell lines, HUH6, HepT1, and HepG2, also displayed a high abundance of *UHRF1* (**Figure 15**). However, no significant differences in the relative gene expression of *USP7* or *DNMT1* could be identified (**Figure 15**), neither in the tumors nor in the hepatoblastoma cell lines.

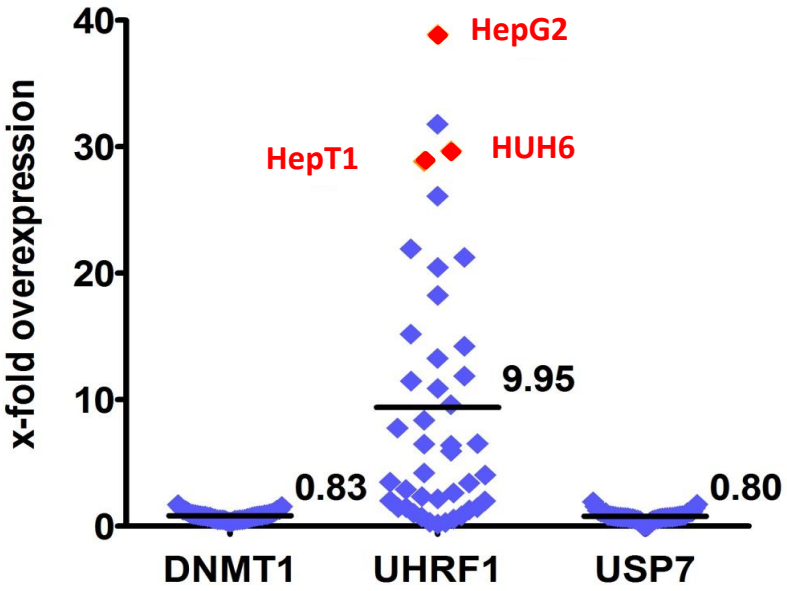


Figure 15: **Expression of *DNMT1*, *UHRF1* and *USP7* in hepatoblastoma**. mRNA abundance of *DNMT1*, *UHRF1* and *USP7* in tumor samples and the three hepatoblastoma cell lines (in red) compared to the mean of 7 normal liver tissues are given.

Promoter methylation has been described as a molecular mechanism that suppresses the gene expression of negative regulators of tumor growth [202]. Since the gene expression of HHIP, IGFBP3, and SFRP1, TSGs relevant in hepatoblastoma, have been described to be downregulated in a variety of other cancers we performed MSP analysis in order to determine the extent of the promoter methylation of the three TSGs; HHIP, IGFBP3, and SFRP1 in the hepatoblastoma cell lines HepT1,

HepG2 and HUH6. A strong methylation within the promoter region of HHIP, IGFBP3 and SFRP1 in all three cell lines was identified, whereas no methylation within the ACTB promoter could be observed (**Figure 16A**). Because promoter methylation has a strong impact on the transcriptional activity, we next wanted to determine the gene expression profiles of HHIP, IGFBP3 and SFRP1 in the hepatoblastoma cell lines. As expected, the promoter methylation of the TSGs was inversely correlated with gene expression of our three candidate genes and expression of ACTB (**Figure 16B**).

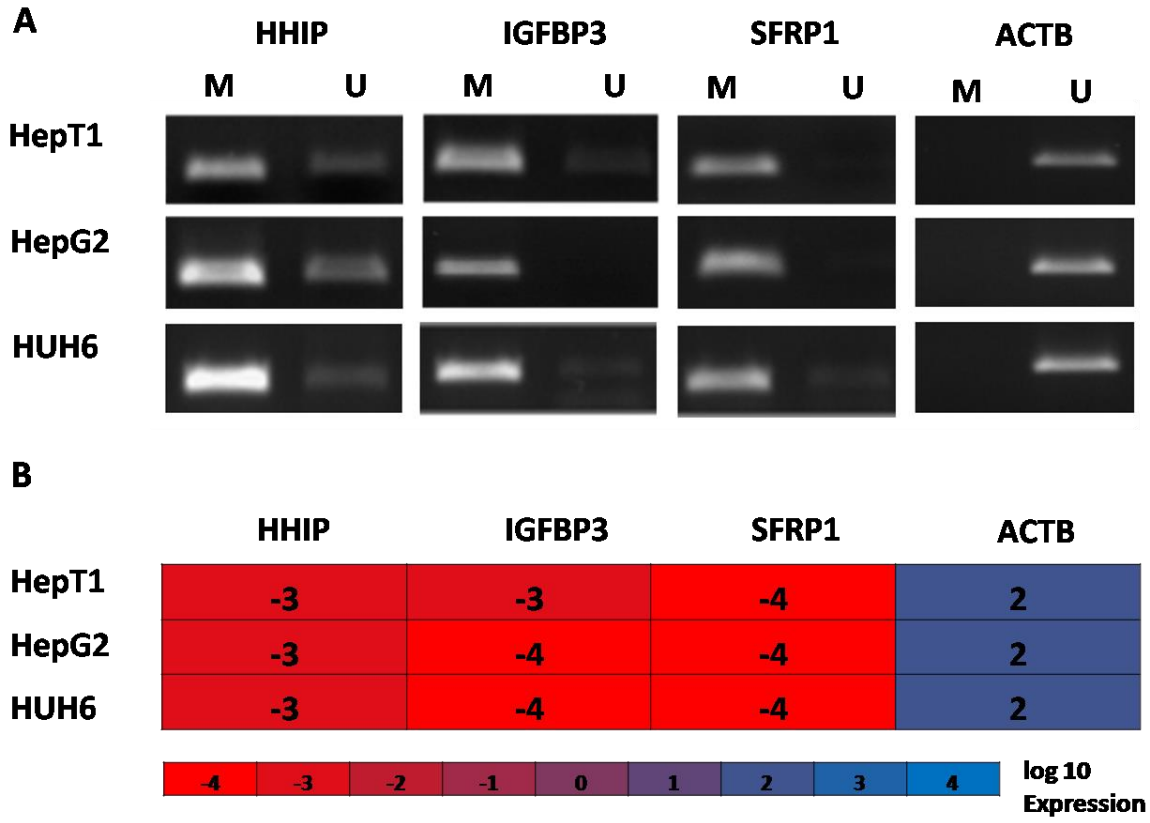


Figure 16: **Methylation state and mRNA abundance of target genes of hepatoblastoma cell lines. (A)** Representative MSP analyses of *HHIP*, *IGFBP3* and *SFRP1* and *ACTB* in the HUH6, HEPT1 and HepG2 cell line are presented. Genes were analyzed for methylated (M) and unmethylated (U) CpG sites within the promoter region. **(B)** Relative mRNA abundance of *HHIP, IGFBP3, SFRP1* and *ACTB* in HUH6, HEPT1 and HepG2 cells were measured by qRT-PCR. The values represent gene expression in relation to the house-keeping gene *TBP*. Color scale illustrates the relative expression level of mRNAs (log10 expression): Blue color represents a high expression level; red color represents a low expression level.

### 4.2.3 Knockdown of *UHRF1* leads to demethylation of tumor suppressor genes

To establish the role of UHRF1 on methylation and gene expression, we first evaluated the consequence of UHRF1 knockdown in the three hepatoblastoma cell lines HUH6, HepT1 and HepG2. Transient knockdown of UHRF1 resulted in significant reduction of UHRF1 expression up to 85 % after 48 h compared to cells transiently transfected with non-targeting control (NTC) siRNA (**Figure 17A**). Knockdown on RNA level was most efficient in HepG2 and least in HepT1. Next, we confirmed

the knockdown of UHRF1 on protein level. UHRF1 protein levels were monitored by Western blot analysis 48 h after transfection. We detected a significant reduction of the UHRF1 protein in all three hepatoblastoma cells lines, being the strongest in HUH6 cells (**Figure 17B**). For further experiments we worked with HUH6 cells due to the strongest UHRF1 downregulation on protein level.

As promoter methylation is in strong inverse correlation with transcriptional activity, we investigated whether knockdown of UHRF1 affects the methylation status of the HHIP, IGFBP3 and SFPR1 promoter regions and re-establishes their expression in HUH6 cells. 48 h after UHRF1 knockdown MSP analysis was performed. We detected a reduced HHIP, IGFBP3 and SFPR1 promoter methylation level in UHRF1 depleted in comparison to control transfected HUH6 cells (**Figure 17**). To support this finding pyrosequencing was performed, which enables quantification of DNA methylation [203]. Comparably to MSP analysis, pyrosequencing revealed a significantly decreased methylation rate within the promoter of HHIP, IGFBP3, SFRP1, showing the strongest reduction for the HHIP promoter, followed by IGFBP3 and SFRP1, respectively (**Figure 17D**). We also analyzed the genome-wide methylation level, which can be estimated using the methylation level of the CpG sites of the long interspersed nuclear element-1 (LINE-1), since LINE-1 methylation correlates with global DNA methylation status [204]. In this study we observed a general hypomethylation of the promoter region of LINE-1 in HUH6 cells compared to genomic DNA and Sss1 treated HUH6 cells, which showed high methylation levels. The downregulation of UHRF1 led to a slight decrease of methylation in HUH6 cells in comparison to siNTC transfected HUH6 cells (**Figure 17D**). Collectively, this data indicate that UHRF1 controls DNA methylation at the promoters of the three TSGs and LINE-1 repeats.

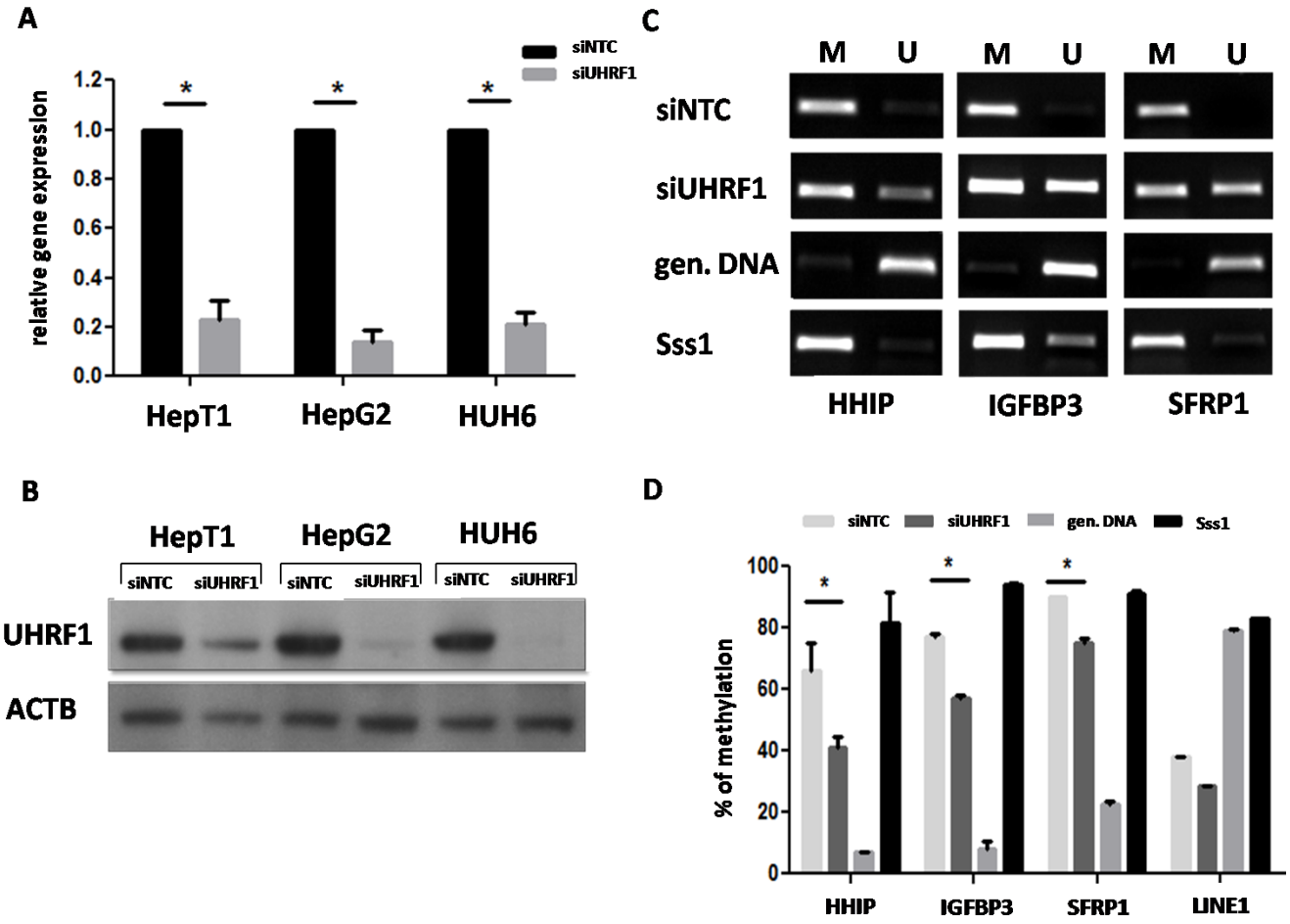


Figure 17: **Demethylation of the *HHIP, IGFBP3* and *SFRP1* promoter region after *UHRF1* knockdown.** HepT1, HepG2 and HUH6 cells were either transfected with siRNA against *UHRF1* (siUHRF1) or transfected with non-targeting control siRNA (siNTC), which has no known vertebrate target gene. Cells were harvested 48 h after transfection. **(A)** Relative gene expression was reduced in cells transfected with siRNA against *UHRF1* compared to negative control. Data represent mean +/- standard deviation, standardized to control and normalized to *TBP* (housekeeping genes) of at least three biological replicates. **(B)** Western blot analysis of HepT1, HepG2 and HUH6 cells after *UHRF1* knockdown. A clear decrease of protein levels was detected in all three cell lines. Immunodetection of beta-actin served as a standard for equal protein loading. **(C)** Promoter region of the *HHIP*, *IGFBP3* and *SFRP1* genes were analyzed for methylated (M) and unmethylated (U) CpG sites by MSP in presence or absence of *UHRF1*. Representative images of MSP experiments are given. Genomic DNA as well as *in vitro* methylated DNA (Sss1) were used as negative and positive controls, respectively. **(D)** Pyrosequencing of HUH6 cells after *UHRF1* knockdown on promoter regions of the *HHIP*, *IGFBP3*, *SFRP1* and *LINE-1* repeats. Pyrosequencing analysis was performed with bisulfite-treated DNA from HUH6 cells 48 h after knockdown. Data represent mean +/- standard deviation of at least three biological replicates. Statistically significant difference versus siNTC transfected cells: *p < 0.05 (unpaired Student´s t-test).

### 4.2.4 Effects of *UHRF1* downregulation on gene expression and proliferation

To directly address the role of UHRF1 in silencing of TSGs, we knocked down UHRF1 for 48 h in HUH6 cells. Surprisingly, although UHRF1 knockdown led to a demethylation of promoters, the strong depletion of UHRF1 did not lead to re-established gene expression of our three silenced candidate genes HHIP, IGFBP3 and SFRP1 (**Figure 18A**). ACTB expression was either not affected after UHRF1 knockdown. However, we additionally analyzed the effect of UHRF1 downregulation on proliferation,

since UHRF1 expression is correlated with cell proliferation [137, 205]. HUH6 cells were transiently transfected and MTT assays were performed. In line with the gene expression data, UHRF1 knockdown did not have an effect on cell viability in a time range of 168 h (**Figure 18B**). Cells transfected with control siRNA showed the same proliferation curve than HUH6 cells transfected with siRNA targeting UHRF1.

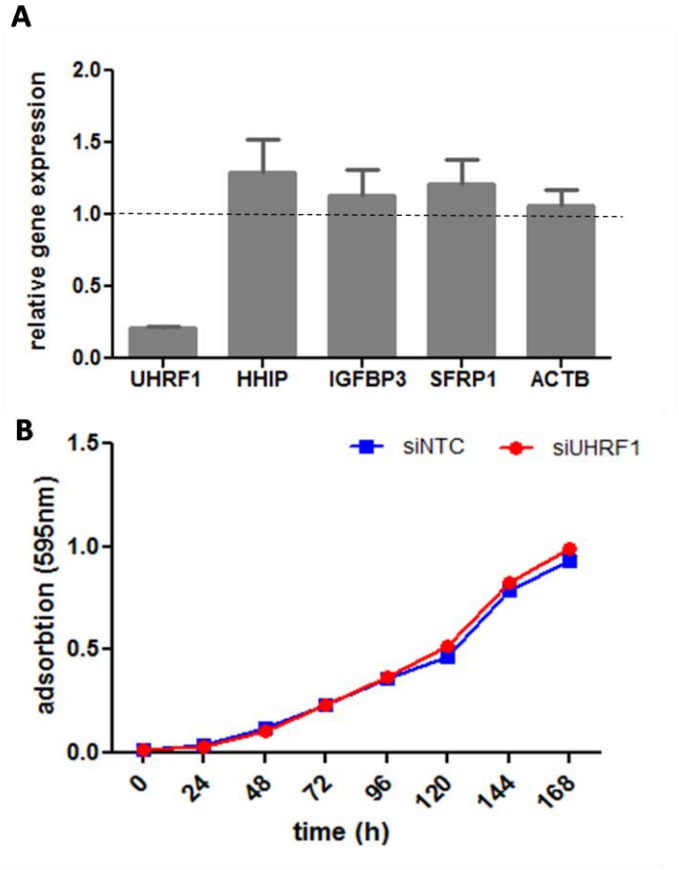


Figure 18: ***UHRF1* knockdown does not influence expression of target genes and cell proliferation. (A)** The mRNA abundance of *HHIP, IGFBP3* and *SFRP1* was revealed after two days of *UHRF1* knockdown in the HUH6 cell line by quantitative real-time PCR. Gene expression of *HHIP, IGFBP3* and *SFRP1* and *ACTB* was not notably changed after *UHRF1* knockdown. Data represent mean +/- SEM, standardized to control and normalized to *TBP* (housekeeping genes) of eight biological replicates. **(B)** Growth properties of *UHRF1* depleted HUH6 cells**.** The cell viability of *UHRF1* transfected cells was assessed at the indicated time points using MTT assays and optical density measurements. The values given represent the mean of four biological replicates +/- SD.

### 4.2.5 *UHRF1* knockdown decreases the repressive marks H3K27me3 and H3K9me2

Since demethylation alone was not sufficient to induce re-expression of our TSGs and UHRF1 is able to influence both, DNA methylation as well as histone modification, we wanted to investigate the effect of UHRF1 knockdown on activating and repressive histone marks. We performed ChIP analysis 48 h after UHRF1 knockdown to evaluate the histone mark setting within the promoter region of our TSGs HHIP, IGFBP3 and SFRP1. The use of antibodies against, RNA Pol II, H3K4me2, H3K27me3 and

H3K9me2 revealed that UHRF1 knockdown in HUH6 cells reduced H3K9 di-methylation and H3K27 tri-methylation on the HHIP promoter. However, UHRF1 downregulation neither changed the low RNA Pol II occupancy, nor methylation status of the activating H3K4 histone mark. This is in accordance with the still existing transcriptional repression observed after UHRF1 knockdown (**Figure 19A**). The histone modification profile within the IGFBP3 and SFRP1 promoters after knockdown was similar to the HHIP promoter regions (**Figure 19B; 19C**). For ACTB an increase for RNA Pol II occupancy and H3K4 di-methylation was observed. The repressive mark H3K27me3 was hardly detectable and H3K9me2 methylation was slightly decreased after UHRF1 knockdown (**Figure 19D**). This data underscore the role of UHRF1 in maintenance of the repressive chromatin state in silenced genes, but also shows that UHRF1 knockdown alone is not sufficient to change histones to an active chromatin state.

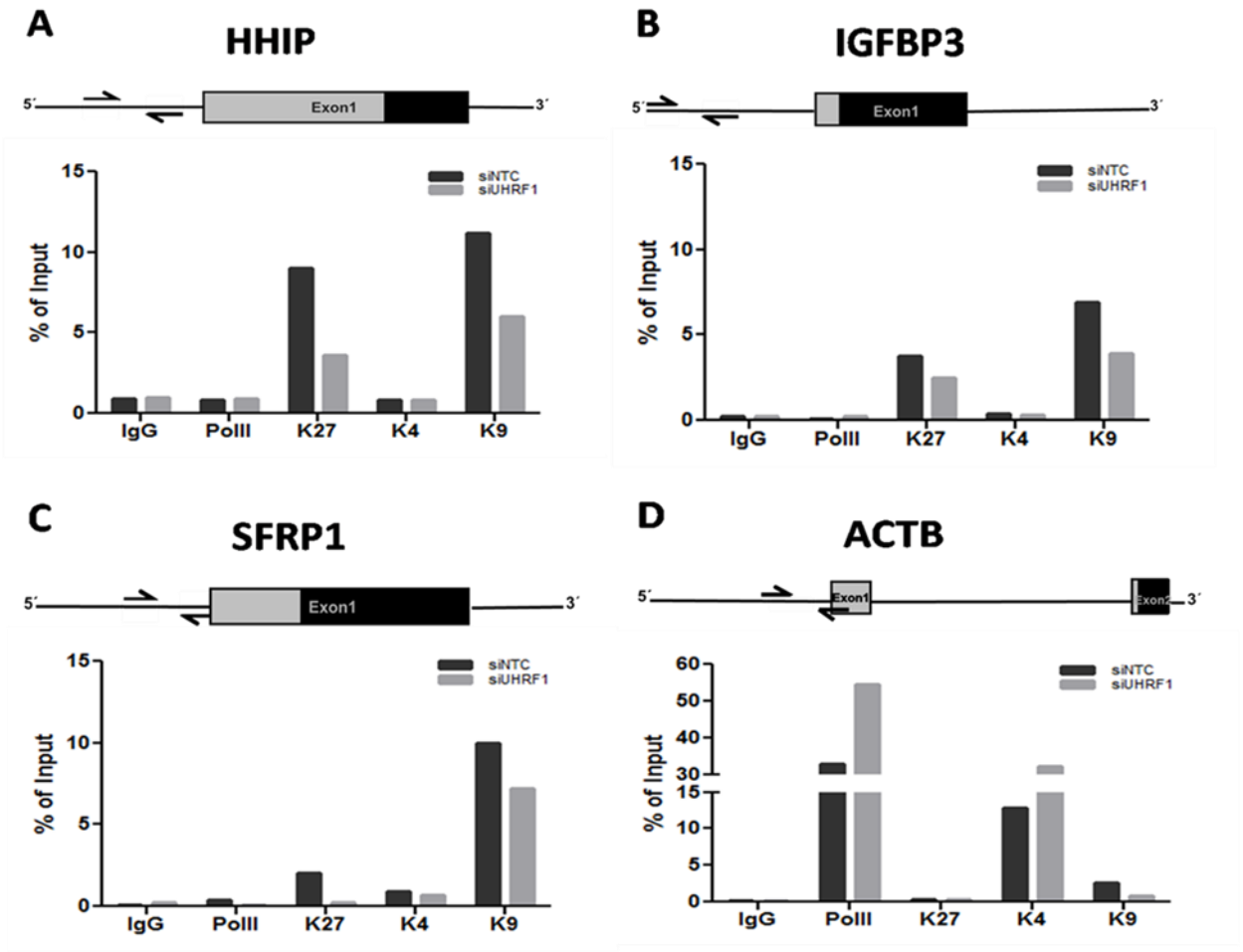


Figure 19: **Chromatin immunoprecipitation of HUH6 cells after *UHRF1* knockdown**. HUH6 cells were transfected with siRNA targeting *UHRF1* or control siRNA and ChIP was performed after 48 h. Alterations of histone modification within the promoter regions of the TSGs *HHIP* **(A)**, *IGFBP3* **(B)**, *SFRP1* **(C)** as well as *ACTB* **(D)** were measured. The locations of the ChIP primer sets within the promoter regions are shown. Boxes emphasize exons of the respective genes with black parts highlighting the translated proportion. ChIP was performed using antibodies against RNA Pol II, H3K27me3, H3K4me2, H3K9me2 and mouse IgG as negative control. Precipitated DNA was analyzed by qRT-PCR and results are shown as percentages of total input. One representative experiment of three biological replicates is given.

### 4.2.6 Clinical relevance of *UHRF1* overexpression in hepatoblastoma

To assess the clinical relevance of UHRF1 we evaluated whether UHRF1 overexpression predominantly occurs in a defined subset of tumors. By correlating UHRF1 expression with the 16gene signature, we found that UHRF1 was significantly increased in the C2 subtype of the 16-gene signature [26], which is associated with poor prognosis in hepatoblastoma (**Figure 20A**). In line with this, the overall survival of patients with high UHRF1 expression was significantly worse (about 60 %) compared to patients with low UHRF1 expression, which was about 90 % (**Figure 20B**). These data suggest that UHRF1 activation might be more relevant as a prognostic marker than as a direct anticancer target in hepatoblastoma patients.

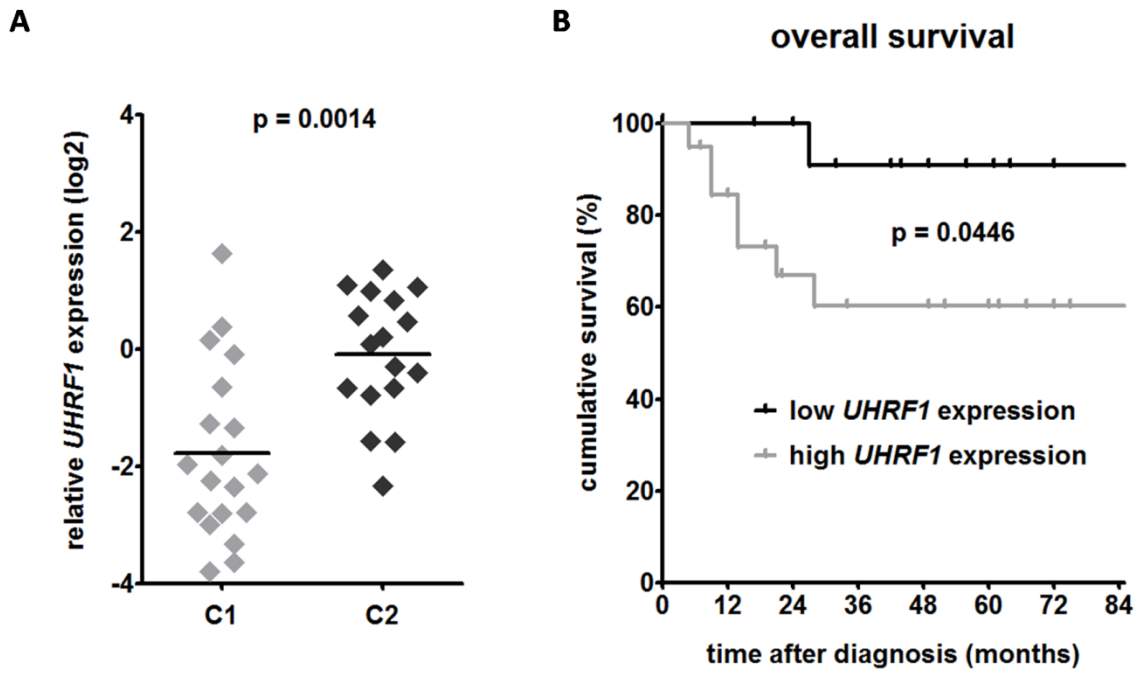


Figure 21: **Clinical relevance of *UHRF1* overexpression in hepatoblastoma**. **(A)** Correlation of the relative *UHRF1* expression in the tumor samples with the subtypes C1 and C2 of the 16-gene signature [25]. The mean expression values (black lines) and statistical significances from the unpaired Student's *t*-test are given. **(B)** Overall survival was calculated as time from diagnosis to death of disease and is plotted for 13 patients with low (black line) and 20 with high (grey line) *UHRF1* expression (defined as >5-fold increased expression than the mean of 6 normal liver tissues) over a period of 84 months. Statistical significance was calculated using Mantel-Cox test.

# 5 Discussion

To date, the development and progression of hepatoblastoma is associated with mutations, genetic syndromes and/or deregulation of embryonic pathways such as the WNT-, the IGF- or hedgehog signaling pathway through downregulation of their inhibitory components via DNA methylation. The misregulation of methylation already suggests that epigenetic mechanisms in addition to genetic alterations play a crucial role in the development of hepatoblastoma. In this study we were able to gain more information about the genetics in hepatoblastoma by the identification of recurrent beta catenin (CTNNB1) and nuclear factor (erythroid-derived 2)-like 2 (NFE2L2) mutations within our tumor cohort. We got a first impression of NFE2L2s role in hepatoblastoma proliferation as well as its relevance in the clinical setting. Furthermore, we recognized the ubiquitin-like with PHD and ring finger domains 1 (UHRF1) as a regulator of DNA methylation in hepatoblastoma and as a potential prognostic marker.

## 5.1 Genetics

The importance of genetic factors in the development of cancer has been very well demonstrated in the last decades. The onco-genetics is a subject of comprehensive research. The medical database system PubMed using the search term "cancer genetics" displayed a total of over 300,000 scientific publications (effective date: 18.03.2015). This high number of publications is impressive and underlines the fundamental importance of genetic mechanisms. Genetic changes drive the pathogenesis of tumors in both adults and children. These changes can be inherited and are, therefore, found in every cell, but more often, they are somatically acquired and restricted to tumor cells. Investigations of childhood cancer genetics have identified that pediatric cancers contain fewer somatic mutations and many of the mutations found in childhood cancers aren’t found in adult cancers. In addition, it was found that genes that encode proteins involved in the epigenetic regulation are mutated at a high frequency in a subset of childhood cancers [206] in comparison to tumors arising in adults where epigenetic regulation is less dominant.

Interestingly, our whole-exome study on hepatoblastoma samples showed that the majority of mutated genes are epigenetic regulatory proteins that affect transcription, chromatin and chromosome organization as well as chromatin modification. As mentioned the predominance of mutation within epigenetic regulators is consistent with findings in other childhood tumors [206]. Sequencing of 21 different pediatric cancer subtypes, including leukemia, brain tumors and different solid malignancies in about 1000 pediatric cancer samples has identified H3F3A, PHF6, ATRX, KDM6A, SMARCA4, ASXL2, CREBBP, EZH2, MLL2, USP7, SETD2, ASXL1, NSD2, SMC1A and ZMYM3, to be

mutated. These genes are responsible or involved in the regulation of different epigenetic processes, such as regulation of transcription, chromatin modification/remodeling through histone (de)acetylation and (de)methylation as well as DNA modifications [206]. Comparably, the genes found in our study, are involved in the same epigenetic processes. HDAC4, KDM5C and KMT2C are directly responsible for the deacetylation and (de)methylation of histones, respectively, while CIR1, BCORL1 indirectly regulate the deacetylation of histones. Genes controlling histone (de)methylation have become increasingly recognized as a common feature of different human cancers. Inactivating mutations, for example, of UTX, which demethylates histone H3K27 have been observed in multiple myelomas, esophageal cancers and renal cell cancers [207]. Additionally, some renal cell cancers contain mutations in the histone methyltransferase gene SETD2 and the histone demethylase gene JARID1C [208]. The histone methyltransferase gene EZH2 has been discovered to be mutated in nonHodgkin's lymphomas [209] and recently, frequent mutations of the chromatin remodeling gene ARID1A have been observed in ovarian clear cell carcinomas [210, 211]. These results clearly demonstrate that alterations of the epigenetic machinery occupy an important role in cancer development since these mutations have the potential to deregulate hundreds of targeted genes, genome wide.

In this context, it is important to elaborate how disrupted epigenetic regulators identified in our study cooperate with changes in known signaling pathways that contribute to hepatoblastoma development. Since hepatoblastoma develops early in life, hepatoblastoma is likely to be driven by only few genetic changes, therefore, it is reasonable to further study the genes mutated in our hepatoblastoma samples in order to distinguish the so-called "driver" mutations, with the ability to promote or "drive" neoplastic processes, from the non-contributing "passenger" mutations, that have no direct or indirect effect on the selective growth advantage of the cell [212, 213]. The identification of such genes is important for understanding pathways and gene functions in normal and cancer tissues. Since *HDAC4* and KDM5C are already described to act as driver mutations in breast cancer [214] and kidney cancer cells [215], respectively, they might also represent a driver mutation in our hepatoblastoma samples. However, the high rates of mutation in epigenetic regulatory genes, strongly underlies the big role of epigenetics in hepatoblastoma development, but simultaneously suggest that the majority of the mutations in hepatoblastoma might be passenger rather than driver mutations based on variety and high number.

A potential non-epigenetic driving force for hepatoblastoma development which we have also described in our study, might be the CTNNB1 mutations and consequently activation of WNT signaling. As found earlier, we identified recurrent mutations of CTNNB1 in our hepatoblastoma samples, a gene, playing a central and critical role in the WNT signaling pathway. In our cohort about

70 %, of all cases carried a CTNNB1 mutation. However, it has been shown that the introduction of activating CTNNB1 mutations in hepatocytes was not sufficient to drive tumorigenesis [38, 39], since CTNNB1 mutations alone only cause immediate proliferation leading to marked hepatomegaly [38, 39]. Recently, Mokapatti et al., refute years of assuming that a CTNNB1 mutation itself is not sufficient to induce HCC or hepatoblastoma. The study demonstrates that the activation of the WNT pathway in a unique population of bipotential fetal liver cells is able to give rise to endogenous HCCs, hepatoblastomas and lung metastasis in adult mice [73]. This is in striking contrast to the absence of tumors when CTNNB1 is stabilized in adult hepatocytes using a Cre-expressing adenovirus or an adolase B promoter–driven transgene expressing stable mutant CTNNB1 protein [75]. Interestingly, the HCCs and hepatoblastomas which developed out of fetal liver cell showed an increase in both canonical (c-Myc, cyclin D1 and AXIN2) and non-canonical WNT targets (GS, GLT1, OAT and LECT2). Such induction of canonical WNT targets was not observed in the prior model in which CTNNB1 was stabilized and no tumor development took place [75]. These differences suggest that the ability of WNT pathway activation which results in HCCs or hepatoblastoma critically depend on the activation of canonical WNT targets. Additionally, this result shows that tumor development is also highly dependent on the cell type wherein a mutation of CTNNB1 arises. Although CTNNB1 seems to be a key driver in liver development and is frequently hit by mutations there are cases that do not lead to tumor development, underscoring the impact on the presence of other mutations. Therefore, the data from Mokapatti et al., might also explain the development of wild type CTNNB1 tumors (about 20 % of our cases) by suggesting other gene mutations within the canonical WNT pathway, such as the APC and AXIN. However, transcriptional WNT pathway activation might also be responsible for tumor development.

The finding of mutations within NFE2L2 and more importantly activation of the NFE2L2-KEAP1 pathway might present an additional or alternative mechanism that may contribute to hepatoblastoma development and progression, based on their recurrency in our samples. Intriguingly, comparable alterations have been detected in HCC in adults, showing either NFE2L2 or KEAP1 mutations in altogether 7.2 % [197], 8.0 % [198], and 8.9 % [216] of all patients, thereby suggesting a broader role of the NFE2L2-KEAP1 pathway in liver cancers. The KEAP1-NFE2L2 pathway is the major regulator of cytoprotective responses to oxidative and electrophilic stress [196, 217]. In normal and premalignant tissues, NFE2L2 regulated downstream pathways prevent cancer initiation and progression while in malignant cells NFE2L2 activity provides growth advantage and mediates chemoresistance [78, 83]. The activation of NFE2L2 is regulated by KEAP1 (Kelch like-ECH associating protein 1), which binds to NFE2L2 and promotes its degradation by the ubiquitin proteasome pathway.

The mutations observed in this study are located either in or adjacent to the DLG and ETGE motifs which have been described to be essential for binding of the KEAP1/CUL3 complex that mediates ubiquitination and proteasomal degradation [193]. The mutations specifically alter amino acids in the motifs, which results in aberrant cellular accumulation of NFE2L2 and insensitivity to degradation, leading to constitutive activation of the pathway. Similar mutations in the NFE2L2 gene have also been observed in other cancers, including lung, head and neck, and esophageal carcinoma [193, 218, 219]. Comparably, in these cancers mutations of NFE2L2 also change the amino acids within the DLG motif or within the ETGE motif [193], resulting in aberrant cellular accumulation of NFE2L2 and constant activation. However, we found half of the tumor cases showing pathway activation without NFE2L2 mutations, thereby suggesting that other yet unidentified activating mechanisms must exist. Transcriptional downregulation of KEAP1 might be one possibility, however we and others have failed to detect significant differences between normal liver and liver tumor samples, although a trend for decreased KEAP1 expression in tumors with KEAP1 mutations has been reported [198]. Accordingly, promoter methylation of KEAP1 as shown for lung cancer [220, 221] prostate [222], malignant glioma [221] and colorectal cancers [223] can be dismissed, too.

Recent studies have shown that NFE2L2 regulates the proliferation of human lung cancer cells, pancreatic cancer and glioblastoma [84, 224-226]. These findings suggest that activation of NFE2L2 in cancer cells provides advantages for the cell proliferation. Based on these results we performed transient NFE2L2 knockdown experiments in our hepatoblastoma cell lines. NFE2L2 siRNA knockdown profoundly inhibited the cellular proliferation of the HepG2 and HUH6 cells, however, a clear inhibitory effect for HepT1 cell proliferation was not observed. This result might reflect the fact that HepG2 cells express high endogenous NFE2L2 and are therefore more sensitive to alterations in NFE2L2 expression. Similar findings were observed in a lung cancer study, where depletion of NFE2L2 resulted in a decrease in cellular proliferation in A549 and H460 cancer cells [227]. Ji and colleagues also observed an inhibition of cell proliferation, an increasing cell apoptosis and inhibition angiogenesis in mouse xenograft model for glioblastoma [228].

The inhibitory effect on cell proliferation and apoptosis in consequence of NFE2L2 depletion may be based on changed regulation of downstream target genes, which include stress response genes, xenobiotics-metabolizing genes, genes involved in the ubiquitin-mediated proteasomal degradation system, cell growth controlling genes and genes important for apoptosis [196, 226, 229].

However, as the NFE2L2 mutated cases were concomitantly mutated in CTNNB1, as described before for adult HCC [197], we hypothesize that activated WNT signaling and activated NFE2L2-KEAP1 signaling might cooperate in liver tumorigenesis. As NFE2L2-KEAP1 signaling is known to prevent apoptosis and promote cell survival [196] and constitutive activation of NFE2L2-KEAP1 signaling in

KEAP1 knockout mice is not sufficient to drive tumor development [230], it is tempting to speculate that NFE2L2 may not initiate tumorigenesis, but rather confers a high survival capacity and thereby positively selects for already WNT-activated premalignant cells, a presumption which was already described in pediatric HCC. Clonality analysis of pediatric HCC predicted that the CTNNB1 mutation was clonal and occurred earlier during carcinogenesis, whereas the NFE2L2 mutation was acquired later [85]. Nevertheless, further genome-wide approaches deciphering genetic and epigenetic alterations on a larger cohort of patients are warranted and will hopefully shed light onto the cause for the widespread activation of the NFE2L2-KEAP1 pathway and a possible crosstalk between WNT and NFE2L2-KEAP1 signaling in liver cancers.

Because, the establishment of molecular markers to aid risk stratification of cancer patients is an ongoing endeavour in pediatric oncology, we investigated the NFE2L2 activation in relation to clinical parameters. Here, we provide evidence that determining the activity of the NFE2L2-KEAP1 pathway might help to identify patients at risk for worse outcome. Accordingly, the high expression of NQO1, which is a target gene of NFE2L2, was associated with two clinical high-risk features, namely metastatic spread and invasive growth into vessels. Consistent with this observation we found a significantly poorer outcome of high expressing patients. In line with this, the C2 subtype of the 16gene signature that has been validated to predict poor prognosis in hepatoblastoma [26] was also significantly associated with high NQO1 expression. Interestingly, NQO1 expression has been described to be commonly elevated in other types of human cancers, including pancreatic, breast and thyroid cancer and is already suggested as a prognostic marker for different cancers [231-233]. In small cell lung cancer for instance, a high level of NQO1 expression was significantly correlated with lower disease-free survival and 5-year survival rates [231]. Similar findings were obtained in gastric adenocarcinoma where NQO1 expression is positively correlated with tumor size, serosal invasion, tumor stage, and both disease-free survival and 5-year survival rates [232]. Based on our data we advocate the measurement of NQO1 expression to be included into the upcoming international treatment protocol for the pre-therapeutic risk assessment of hepatoblastoma patients in order to aid risk-adapted therapy. Collectively, our data indicate that activation of WNT signaling in concert with activation of the NFE2L2-KEAP1 pathway might be the driving force in the development of liver cancers, both in children and adults, thereby offering a new therapeutic target for the treatment of these devastating diseases. Strikingly, a first promising NFE2L2 inhibitor has recently been described, which reduces the protein level of NFE2L2 regardless of the status of KEAP1 or NFE2L2 being wild type or mutated [234].

Although the genetic origin of cancer is widely accepted, recent studies demonstrate that cancer cells harbor global epigenetic abnormalities and that these epigenetic changes may be the key initiating

events in some forms of cancer [87, 235, 236] especially in those having a relatively normal genomic background. Since we identified hepatoblastoma as a genetically very simple tumor and mutations of epigenetic regulators in the first part of this work we started to decipher the impact of the epigenetic factor UHRF1 in hepatoblastoma development and/or progression.

## 5.2 Epigenetic

Epigenetic mechanisms contribute to the development and progression of different tumor species by being involved in transcriptional repression of tumor suppressor genes (TSGs), epigenetic activation of proto-oncogenes and imprinting. Recently, UHRF1 emerged as a key regulator of these events by controlling both DNA methylation as well as histone modification. UHRF1 is an essential cofactor for the maintenance of DNA methylation [118, 122] by binding to hemi-methylated DNA, by interaction and co-localization with DNMT1 [116]. The strong methylation within the promoter region of various genes, mediated by DNMT1 involved complexes, is a common phenomenon in tumor development [114, 237]. Due to the hypermethylation of CpG islands decommissioning of gene expression takes place. TSGs but even so genes involved in signaling pathways are the genes mainly affected [238]. Their usual involvement in the regulation the cell cycle and of cell proliferation causes a growth advantage and cell survival for neoplastic cells.

In this work we identified the hepatoblastoma derived cell lines HepT1, HepG2 and HUH6 to possess a strong CpG promoter methylation in inhibitory components of WNT-, IGF- and Hedgehog signaling pathway, namely, Hedgehog-interacting protein (HHIP), Insulin-like growth factor-binding protein 3 (IGFBP3) and Secreted frizzled-related protein 1 (SFRP1). Methylation analysis of these genes and subsequent analysis of gene expression revealed a strong relationship between methylation and expression, resulting in a strong suppression of gene transcription. Comparative methylation profiles of these genes have been obtained in other tumor identities [141], suggesting an important role for SFRP1, IGFBP3 or HHIP silencing in carcinogenesis. SFRP1 for example, has been identified to be transcriptional silenced in gastric tumors [239], breast cancer [240], colorectal tumors [241], in HCC [242] and even so in systemic sclerosis [243]. IGFBP3 is epigenetically regulated by methylation in renal tumors, HCC, breast cancer, gastric and colon carcinomas [244-246]. A deregulation of methylation within the promoter of HHIP was identified in medulloblastoma [247], gastric [248], hepatic [147, 249] and pancreatic cancer [250]. For SFRP1 it is noteworthy, that an increased SFRP1 expression or re-expression of SFRP1 inhibits the growth of tumor cells independent of the CTNNB1 status of the canonical WNT signaling pathway, which was first described by Suzuki and colleagues [251] in colorectal carcinoma. The overexpression of SFRP1, SFRP2 and SFRP5 reduced the CTNNB1

protein level in both the mutant variant as well as the wild-type form [251]. This observation is of great interest in CTNNB1 mutated hepatoblastoma cases, since the re-activation through SFRP1 promoter demethylation would serve as an approach to deal with the misregulated WNT pathway based on CTNNB1 mutations.

In this context, several studies have shown that treatment with the demethylating agent 5-Aza-dC leads to reactivation of gene expression in the corresponding cell lines [147, 148, 243]. This suggests that changes to any component of the methylation apparatus, might be able to influence methylation and consequently, render gene expression of silenced genes. Since UHRF1 is closely linked with the DNA methylation and histone methylation, we wanted to validate UHRF1 binding as well as changes of methylation levels in the promoter regions in the hepatoblastoma relevant TSGs after UHRF1 downregulation.

Colleagues of mine identified a trimeric complex comprising DNMT1, Ubiquitin-specific-processing protease 7 (USP7) and UHRF1 [141], occupying an import role in the methylation process of DNA [141]. The complex was described to bind on the promoter region of the silenced TSGs HHIP, IGFBP3 and SFRP1 in the colon carcinoma cell line HCT-116 [141]. In this work, we were able to confirm the results of Felle and colleagues that UHRF1 binds together with DNMT1 and USP7 on the promoters of the silenced TSGs in the hepatoblastoma cell line HUH6. Moreover, we were able to show that the UHRF1 expression is markedly increased in our hepatoblastoma cohort, a phenomenon already known for cancer in bladder [132], breast [116, 121], pancreatic [133], colon [134] and HCC [135]. The expression profile of USP7 and DNMT1 was comparable to normal liver tissue. Furthermore, the UHRF1 overexpression has been identified to correlate with increased DNA methylation in lung cancer [130, 136, 140]. Thus, UHRF1 activity seems to be quite important in maintaining the hypermethylation of certain TSGs. This is also supported by findings in breast tumors, where UHRF1 overexpression was correlated with BRCA1 promoter hypermethylation [121]. Therefore, enhanced UHRF1 expression in cancer cells is considered to be associated with TSG silencing and cellular proliferation. These results suggest UHRF1 as a promising therapeutic target, especially as its expression is only detectable in proliferating cells including tumor tissues and different types of primary cancers [129, 132, 252]. Thus, we suggest that UHRF1 inhibition is of high selectivity for tumor cells.

The high expression of UHRF1 in tumor cells and its strong role in proliferation propose UHRF1 depletion as an anti-tumor action. First depletion experiments in several types of cancer have shown that UHRF1 mediates antitumor activities. We therefore performed UHRF1 knockdown in our

hepatoblastoma cell line HUH6. The knockdown of UHRF1 strongly decreased the methylation level of the promoter regions of HHIP, IGFBP3 and SFRP1. Interestingly, comparable results were obtained in RASSF1, CYGB, and CDH13 promoters in A549 lung adenocarcinoma cells [140]. The methylation status of all three promoters was consistently reduced after UHRF1 knockdown. Moreover, it has been shown that downregulation of UHRF1 resulted in a robust demethylation at the SFRP1, IGFBP3 and HHIP promoters in the human colon adenocarcinoma cells HCT-116 [141], underscoring the impact of UHRF1 in the methylation process of different TSGs. We also analyzed the genome-wide methylation level, represented by LINE-1 methylation, since several studies have demonstrated cancer associated hypomethylation of LINE-1 [253-255]. LINE-1 sequences are highly repeated human retrotransposon sequences and constitute about 17 % of the human genome [256]. The genome-wide loss of methylation in core CpG sites of the promoter is regarded as a common epigenetic event in malignancies and is suggested to a play a crucial role in genomic instability [257] and in carcinogenesis [258, 259]. Interestingly, we observed a hypomethylation of LINE-1 in our hepatoblastoma cell line HUH6 a phenomena, which has already been described in other cancers. LINE-1 hypomethylation was observed in urinary bladder carcinomas [260], in chronic lymphocytic leukemia in comparison to normal mononuclear blood cells [261], hepatocellular carcinomas [255], and prostate carcinomas compared to normal prostate tissue [262]. The consequences of LINE-1 hypomethylation are genomic instability and alteration of gene expression. Interestingly, UHRF1 is described to be involved in the methylation of the LINE-1 promoter and that the inhibition or the dysfunction of the DNA methylation machinery promotes further DNA hypomethylation on DNA repeat elements, such as LINE-1 [263]. This is in line with our observed data, that the downregulation of UHRF1 decreases the methylation level of the already hypomethylated LINE-1.

Unfortunately, we could not observe or confirm the results of other groups where UHRF1 knockdown led to a reactivation of silenced TSGs. HHIP, IGFBP3 and SFRP1 gene expression remained silenced after UHRF1 knockdown in our hepatoblastoma cell line HUH6. In contrast to our results, Sabatino and colleagues observed a reactivation of PPARG after UHRF1 knockdown in colorectal cancer, accompanied by histone mark changes and DNA demethylation [264]. Interestingly, first studies with the methylated genes HHIP and IGBFP3 in hepatoblastoma showed that the 5-Aza-dC treatment alone is sufficient to induce reactivation of gene expression, respectively [147, 148]. The DNA demethylating agent 5-aza 2´-deoxycytidine (5-Aza-dC) incorporates into DNA, where it induces an irreversible inactivation of DNA methyltransferases [265] and is widely used for studying the role of DNA methylation in biological processes and is already used as a clinical treatment for certain leukemia's [266]. Both, 5-Aza-dC treatment and UHRF1 knockdown induce demethylation of DNA, while in consequence only 5-Aza-dC treatment results in gene reactivation, suggesting that additional

mechanisms others than demethylation must exist that influence the activation of silenced genes. The effect on different histone tail modifications or histone replacement by 5-Aza-dC treatment might be one possibility. Most studies describe that 5-Aza-dC treatment is closely and consistently linked with demethylation of DNA and significantly decreases histone H3 lysine 9 di-methylation (H3K9me2) on promoters, a phenomenon also observed for UHRF1 knockdown in this study. However, Kondo et al. have reported that 5-Aza-dC treatment slightly increases lysine-9 acetylation (K9ac) and moderately increases histone H3 lysine 4 di-methylation (H3K4me2) in addition to a reduction of histone H3 Lys-9 di/tri-methylation [267, 268]. An increase in histone H3K4me2 as well as an increase K9ac is associated with gene re-expression. Furthermore, there have been reports revealing that 5Aza-dC treatment influences histone H3 methylation and acetylation even at genes that are not subject to CpG methylation, since these genes are already expressed [268, 269]. Thus, these authors also found that 5-Aza-dC alters the patterns and levels of histone modifications in local regions independent of CpG methylation status or transcriptional activity. Therefore, 5-Aza-dC might directly influence, in contrast to UHRF1 knockdown, acetylation of histones, even though the mechanism is not fully understood yet.

Even if, no reactivation of our three TSGs takes place, we wanted to investigate the effect of UHRF1 knockdown on tumor cell proliferation. As mentioned above, UHRF1 has been reported to be essential for cell proliferation and UHRF1 knockdown may regulate other genes that mediate an antitumor effect. Depletion of UHRF1 has been shown to reduce the growth rates of several cell types. Transient knockdown of UHRF1 was carried out to examine proliferation of the tumor cell line HUH6 over a timeframe of 168 h. We failed to detect a significant difference in cell viability between control transfected and UHRF1 siRNA transfected cells. This result is in marked contrast to already published studies in breast, gallbladder and colon cancer. In here, a remarkable decrease in proliferation in the human breast cancer cell lines MDA-MB-231 and MCF-7 after UHRF1-shRNA treatment was observed [139]. In addition, UHRF1 depletion in gallbladder cancer cells markedly inhibited proliferation, migration in vitro and the ability of these cells to form tumors in vivo [270]. Knockdown of UHRF1 expression suppressed cellular growth in colon cancer cell lines, HCT-116 and SW620 [134]. Interestingly, there are studies showing that UHRF1 expression is downregulated in apoptosis-induced cells and that UHRF1 promotes the proliferation of breast cancer cells by apoptosis inhibition, G1 phase shortage and promotion of tumor vessel formation [128]. However, it has previously been noted that the consequences of UHRF1 depletion for cell proliferation are rather variable depending on the cell model used [271], which may explain the discrepancies of other tumor cells to our cell line.

Because alterations of chromatin organization are a common mechanism of oncogenesis and several studies have identified a role for UHRF1 in the maintenance of heterochromatin [272], we investigated the influence of UHRF1 knockdown on histone modifications responsible for the condensed chromatin state. Chromatin immunoprecipitation revealed a strong enrichment of H3K27me3 and H3K9me2 on the promoter loci of our three TSGs, histone marks indicative for a suppressed transcriptional state, as observed for our TSGs. The presence of H3K4me2 (activating histone mark) and RNA Poll were hardly detectable. Although UHRF1 knockdown did not reactivate gene expression of our silenced genes HHIP, IGFBP3 and SFRP1, changes in histone marks after knockdown were observed. Downregulation of UHRF1 resulted in significant reduction of repressive histone marks H3K9me2 and H3K27me3 on the promoter regions, while no difference in H3K4me2 has been observed. Consistent with our findings, previous studies demonstrated a decrease of H3K9me2 after UHRF1 depletion which was explained by the disruption of UHRF1/G9a interaction in consequence of decreased UHRF1 levels [273, 274]. UHRF1 has been described to read H3K9me2/3 and to be responsible for the recruitment of the histone lysine methyltransferase G9a, which than performs H3K9 di- and tri-methylation [274]. Thus, the recruitment of G9a, and consequently dimethylation of H3K9, is disturbed, since H3K9me2 decreases after UHRF1 knockdown. This observation emphasizes that UHRF1 acts as an in important interface for mediating methylation of H3K9me2 and to ensure the action and functionality of G9a. Interestingly, there are recent reports that have shown that G9a is also involved in H1 and H3K27 methylation in vivo [275-277]. Our data suggest that the interaction of G9a and UHRF1 might also take part in vitro, since H3K27 methylation decreases after UHRF1 knockdown in our study.

However, a parallel and convergent pathway might also explain the strong enrichment and reduction of H3K27 methylation observed in our study. The Enhancer of zeste 2 (EZH2), a methyltransferase and component of the polycomb repressive complex 2 (PRC2), plays an essential role in the epigenetic maintenance of the H3K27me3 repressive chromatin mark [278], which prevents initiation of transcription. There have been studies showing a strong mechanistic link between EZH2, its associated histone mark, H3K27me3 and DNA methylation [279, 280] an interaction important to ensure a stable repressive state. Interestingly, H3K27me3 and DNA methylation are compatible and overlapping throughout most of the genome, except at CpG islands, where these two marks are mutually exclusive [281]. It has been shown that binding of DNMTs to EZH2-repressed genes depends on the presence of EZH2 and bisulfite genomic sequencing clearly showed that EZH2 is required for DNA methylation of EZH2-target promoters [279]. A remarkable reduction of DNA was observed by depletion of EZH2, methylation at a number of CpG sites within the MYT1 and WNT1 promoters, suggesting that EZH2 directly controls DNA methylation [279, 282, 283] or at least serves as a

recruitment platform for DNA methyltransferases [279]. However, it is not completely understood, which molecular mechanisms link these two systems. The results of our study suggest that UHRF1 plays an important part in this interaction, since UHRF1 strongly interacts with the DNMTs and the depletion of UHRF1 effects both DNA methylation and H3K27me3. Our observation also shows that there is no one-sided dependency of the mechanism since reduction of UHRF1 spans both the DNA methylation and the H3K27me3 methylation. In this context, it would be interesting to further study, the interaction of EZH2 with UHRF1 and in this setting whether UHRF1 depletion directly or indirectly influence histone H3 tri-methylation at lysine 27.

Taking together, our data show that the depletion of UHRF1 alone influences histone modifications and DNA methylation, which are important regulating mechanisms for gene silencing in tumor cells. Nonetheless, the depletion of UHRF1 is not sufficient to reactivate the TSGs HHIP, IGFBP3 and SFRP1 in our hepatoblastoma cells.

Although our study did not show the expected therapeutic potential of UHRF1 regulation on tumor cell growth and we identified a diagnostic and prognostic value of UHRF1 in our tumor set, since we observed a significant overexpression of *UHRF1* in hepatoblastoma tissue compared to normal liver tissue. By investigating parameters relevant for the clinic we were able to show that high levels of UHRF1 are associated with a more advanced tumor state in our hepatoblastoma patients, a phenomenon which has already been shown for lung, bladder and prostate cancers [132, 136, 273]. The high UHRF1 expression observed correlates on the one hand with the C2 signature, predictive for poor prognosis in hepatoblastoma and on the other hand with the lower survival rate, suggesting that a high UHRF1 expression might be used as a marker for worse outcome. Comparably, breast cancer studies have identified powerful associations between clinical parameters and outcome [284]. Breast cancer patients with advanced disease stage, with lymph node metastasis and ERBB2 positive status show significantly high UHRF1 levels in both plasma and tissue. Thus, the expression data are closely related to advanced disease state and prognosis. Additionally, there are similar results for kidney tumors and bladder cancers showing a correlation of UHRF1 expression levels and with a low 5-year survival rate [132]. So far, UHRF1 is suggested to act as prognostic marker in bladder cancer and the cervical cancer. Based on our obtained data we propose UHRF1 as a potential prognostic factor for hepatoblastoma, although further UHRF1 based investigations and analysis need to be performed to confirm and validate UHRF1s possible use as a diagnostic marker for hepatoblastoma.

## 5.3 Perspectives and future plans

The KEAP1-NFE2L2 pathway is the major regulator of cytoprotective responses to endogenous and exogenous stresses caused by reactive oxygen species (ROS) and electrophiles, and therefore provides an interesting research target for studying chemoresistance. In line with this assumption, studies have shown that ectopic expression of NFE2L2 in cancer cell lines that have low basal levels of NFE2L2 renders these cells to be more resistant to a variety of anti-cancer agents, whereas siRNA mediated inhibition of NFE2L2 in cells with high levels of NFE2L2 has been shown to reverse drug resistance [84, 199, 220, 224, 285]. In addition, human cancer cells that have adopted chemotherapeutic resistance have also been shown to express high levels of NFE2L2. For instance, human ovarian cancer cells selected for doxorubicin resistance show elevated NFE2L2 levels in comparison to wild-type cells. A depletion of NFE2L2 restores drug sensitivity in these resistant cells. Thus, it would be highly interesting to stably overexpress NFE2L2 in hepatoblastoma cells in order to study the effect on cell proliferation, survival as well as the response to chemotherapeutic agents. Moreover, it is important to mimic the NFE2L2 mutations observed in our study in order to transfect the NFE2L2 mutations in hepatoblastoma cells to get more information about their roles for proliferation, migration, invasion and their potential to induce chemoresistance. The knockdown of NFE2L2 is another interesting approach for this research to study the susceptibility of cells transfected with NFE2L2 siRNA or control siRNA to chemotherapeutic drugs. It allows investigation of the therapeutic potential of NFE2L2 interference. The effect of NFE2L2 depletion on tumor cells can be validated for further approaches such as the drug development of NFE2L2 inhibitors in cell culture to decrease proliferation and to increase efficiency of chemotherapeutic drugs in hepatoblastoma treatment. The insights that will be gained with these experiments may be of relevance to other solid childhood as well as adult tumors.

Since, the establishment of molecular markers to aid risk stratification of cancer patients is an ongoing endeavor in pediatric oncology; it would be interesting to further study the role of UHRF1 as a prognostic and diagnostic marker for hepatoblastoma patients as it is already suggested in other cancers. As UHRF1 is overexpressed in hepatoblastoma and its expression is associated with a poor prognosis in hepatoblastoma patients, it is important to study more clinicopathological parameters in relation to UHRF1 in order to validate the prognostic significance for UHRF1.

# 6 Summary / Zusammenfassung

## 6.1 Summary

Hepatoblastoma is a malignant disease of the liver. It accounts for about 1 % of all childhood cancers and is the most common malignant liver tumor in infancy. Hepatoblastoma is assumed to arise from immature liver progenitor cells by aberrant activation of genes important in the embryonic development. Based on its early manifestation it is generally assumed that hepatoblastoma displays a relatively normal genomic background.

Whole-exome sequencing performed in our group identified hepatoblastoma as one of the genetically simplest tumors ever described, with recurrent mutations in beta-catenin (CTNNB1) and nuclear factor (erythroid-derived 2)-like 2 (NFE2L2). Based on this finding we performed targeted genotyping of a large cohort of primary hepatoblastomas, hepatoblastoma cell lines and transitional liver cell tumors and identified CTNNB1 and NFE2L2 to be mutated in 72.5 % and 9.8 % of cases, respectively. CTNNB1 is a key effector molecule of canonical WNT signaling pathway, a pathway that is essential in organogenesis and cellular processes such as cell proliferation, differentiation, survival and apoptosis. However, NFE2L2 is involved in the activation of the cellular antioxidant response to combat the harmful effects such as xenobiotics and oxidative stress. Interestingly, all NFE2L2 mutations were located in or adjacent to the DLG and ETGE motifs of the NFE2L2 protein that are needed to get recognized by the KEAP1/CUL3 complex for proteasomal degradation. Functional analysis showed that cells transfected with mutant NFE2L2 were insensitive to KEAP1-mediated downregulation of NFE2L2 signaling and that depletion of the NFE2L2 via siRNA downregulates the NAD(P)H dehydrogenase (quinine) 1 (NQO1), a target gene of NFE2L2, and inhibits proliferation. In the clinical setting, NQO1 overexpression in tumors was significantly associated with metastasis, vascular invasion, the adverse prognostic C2 gene signature as well as poor outcome.

RNA sequencing in our group identified the ubiquitin-like with PHD and ring finger domains 1 (UHRF1), a protein known to preferentially bind to hemi-methylated DNA, to be highly overexpressed in hepatoblastoma tumors. UHRF1 is as a key regulator in the epigenetic crosstalk, by controlling DNA methylation and histone modification. Using immunoprecipitation, we were able to show that UHRF1 binds in concert with DNA methyltransferase 1 (DNMT1) and ubiquitin specific peptidase 7 (USP7) as a trimeric complex to promoter regions of tumor suppressor genes (TSG) relevant in hepatoblastoma, such as hedgehog interacting protein (HHIP), insulin-like growth factor binding protein 3 (IGFBP3), and secreted frizzled-related protein 1 (SFRP1). These genes are epigenetically silenced in

hepatoblastoma, as evidenced by heavy DNA methylation and enrichment of the repressive H3K27me3 and H3K9me2 chromatin mark. Interestingly, knockdown of UHRF1 expression via RNA interference resulted in promoter demethylation, but no reactivation of TSG gene expression. Additionally, no effect on tumor cell proliferation was observed after UHRF1 knockdown. Chromatin immunoprecipitation experiments revealed a decrease of the repressive chromatin marks H3K27me3 and H3K9me2 after UHRF1 depletion, but neither a clear shift towards the active H3K4me2 chromatin mark nor enrichment of RNA Polymerase at the TSG loci was observed. Statistical analyses revealed that a high expression of UHRF1 was associated with advanced disease state and a worse overall survival.

Taken together our study demonstrates that activation of WNT signaling in concert with activation of the NFE2L2-KEAP1 pathway might be the driving force in the development of liver cancers. Moreover, we defined aberrant NQO1 expression as a marker for adverse course of disease and poor outcome. In addition, we showed that an aberrant expression of the epigenetic regulator UHRF1 and its excessive binding on promoter regions results in methylation of TSGs. This may represent an important mechanism in the initial phases of embryonal tumorigenesis. However, UHRF1 depletion alone was not sufficient to re-induce TSG expression. Therefore, UHRF1 might be more useful as a biomarker for the prognosis of hepatoblastoma than a direct anti-cancer target for hepatoblastoma therapy.

## 6.2 Zusammenfassung

Das Hepatoblastom ist der häufigste maligne Lebertumor im Kindesalter und nimmt ca. 1 % aller malignen Tumoren des Kindesalters ein. Die auffallend frühe Manifestation lässt vermuten, dass vergleichsweise wenige genetische Schritte bis zum malignen Phänotyp notwendig sind und es dadurch einen relativ normalen genomischen Hintergrund aufweist. Da neben genetischen Veränderungen auch epigenetische Veränderungen zur Tumorentstehung beitragen können, war es Ziel dieser Arbeit, bereits bekannte Mutationen in unserer Tumorkohorte zu überprüfen und/oder epigenetischen Veränderungen im Hepatoblastom zu identifizieren, die bei der Tumorentstehung und Progression eine Rolle spielen könnten.

Mit Hilfe der Exom-Sequenzierungs Technologie konnte das Hepatoblastom als genetisch einfacher Tumor identifiziert werden. Wiederkehrende Mutationen fanden sich im beta-catenin (CTNNB1) Gen und im Transkriptionsfaktor Nuclear factor (erythroid-derived 2)-like 2 (NFE2L2). Auf Grundlage der

erwähnten Studie, wurde in dieser Arbeit eine gezielte Genotypisierung einer großen Kohorte an Hepatoblastomen, transitionalen Leberzelltumoren sowie von Hepatoblastom-Zelllinien durchgeführt. Hierbei konnte gezeigt werden, dass 72,5 % aller untersuchten Fälle eine CTNNB1 Mutation und 9,8 % aller Fälle eine NFE2L2 Mutation tragen. CTNNB1 ist ein Schlüssel Effektormolekül des WNT-Signalwegs, der im wesentlich an der Organogenese und zellulären Prozessen, wie Zellproliferation, Differenzierung und Apoptose beteiligt ist. NFE2L2 hingegen ist bei der Aktivierung der zellulären Antioxidationsprozesse beteiligt, die der Bekämpfung von oxidativen Stress aber auch der Eliminierung von schädlichen Stoffen dienen. Interessanterweise lagen die NFE2L2 Mutationen in oder benachbart zum DLG- oder ETGE-Motiv des NFE2L2 Proteins, die als Erkennungssequenz für den proteasomalen Abbau dienen. Die identifizierten NFE2L2 Mutationen wurden im Laufe dieser Arbeit kloniert und in unterschiedliche Zelllinien eingebracht. Transfizierte Zellen, die das mutierte NFE2L2 tragen, zeigten sich unempfindlicher gegenüber dem KEAP1 vermittelte Abbau. Darüber hinaus konnte gezeigt werden, dass die Überexpression der NAD(P)H dehydrogenase (quinine) 1 (NQO1), einem Zielgen von NFE2L2, verstärkt in Fällen mit NFE2L2 Mutation auftritt und stark mit der Metastasierung, der Gefäßinvasion, der Gen-Signatur C2 und schlechter Prognose assoziiert ist. Der Knockdown von NFE2L2 bewirkt eine verminderte Expression von NQO1 sowie eine verminderter Zellproliferation.

In dieser Arbeit konnte außerdem eine stark erhöhte Expression des UHRF1-Gens in Hepatoblastomen beobachtet werden. UHRF1, ist ein Protein, das bevorzugt an hemi-methylierte DNA bindet und die DNA Methyltransferase 1 (DNMT1) rekrutiert. UHRF1 nimmt eine Schlüsselrolle in der epigenetischen Regulation ein, da es sowohl die DNA-Methylierung als auch bestimmte Histonmodifikationen vermittelt. UHRF1 bindet zusammen mit DNMT1 und der Ubiquitin-spezifischen Peptidase 7 (USP7) an die Promoterregionen des Hedgehog interacting Proteins (HHIP), des Insulin-like growth factor-binding Proteins 3 (IGFBP3) und des Secreted frizzled-related Proteins 1 (SFRP1), Tumorsuppressorgene (TSG), die eine relevante Rolle in der Hepatoblastomentstehung und Progression spielen. Die starke DNA-Methylierung sowie die Anreicherung der reprimierenden Histonmarks H3K27me3 und H3K9me2 im Promoterbereich führen zum epigenetischen Stilllegen ihrer Genaktivität. Ein gezielter Knockdown von UHRF1 bedingt eine Demethylierung der Promotoren, jedoch keine Reaktivierung der TSG Expression. Auch im Wachstum der Tumorzellen konnte keine Veränderung beobachtet werden. Die näherer Betrachtung der Chromatinstruktur nach UHRF1 Knockdown zeigte eine Verminderung der repressiven Chromatinmarks H3K27me3 und H3K9me2, jedoch weder Verschiebung in Richtung des aktivierenden H3K4me2 Histonmarks noch eine Anreicherung der RNA-Polymerase. Darüber hinaus konnte gezeigt werden, dass eine hohe

Expression von UHRF1 im Zusammenhang mit einem fortgeschrittenen Krankheitszustand (aggressiver Tumortyp) und einer schlechteren Gesamtüberlebensrate steht.

Zusammenfassend lässt sich sagen, dass die Aktivierung der WNT Signalwegs in Kombination mit der Aktivierung des NFE2L2-KEAP1 Signalwegs als eine der treibenden Kräfte in der Leberkrebs-entwicklung angesehen werden kann. Darüber hinaus waren wir in der Lage, die veränderte Expression von NQO1 als Marker für einen ungünstigen Krankheitsverlauf und schlechte Prognose zu identifizieren. In dieser Arbeit konnte außerdem gezeigt werden, dass UHRF1 stark an der Methylierung von TSG beteiligt ist, einem Prozess der zur Stilllegung der Genaktivität führt und als wichtiger Mechanismus in den ersten Phasen der embryonalen Tumorentstehung betrachtet wird. Der Knockdown von UHRF1 allein ist allerdings nicht ausreichend, um die Genexpression zu reaktivieren, welches die Annahme zulässt, dass neben der Methylierung, andere Prozesse eine wichtige Rolle in der Stilllegung von TSG spielen. Aus klinischer Sicht stellt sich UHRF1 jedoch als nützlicher Biomarker für die Prognose von Hepatoblastomen dar.

# 7 References


1. Eichenmuller, M., et al., *The genomic landscape of hepatoblastoma and their progenies with HCC-like features.* J Hepatol, 2014.
2. Steliarova-Foucher, E., et al., *Geographical patterns and time trends of cancer incidence and survival among children and adolescents in Europe since the 1970s (the ACCISproject): an epidemiological study.* Lancet, 2004. **364**(9451): p. 2097-105.
3. Gatta, G., et al., *Childhood cancer survival in Europe 1999-2007: results of EUROCARE-5--a population-based study.* Lancet Oncol, 2014. **15**(1): p. 35-47.
4. Howlader N, N.A., Krapcho M, Garshell J, Miller D, Altekruse SF, Kosary CL, Yu M, Ruhl J, Tatalovich Z,Mariotto A, Lewis DR, Chen HS, Feuer EJ, Cronin KA (eds). SEER Cancer Statistics Review, 1975-2011, National Cancer Institute. Bethesda, MD, http://seer.cancer.gov/csr/1975_2011/, based on November 2013 SEER data submission, posted to the SEER web site, April 2014.
5. Miller, R.W., J.L. Young, Jr., and B. Novakovic, *Childhood cancer.* Cancer, 1995. **75**(1 Suppl): p. 395-405.
6. Stiller, C.A., *Epidemiology and genetics of childhood cancer.* Oncogene, 2004. **23**(38): p. 6429-44.
7. Perilongo, G. and E.A. Shafford, *Liver tumours.* Eur J Cancer, 1999. **35**(6): p. 953-8; discussion 958-9.
8. Weinberg, A.G. and M.J. Finegold, *Primary hepatic tumors of childhood.* Hum Pathol, 1983. **14**(6): p. 512-37.
9. Meyers, R.L., *Tumors of the liver in children.* Surg Oncol, 2007. **16**(3): p. 195-203.
10. Perilongo, G., et al., *Risk-adapted treatment for childhood hepatoblastoma. final report of the second study of the International Society of Paediatric Oncology--SIOPEL 2.* Eur J Cancer, 2004. **40**(3): p. 411-21.
11. Pritchard, J., et al., *Cisplatin, doxorubicin, and delayed surgery for childhood hepatoblastoma: a successful approach--results of the first prospective study of the International Society of Pediatric Oncology.* J Clin Oncol, 2000. **18**(22): p. 3819-28.
12. Ortega, J.A., et al., *Randomized comparison of cisplatin/vincristine/fluorouracil and cisplatin/continuous infusion doxorubicin for treatment of pediatric hepatoblastoma: A report from the Children's Cancer Group and the Pediatric Oncology Group.* J Clin Oncol, 2000. **18**(14): p. 2665-75.
13. Spector, L.G., J.H. Feusner, and J.A. Ross, *Hepatoblastoma and low birth weight.* Pediatr Blood Cancer, 2004. **43**(6): p. 706.
14. Ross, J.A., *Hepatoblastoma and birth weight: too little, too big, or just right?* J Pediatr, 1997. **130**(4): p. 516-7.
15. Stocker, J.T., *Hepatoblastoma.* Semin Diagn Pathol, 1994. **11**(2): p. 136-43.
16. Haas, J.E., et al., *Histopathology and prognosis in childhood hepatoblastoma and hepatocarcinoma.* Cancer, 1989. **64**(5): p. 1082-95.
17. Wu, J.T., L. Book, and K. Sudar, *Serum alpha fetoprotein (AFP) levels in normal infants.* Pediatr Res, 1981. **15**(1): p. 50-2.
18. Tsuchida, Y., et al., *Evaluation of alpha-fetoprotein in early infancy.* J Pediatr Surg, 1978. **13**(2): p. 155-62.
19. De Ioris, M., et al., *Hepatoblastoma with a low serum alpha-fetoprotein level at diagnosis: the SIOPEL group experience.* Eur J Cancer, 2008. **44**(4): p. 545-50.
20. Koh, K.N., et al., *Prognostic implications of serum alpha-fetoprotein response during treatment of hepatoblastoma.* Pediatr Blood Cancer, 2011. **57**(4): p. 554-60.
21. Brown, J., et al., *Pretreatment prognostic factors for children with hepatoblastoma-- results from the International Society of Paediatric Oncology (SIOP) study SIOPEL 1.* Eur J Cancer, 2000. **36**(11): p. 1418-25.
22. Schnater, J.M., et al., *Where do we stand with hepatoblastoma? A review.* Cancer, 2003. **98**(4): p. 668-78.
23. Roebuck, D.J., et al., *2005 PRETEXT: a revised staging system for primary malignant liver tumours of childhood developed by the SIOPEL group.* Pediatr Radiol, 2007. **37**(2): p. 123-32; quiz 249-50.
24. Litten, J.B. and G.E. Tomlinson, *Liver tumors in children.* Oncologist, 2008. **13**(7): p. 812-20.
25. Meyers, R.L., H.M. Katzenstein, and M.H. Malogolowkin, *Predictive value of staging systems in hepatoblastoma.* J Clin Oncol, 2007. **25**(6): p. 737; author reply 737-8.
26. Cairo, S., et al., *Hepatic stem-like phenotype and interplay of Wnt/beta-catenin and Myc signaling in aggressive childhood liver cancer.* Cancer Cell, 2008. **14**(6): p. 471-84.

27. Goga, A., et al., *Inhibition of CDK1 as a potential therapy for tumors over-expressing MYC.* Nat Med, 2007. **13**(7): p. 820-7.
28. Haeberle, B. and D. Schweinitz, *Treatment of hepatoblastoma in the German cooperative pediatric liver tumor studies.* Front Biosci (Elite Ed), 2012. **4**: p. 493-8.
29. Zsiros, J., et al., *Successful treatment of childhood high-risk hepatoblastoma with dose-intensive multiagent chemotherapy and surgery: final results of the SIOPEL-3HR study.* J Clin Oncol, 2010. **28**(15): p. 2584-90.
30. Oue, T., et al., *Transcatheter arterial chemoembolization in the treatment of hepatoblastoma.* J Pediatr Surg, 1998. **33**(12): p. 1771-5.
31. Han, Y.M., et al., *Effectiveness of preoperative transarterial chemoembolization in presumed inoperable hepatoblastoma.* J Vasc Interv Radiol, 1999. **10**(9): p. 1275-80.
32. Sue, K., et al., *Intrahepatic arterial injections of cisplatin-phosphatidylcholine-Lipiodol suspension in two unresectable hepatoblastoma cases.* Med Pediatr Oncol, 1989. **17**(6): p. 496-500.
33. Czauderna, P., *Hepatoblastoma throughout SIOPEL trials - clinical lessons learnt.* Front Biosci (Elite Ed), 2012. **4**: p. 470-9.
34. Sivaprakasam, P., et al., *Survival and long-term outcomes in children with hepatoblastoma treated with continuous infusion of cisplatin and doxorubicin.* J Pediatr Hematol Oncol, 2011. **33**(6): p. e226-30.
35. Knight, K.R., D.F. Kraemer, and E.A. Neuwelt, *Ototoxicity in children receiving platinum chemotherapy: underestimating a commonly occurring toxicity that may influence academic and social development.* J Clin Oncol, 2005. **23**(34): p. 8588-96.
36. Schultz, K.A., et al., *Behavioral and social outcomes in adolescent survivors of childhood cancer: a report from the childhood cancer survivor study.* J Clin Oncol, 2007. **25**(24): p. 3649-56.
37. Chang, M.H., *Hepatocellular carcinoma in children.* Zhonghua Min Guo Xiao Er Ke Yi Xue Hui Za Zhi, 1998. **39**(6): p. 366-70.
38. Yu, S.B., et al., *Clinical characteristics and prognosis of pediatric hepatocellular carcinoma.* World J Surg, 2006. **30**(1): p. 43-50.
39. Czauderna, P., et al., *Hepatocellular carcinoma in children: results of the first prospective study of the International Society of Pediatric Oncology group.* J Clin Oncol, 2002. **20**(12): p. 2798-804.
40. Prokurat, A., et al., *Transitional liver cell tumors (TLCT) in older children and adolescents: a novel group of aggressive hepatic tumors expressing beta-catenin.* Med Pediatr Oncol, 2002. **39**(5): p. 510-8.
41. Tomlinson, G.E. and R. Kappler, *Genetics and epigenetics of hepatoblastoma.* Pediatr Blood Cancer, 2012. **59**(5): p. 785-92.
42. Kingston, J.E., G.J. Draper, and J.R. Mann, *Hepatoblastoma and polyposis coli.* Lancet, 1982. **1**(8269): p. 457.
43. Buckley, J.D., et al., *A case-control study of risk factors for hepatoblastoma. A report from the Childrens Cancer Study Group.* Cancer, 1989. **64**(5): p. 1169-76.
44. Hughes, L.J. and V.V. Michels, *Risk of hepatoblastoma in familial adenomatous polyposis.* Am J Med Genet, 1992. **43**(6): p. 1023-5.
45. Fukuzawa, R., et al., *Beckwith-Wiedemann syndrome-associated hepatoblastoma: wnt signal activation occurs later in tumorigenesis in patients with 11p15.5 uniparental disomy.* Pediatr Dev Pathol, 2003. **6**(4): p. 299-306.
46. DeBaun, M.R. and M.A. Tucker, *Risk of cancer during the first four years of life in children from The Beckwith-Wiedemann Syndrome Registry.* J Pediatr, 1998. **132**(3 Pt 1): p. 398-400.
47. Mateos, M.E., et al., *Simpson-Golabi-Behmel syndrome type 1 and hepatoblastoma in a patient with a novel exon 2-4 duplication of the GPC3 gene.* Am J Med Genet A, 2013. **161A**(5): p. 1091-5.
48. Kato, M., et al., *Hepatoblastoma in a patient with sotos syndrome.* J Pediatr, 2009. **155**(6): p. 937-9.
49. Mussa, A., et al., *The overlap between Sotos and Beckwith-Wiedemann syndromes.* J Pediatr, 2010. **156**(6): p. 1035-6; author reply 1036.
50. Swarts, S., J. Wisecarver, and J.A. Bridge, *Significance of extra copies of chromosome 20 and the long arm of chromosome 2 in hepatoblastoma.* Cancer Genet Cytogenet, 1996. **91**(1): p. 65-7.
51. Tomlinson, G.E., *Cytogenetics of hepatoblastoma.* Front Biosci (Elite Ed), 2012. **4**: p. 1287-92.
52. Weber, R.G., et al., *Characterization of genomic alterations in hepatoblastomas. A role for gains on chromosomes 8q and 20 as predictors of poor outcome.* Am J Pathol, 2000. **157**(2): p. 571-8.
53. Schneider, N.R., et al., *The first recurring chromosome translocation in hepatoblastoma: der(4)t(1;4)(q12;q34).* Genes Chromosomes Cancer, 1997. **19**(4): p. 291-4.
54. Tomlinson, G.E., et al., *Cytogenetic evaluation of a large series of hepatoblastomas: numerical abnormalities with recurring aberrations involving 1q12-q21.* Genes Chromosomes Cancer, 2005. **44**(2): p. 177-84.

55. Hartmann, W., et al., *Activation of phosphatidylinositol-3'-kinase/AKT signaling is essential in hepatoblastoma survival.* Clin Cancer Res, 2009. **15**(14): p. 4538-45.
56. Rumbajan, J.M., et al., *Comprehensive analyses of imprinted differentially methylated regions reveal epigenetic and genetic characteristics in hepatoblastoma.* BMC Cancer, 2013. **13**: p. 608.
57. Zatkova, A., et al., *Amplification and overexpression of the IGF2 regulator PLAG1 in hepatoblastoma.* Genes Chromosomes Cancer, 2004. **39**(2): p. 126-37.
58. Koch, A., et al., *Childhood hepatoblastomas frequently carry a mutated degradation targeting box of the beta-catenin gene.* Cancer Res, 1999. **59**(2): p. 269-73.
59. Cadigan, K.M. and R. Nusse, *Wnt signaling: a common theme in animal development.* Genes Dev, 1997. **11**(24): p. 3286-305.
60. Morin, P.J., et al., *Activation of beta-catenin-Tcf signaling in colon cancer by mutations in beta-catenin or APC.* Science, 1997. **275**(5307): p. 1787-90.
61. Rubinfeld, B., et al., *Stabilization of beta-catenin by genetic defects in melanoma cell lines.* Science, 1997. **275**(5307): p. 1790-2.
62. Sakanaka, C., J.B. Weiss, and L.T. Williams, *Bridging of beta-catenin and glycogen synthase kinase3beta by axin and inhibition of beta-catenin-mediated transcription.* Proc Natl Acad Sci U S A, 1998. **95**(6): p. 3020-3.
63. Behrens, J., et al., *Functional interaction of beta-catenin with the transcription factor LEF-1.* Nature, 1996. **382**(6592): p. 638-42.
64. Huber, O., et al., *Nuclear localization of beta-catenin by interaction with transcription factor LEF-1.* Mech Dev, 1996. **59**(1): p. 3-10.
65. Shtutman, M., et al., *The cyclin D1 gene is a target of the beta-catenin/LEF-1 pathway.* Proc Natl Acad Sci U S A, 1999. **96**(10): p. 5522-7.
66. He, T.C., et al., *Identification of c-MYC as a target of the APC pathway.* Science, 1998. **281**(5382): p. 1509-12.
67. Kioussi, C., et al., *Identification of a Wnt/Dvl/beta-Catenin --> Pitx2 pathway mediating cell-typespecific proliferation during development.* Cell, 2002. **111**(5): p. 673-85.
68. Oda, H., et al., *Somatic mutations of the APC gene in sporadic hepatoblastomas.* Cancer Res, 1996. **56**(14): p. 3320-3.
69. Taniguchi, K., et al., *Mutational spectrum of beta-catenin, AXIN1, and AXIN2 in hepatocellular carcinomas and hepatoblastomas.* Oncogene, 2002. **21**(31): p. 4863-71.
70. Koch, A., et al., *Mutations and elevated transcriptional activity of conductin (AXIN2) in hepatoblastomas.* J Pathol, 2004. **204**(5): p. 546-54.
71. de La Coste, A., et al., *Somatic mutations of the beta-catenin gene are frequent in mouse and human hepatocellular carcinomas.* Proc Natl Acad Sci U S A, 1998. **95**(15): p. 8847-51.
72. Buendia, M.A., *Genetic alterations in hepatoblastoma and hepatocellular carcinoma: common and distinctive aspects.* Med Pediatr Oncol, 2002. **39**(5): p. 530-5.
73. Mokkapati, S., et al., *beta-catenin activation in a novel liver progenitor cell type is sufficient to cause hepatocellular carcinoma and hepatoblastoma.* Cancer Res, 2014. **74**(16): p. 4515-25.
74. Harada, N., et al., *Lack of tumorigenesis in the mouse liver after adenovirus-mediated expression of a dominant stable mutant of beta-catenin.* Cancer Res, 2002. **62**(7): p. 1971-7.
75. Cadoret, A., et al., *Hepatomegaly in transgenic mice expressing an oncogenic form of beta-catenin.* Cancer Res, 2001. **61**(8): p. 3245-9.
76. Vilarinho, S., et al., *Paediatric hepatocellular carcinoma due to somatic CTNNB1 and NFE2L2 mutations in the setting of inherited bi-allelic ABCB11 mutations.* J Hepatol, 2014.
77. Zhang, Y. and G.B. Gordon, *A strategy for cancer prevention: stimulation of the Nrf2-ARE signaling pathway.* Mol Cancer Ther, 2004. **3**(7): p. 885-93.
78. Lau, A., et al., *Dual roles of Nrf2 in cancer.* Pharmacol Res, 2008. **58**(5-6): p. 262-70.
79. Abazeed, M.E., et al., *Integrative radiogenomic profiling of squamous cell lung cancer.* Cancer Res, 2013. **73**(20): p. 6289-98.
80. Hirotsu, Y., et al., *Nrf2-MafG heterodimers contribute globally to antioxidant and metabolic networks.* Nucleic Acids Res, 2012. **40**(20): p. 10228-39.
81. Itoh, K., et al., *An Nrf2/small Maf heterodimer mediates the induction of phase II detoxifying enzyme genes through antioxidant response elements.* Biochem Biophys Res Commun, 1997. **236**(2): p. 313-22.
82. Nguyen, T., H.C. Huang, and C.B. Pickett, *Transcriptional regulation of the antioxidant response element. Activation by Nrf2 and repression by MafK.* J Biol Chem, 2000. **275**(20): p. 15466-73.
83. Sporn, M.B. and K.T. Liby, *NRF2 and cancer: the good, the bad and the importance of context.* Nat Rev Cancer, 2012. **12**(8): p. 564-71.

84. Homma, S., et al., *Nrf2 enhances cell proliferation and resistance to anticancer drugs in human lung cancer.* Clin Cancer Res, 2009. **15**(10): p. 3423-32.
85. Vilarinho, S., et al., *Paediatric hepatocellular carcinoma due to somatic CTNNB1 and NFE2L2 mutations in the setting of inherited bi-allelic ABCB11 mutations.* J Hepatol, 2014. **61**(5): p. 1178-83.
86. Bird, A., *DNA methylation patterns and epigenetic memory.* Genes Dev, 2002. **16**(1): p. 6-21.
87. Jones, P.A. and S.B. Baylin, *The fundamental role of epigenetic events in cancer.* Nat Rev Genet, 2002. **3**(6): p. 415-28.
88. Rodenhiser, D. and M. Mann, *Epigenetics and human disease: translating basic biology into clinical applications.* CMAJ, 2006. **174**(3): p. 341-8.
89. Kouzarides, T., *Chromatin modifications and their function.* Cell, 2007. **128**(4): p. 693-705.
90. Verdone, L., M. Caserta, and E. Di Mauro, *Role of histone acetylation in the control of gene expression.* Biochem Cell Biol, 2005. **83**(3): p. 344-53.
91. Wade, P.A., *Transcriptional control at regulatory checkpoints by histone deacetylases: molecular connections between cancer and chromatin.* Hum Mol Genet, 2001. **10**(7): p. 693-8.
92. Vermeulen, M., et al., *Selective anchoring of TFIID to nucleosomes by trimethylation of histone H3 lysine 4.* Cell, 2007. **131**(1): p. 58-69.
93. Bernstein, B.E., A. Meissner, and E.S. Lander, *The mammalian epigenome.* Cell, 2007. **128**(4): p. 66981.
94. Wang, Z., et al., *Combinatorial patterns of histone acetylations and methylations in the human genome.* Nat Genet, 2008. **40**(7): p. 897-903.
95. Kim, J., et al., *Tudor, MBT and chromo domains gauge the degree of lysine methylation.* EMBO Rep, 2006. **7**(4): p. 397-403.
96. Smith, B.C. and J.M. Denu, *Chemical mechanisms of histone lysine and arginine modifications.* Biochim Biophys Acta, 2009. **1789**(1): p. 45-57.
97. Shilatifard, A., *Chromatin modifications by methylation and ubiquitination: implications in the regulation of gene expression.* Annu Rev Biochem, 2006. **75**: p. 243-69.
98. Wysocka, J., *Identifying novel proteins recognizing histone modifications using peptide pull-down assay.* Methods, 2006. **40**(4): p. 339-43.
99. Eissenberg, J.C., *Molecular biology of the chromo domain: an ancient chromatin module comes of age.* Gene, 2001. **275**(1): p. 19-29.
100. Shi, X., et al., *Proteome-wide analysis in Saccharomyces cerevisiae identifies several PHD fingers as novel direct and selective binding modules of histone H3 methylated at either lysine 4 or lysine 36.* J Biol Chem, 2007. **282**(4): p. 2450-5.
101. Wysocka, J., et al., *WDR5 associates with histone H3 methylated at K4 and is essential for H3 K4 methylation and vertebrate development.* Cell, 2005. **121**(6): p. 859-72.
102. Razin, A. and A.D. Riggs, *DNA methylation and gene function.* Science, 1980. **210**(4470): p. 604-10.
103. Bestor, T.H., *The DNA methyltransferases of mammals.* Hum Mol Genet, 2000. **9**(16): p. 2395-402.
104. Raynal, N.J., et al., *DNA methylation does not stably lock gene expression but instead serves as a molecular mark for gene silencing memory.* Cancer Res, 2012. **72**(5): p. 1170-81.
105. Leonhardt, H., et al., *A targeting sequence directs DNA methyltransferase to sites of DNA replication in mammalian nuclei.* Cell, 1992. **71**(5): p. 865-73.
106. Luijsterburg, M.S., et al., *The major architects of chromatin: architectural proteins in bacteria, archaea and eukaryotes.* Crit Rev Biochem Mol Biol, 2008. **43**(6): p. 393-418.
107. Bachman, K.E., M.R. Rountree, and S.B. Baylin, *Dnmt3a and Dnmt3b are transcriptional repressors that exhibit unique localization properties to heterochromatin.* J Biol Chem, 2001. **276**(34): p. 32282-7.
108. Latham, T., N. Gilbert, and B. Ramsahoye, *DNA methylation in mouse embryonic stem cells and development.* Cell Tissue Res, 2008. **331**(1): p. 31-55.
109. Robertson, K.D., *DNA methylation and chromatin - unraveling the tangled web.* Oncogene, 2002. **21**(35): p. 5361-79.
110. Hermann, A., H. Gowher, and A. Jeltsch, *Biochemistry and biology of mammalian DNA methyltransferases.* Cell Mol Life Sci, 2004. **61**(19-20): p. 2571-87.
111. Ehrlich, M., et al., *Amount and distribution of 5-methylcytosine in human DNA from different types of tissues of cells.* Nucleic Acids Res, 1982. **10**(8): p. 2709-21.
112. Wang, Y. and F.C. Leung, *An evaluation of new criteria for CpG islands in the human genome as gene markers.* Bioinformatics, 2004. **20**(7): p. 1170-7.
113. Hoelzer, K., L.A. Shackelton, and C.R. Parrish, *Presence and role of cytosine methylation in DNA viruses of animals.* Nucleic Acids Res, 2008. **36**(9): p. 2825-37.
114. Esteller, M., *Epigenetics in cancer.* N Engl J Med, 2008. **358**(11): p. 1148-59.

115. Alhosin, M., et al., *Down-regulation of UHRF1, associated with re-expression of tumor suppressor genes, is a common feature of natural compounds exhibiting anti-cancer properties.* J Exp Clin Cancer Res, 2011. **30**: p. 41.
116. Unoki, M., T. Nishidate, and Y. Nakamura, *ICBP90, an E2F-1 target, recruits HDAC1 and binds to methyl-CpG through its SRA domain.* Oncogene, 2004. **23**(46): p. 7601-10.
117. Bronner, C., et al., *UHRF1 Links the Histone code and DNA Methylation to ensure Faithful Epigenetic Memory Inheritance.* Genet Epigenet, 2010. **2009**(2): p. 29-36.
118. Sharif, J., et al., *The SRA protein Np95 mediates epigenetic inheritance by recruiting Dnmt1 to methylated DNA.* Nature, 2007. **450**(7171): p. 908-12.
119. Berkyurek, A.C., et al., *The DNA methyltransferase Dnmt1 directly interacts with the SET and RING finger-associated (SRA) domain of the multifunctional protein Uhrf1 to facilitate accession of the catalytic center to hemi-methylated DNA.* J Biol Chem, 2014. **289**(1): p. 379-86.
120. Cheng, J., et al., *Structural insight into coordinated recognition of trimethylated histone H3 lysine 9 (H3K9me3) by the plant homeodomain (PHD) and tandem tudor domain (TTD) of UHRF1 (ubiquitinlike, containing PHD and RING finger domains, 1) protein.* J Biol Chem, 2013. **288**(2): p. 1329-39.
121. Jin, W., et al., *UHRF1 is associated with epigenetic silencing of BRCA1 in sporadic breast cancer.* Breast Cancer Res Treat, 2010. **123**(2): p. 359-73.
122. Bostick, M., et al., *UHRF1 plays a role in maintaining DNA methylation in mammalian cells.* Science, 2007. **317**(5845): p. 1760-4.
123. Muto, M., et al., *Targeted disruption of Np95 gene renders murine embryonic stem cells hypersensitive to DNA damaging agents and DNA replication blocks.* J Biol Chem, 2002. **277**(37): p. 34549-55.
124. Bonapace, I.M., et al., *Np95 is regulated by E1A during mitotic reactivation of terminally differentiated cells and is essential for S phase entry.* J Cell Biol, 2002. **157**(6): p. 909-14.
125. Jenkins, Y., et al., *Critical role of the ubiquitin ligase activity of UHRF1, a nuclear RING finger protein, in tumor cell growth.* Mol Biol Cell, 2005. **16**(12): p. 5621-9.
126. Tien, A.L., et al., *UHRF1 depletion causes a G2/M arrest, activation of DNA damage response and apoptosis.* Biochem J, 2011. **435**(1): p. 175-85.
127. Arima, Y., et al., *Down-regulation of nuclear protein ICBP90 by p53/p21Cip1/WAF1-dependent DNAdamage checkpoint signals contributes to cell cycle arrest at G1/S transition.* Genes Cells, 2004. **9**(2): p. 131-42.
128. Abbady, A.Q., et al., *ICBP90 expression is downregulated in apoptosis-induced Jurkat cells.* Ann N Y Acad Sci, 2003. **1010**: p. 300-3.
129. Hopfner, R., et al., *ICBP90, a novel human CCAAT binding protein, involved in the regulation of topoisomerase IIalpha expression.* Cancer Res, 2000. **60**(1): p. 121-8.
130. Mousli, M., et al., *ICBP90 belongs to a new family of proteins with an expression that is deregulated in cancer cells.* Br J Cancer, 2003. **89**(1): p. 120-7.
131. Jeanblanc, M., et al., *The retinoblastoma gene and its product are targeted by ICBP90: a key mechanism in the G1/S transition during the cell cycle.* Oncogene, 2005. **24**(49): p. 7337-45.
132. Unoki, M., et al., *UHRF1 is a novel molecular marker for diagnosis and the prognosis of bladder cancer.* Br J Cancer, 2009. **101**(1): p. 98-105.
133. Crnogorac-Jurcevic, T., et al., *Proteomic analysis of chronic pancreatitis and pancreatic adenocarcinoma.* Gastroenterology, 2005. **129**(5): p. 1454-63.
134. Kofunato, Y., et al., *UHRF1 expression is upregulated and associated with cellular proliferation in colorectal cancer.* Oncol Rep, 2012. **28**(6): p. 1997-2002.
135. Mudbhary, R., et al., *UHRF1 Overexpression Drives DNA Hypomethylation and Hepatocellular Carcinoma.* Cancer Cell, 2014. **25**(2): p. 196-209.
136. Unoki, M., et al., *UHRF1 is a novel diagnostic marker of lung cancer.* Br J Cancer, 2010. **103**(2): p. 217-22.
137. Lorenzato, M., et al., *Cell cycle and/or proliferation markers: what is the best method to discriminate cervical high-grade lesions?* Hum Pathol, 2005. **36**(10): p. 1101-7.
138. Mulder, K.W., et al., *Diverse epigenetic strategies interact to control epidermal differentiation.* Nat Cell Biol, 2012. **14**(7): p. 753-63.
139. Yan, F., et al., *Inhibition effect of siRNA-downregulated UHRF1 on breast cancer growth.* Cancer Biother Radiopharm, 2011. **26**(2): p. 183-9.
140. Daskalos, A., et al., *UHRF1-mediated tumor suppressor gene inactivation in nonsmall cell lung cancer.* Cancer, 2011. **117**(5): p. 1027-37.

141. Felle, M., et al., *The USP7/Dnmt1 complex stimulates the DNA methylation activity of Dnmt1 and regulates the stability of UHRF1.* Nucleic Acids Res, 2011. **39**(19): p. 8355-65.
142. Robert, M.F., et al., *DNMT1 is required to maintain CpG methylation and aberrant gene silencing in human cancer cells.* Nat Genet, 2003. **33**(1): p. 61-5.
143. Freitag, M. and E.U. Selker, *Controlling DNA methylation: many roads to one modification.* Curr Opin Genet Dev, 2005. **15**(2): p. 191-9.
144. Qin, W., H. Leonhardt, and F. Spada, *Usp7 and Uhrf1 control ubiquitination and stability of the maintenance DNA methyltransferase Dnmt1.* J Cell Biochem, 2011. **112**(2): p. 439-44.
145. Scotting, P.J., D.A. Walker, and G. Perilongo, *Childhood solid tumours: a developmental disorder.* Nat Rev Cancer, 2005. **5**(6): p. 481-8.
146. Hayslip, J. and A. Montero, *Tumor suppressor gene methylation in follicular lymphoma: a comprehensive review.* Mol Cancer, 2006. **5**: p. 44.
147. Eichenmuller, M., et al., *Blocking the hedgehog pathway inhibits hepatoblastoma growth.* Hepatology, 2009. **49**(2): p. 482-90.
148. Regel, I., et al., *IGFBP3 impedes aggressive growth of pediatric liver cancer and is epigenetically silenced in vascular invasive and metastatic tumors.* Mol Cancer, 2012. **11**: p. 9.
149. Bellusci, S., et al., *Involvement of Sonic hedgehog (Shh) in mouse embryonic lung growth and morphogenesis.* Development, 1997. **124**(1): p. 53-63.
150. Hardcastle, Z., et al., *The Shh signalling pathway in tooth development: defects in Gli2 and Gli3 mutants.* Development, 1998. **125**(15): p. 2803-11.
151. Marigo, V. and C.J. Tabin, *Regulation of patched by sonic hedgehog in the developing neural tube.* Proc Natl Acad Sci U S A, 1996. **93**(18): p. 9346-51.
152. Riddle, R.D., et al., *Sonic hedgehog mediates the polarizing activity of the ZPA.* Cell, 1993. **75**(7): p. 1401-16.
153. St-Jacques, B., et al., *Sonic hedgehog signaling is essential for hair development.* Curr Biol, 1998. **8**(19): p. 1058-68.
154. Beachy, P.A., S.S. Karhadkar, and D.M. Berman, *Tissue repair and stem cell renewal in carcinogenesis.* Nature, 2004. **432**(7015): p. 324-31.
155. Omenetti, A., et al., *Hedgehog-mediated mesenchymal-epithelial interactions modulate hepatic response to bile duct ligation.* Lab Invest, 2007. **87**(5): p. 499-514.
156. Sicklick, J.K., et al., *Role for hedgehog signaling in hepatic stellate cell activation and viability.* Lab Invest, 2005. **85**(11): p. 1368-80.
157. Sicklick, J.K., et al., *Hedgehog signaling maintains resident hepatic progenitors throughout life.* Am J Physiol Gastrointest Liver Physiol, 2006. **290**(5): p. G859-70.
158. Litingtung, Y., et al., *Sonic hedgehog is essential to foregut development.* Nat Genet, 1998. **20**(1): p. 5861.
159. Bitgood, M.J., L. Shen, and A.P. McMahon, *Sertoli cell signaling by Desert hedgehog regulates the male germline.* Curr Biol, 1996. **6**(3): p. 298-304.
160. St-Jacques, B., M. Hammerschmidt, and A.P. McMahon, *Indian hedgehog signaling regulates proliferation and differentiation of chondrocytes and is essential for bone formation.* Genes Dev, 1999. **13**(16): p. 2072-86.
161. Vortkamp, A., et al., *Regulation of rate of cartilage differentiation by Indian hedgehog and PTHrelated protein.* Science, 1996. **273**(5275): p. 613-22.
162. Lee, J.J., et al., *Autoproteolysis in hedgehog protein biogenesis.* Science, 1994. **266**(5190): p. 1528-37.
163. Marigo, V., et al., *Biochemical evidence that patched is the Hedgehog receptor.* Nature, 1996. **384**(6605): p. 176-9.
164. Stone, D.M., et al., *The tumour-suppressor gene patched encodes a candidate receptor for Sonic hedgehog.* Nature, 1996. **384**(6605): p. 129-34.
165. Nakano, Y., et al., *A protein with several possible membrane-spanning domains encoded by the Drosophila segment polarity gene patched.* Nature, 1989. **341**(6242): p. 508-13.
166. Alcedo, J. and M. Noll, *Hedgehog and its patched-smoothened receptor complex: a novel signalling mechanism at the cell surface.* Biol Chem, 1997. **378**(7): p. 583-90.
167. Chen, Y. and G. Struhl, *In vivo evidence that Patched and Smoothened constitute distinct binding and transducing components of a Hedgehog receptor complex.* Development, 1998. **125**(24): p. 4943-8.
168. Corcoran, R.B. and M.P. Scott, *Oxysterols stimulate Sonic hedgehog signal transduction and proliferation of medulloblastoma cells.* Proc Natl Acad Sci U S A, 2006. **103**(22): p. 8408-13.
169. Dwyer, J.R., et al., *Oxysterols are novel activators of the hedgehog signaling pathway in pluripotent mesenchymal cells.* J Biol Chem, 2007. **282**(12): p. 8959-68.

170. Kenney, A.M., M.D. Cole, and D.H. Rowitch, *Nmyc upregulation by sonic hedgehog signaling promotes proliferation in developing cerebellar granule neuron precursors.* Development, 2003. **130**(1): p. 15-28.
171. Hahn, H., et al., *Patched target Igf2 is indispensable for the formation of medulloblastoma and rhabdomyosarcoma.* J Biol Chem, 2000. **275**(37): p. 28341-4.
172. Kenney, A.M. and D.H. Rowitch, *Sonic hedgehog promotes G(1) cyclin expression and sustained cell cycle progression in mammalian neuronal precursors.* Mol Cell Biol, 2000. **20**(23): p. 9055-67.
173. Katoh, Y. and M. Katoh, *Hedgehog target genes: mechanisms of carcinogenesis induced by aberrant hedgehog signaling activation.* Curr Mol Med, 2009. **9**(7): p. 873-86.
174. Hirose, Y., T. Itoh, and A. Miyajima, *Hedgehog signal activation coordinates proliferation and differentiation of fetal liver progenitor cells.* Exp Cell Res, 2009. **315**(15): p. 2648-57.
175. Huang, S., et al., *Activation of the hedgehog pathway in human hepatocellular carcinomas.* Carcinogenesis, 2006. **27**(7): p. 1334-40.
176. Sicklick, J.K., et al., *Dysregulation of the Hedgehog pathway in human hepatocarcinogenesis.* Carcinogenesis, 2006. **27**(4): p. 748-57.
177. Jung, Y., et al., *Bile ductules and stromal cells express hedgehog ligands and/or hedgehog target genes in primary biliary cirrhosis.* Hepatology, 2007. **45**(5): p. 1091-6.
178. Oue, T., et al., *Increased expression of the hedgehog signaling pathway in pediatric solid malignancies.* J Pediatr Surg, 2010. **45**(2): p. 387-92.
179. Foulstone, E., et al., *Insulin-like growth factor ligands, receptors, and binding proteins in cancer.* J Pathol, 2005. **205**(2): p. 145-53.
180. Grimberg, A. and P. Cohen, *Role of insulin-like growth factors and their binding proteins in growth control and carcinogenesis.* J Cell Physiol, 2000. **183**(1): p. 1-9.
181. Hartmann, W., et al., *p57(KIP2) is not mutated in hepatoblastoma but shows increased transcriptional activity in a comparative analysis of the three imprinted genes p57(KIP2), IGF2, and H19.* Am J Pathol, 2000. **157**(4): p. 1393-403.
182. Li, X., et al., *Expression, promoter usage and parental imprinting status of insulin-like growth factor II (IGF2) in human hepatoblastoma: uncoupling of IGF2 and H19 imprinting.* Oncogene, 1995. **11**(2): p. 221-9.
183. Honda, S., et al., *Loss of imprinting of IGF2 correlates with hypermethylation of the H19 differentially methylated region in hepatoblastoma.* Br J Cancer, 2008. **99**(11): p. 1891-9.
184. Hanafusa, T., et al., *Functional promoter upstream p53 regulatory sequence of IGFBP3 that is silenced by tumor specific methylation.* BMC Cancer, 2005. **5**: p. 9.
185. Turashvili, G., et al., *Wnt signaling pathway in mammary gland development and carcinogenesis.* Pathobiology, 2006. **73**(5): p. 213-23.
186. Huelsken, J. and J. Behrens, *The Wnt signalling pathway.* J Cell Sci, 2002. **115**(Pt 21): p. 3977-8.
187. Kawano, Y. and R. Kypta, *Secreted antagonists of the Wnt signalling pathway.* J Cell Sci, 2003. **116**(Pt 13): p. 2627-34.
188. Ai, L., et al., *Inactivation of Wnt inhibitory factor-1 (WIF1) expression by epigenetic silencing is a common event in breast cancer.* Carcinogenesis, 2006. **27**(7): p. 1341-8.
189. Sogabe, Y., et al., *Epigenetic inactivation of SFRP genes in oral squamous cell carcinoma.* Int J Oncol, 2008. **32**(6): p. 1253-61.
190. Aguilera, O., et al., *Epigenetic inactivation of the Wnt antagonist DICKKOPF-1 (DKK-1) gene in human colorectal cancer.* Oncogene, 2006. **25**(29): p. 4116-21.
191. Pietsch, T., et al., *Characterization of the continuous cell line HepT1 derived from a human hepatoblastoma.* Lab Invest, 1996. **74**(4): p. 809-18.
192. Lopez-Terrada, D., et al., *Hep G2 is a hepatoblastoma-derived cell line.* Hum Pathol, 2009. **40**(10): p. 1512-5.
193. Shibata, T., et al., *Cancer related mutations in NRF2 impair its recognition by Keap1-Cul3 E3 ligase and promote malignancy.* Proc Natl Acad Sci U S A, 2008. **105**(36): p. 13568-73.
194. Pfaffl, M.W., *A new mathematical model for relative quantification in real-time RT-PCR.* Nucleic Acids Res, 2001. **29**(9): p. e45.
195. Garber, J.E., et al., *Hepatoblastoma and familial adenomatous polyposis.* J Natl Cancer Inst, 1988. **80**(20): p. 1626-8.
196. Taguchi, K., H. Motohashi, and M. Yamamoto, *Molecular mechanisms of the Keap1-Nrf2 pathway in stress response and cancer evolution.* Genes Cells, 2011. **16**(2): p. 123-40.
197. Guichard, C., et al., *Integrated analysis of somatic mutations and focal copy-number changes identifies key genes and pathways in hepatocellular carcinoma.* Nat Genet, 2012. **44**(6): p. 694-8.

198. Cleary, S.P., et al., *Identification of driver genes in hepatocellular carcinoma by exome sequencing.* Hepatology, 2013. **58**(5): p. 1693-702.
199. Shibata, T., et al., *Genetic alteration of Keap1 confers constitutive Nrf2 activation and resistance to chemotherapy in gallbladder cancer.* Gastroenterology, 2008. **135**(4): p. 1358-1368, 1368 e1-4.
200. Dinkova-Kostova, A.T. and P. Talalay, *NAD(P)H:quinone acceptor oxidoreductase 1 (NQO1), a multifunctional antioxidant enzyme and exceptionally versatile cytoprotector.* Arch Biochem Biophys, 2010. **501**(1): p. 116-23.
201. Ooi, A., et al., *CUL3 and NRF2 mutations confer an NRF2 activation phenotype in a sporadic form of papillary renal cell carcinoma.* Cancer Res, 2013. **73**(7): p. 2044-51.
202. Baylin, S.B. and J.E. Ohm, *Epigenetic gene silencing in cancer - a mechanism for early oncogenic pathway addiction?* Nat Rev Cancer, 2006. **6**(2): p. 107-16.
203. Tost, J. and I.G. Gut, *Analysis of gene-specific DNA methylation patterns by pyrosequencing technology.* Methods Mol Biol, 2007. **373**: p. 89-102.
204. Yang, A.S., et al., *A simple method for estimating global DNA methylation using bisulfite PCR of repetitive DNA elements.* Nucleic Acids Res, 2004. **32**(3): p. e38.
205. Obata, Y., et al., *The epigenetic regulator Uhrf1 facilitates the proliferation and maturation of colonic regulatory T cells.* Nat Immunol, 2014. **15**(6): p. 571-9.
206. Huether, R., et al., *The landscape of somatic mutations in epigenetic regulators across 1,000 paediatric cancer genomes.* Nat Commun, 2014. **5**: p. 3630.
207. van Haaften, G., et al., *Somatic mutations of the histone H3K27 demethylase gene UTX in human cancer.* Nat Genet, 2009. **41**(5): p. 521-3.
208. Dalgliesh, G.L., et al., *Systematic sequencing of renal carcinoma reveals inactivation of histone modifying genes.* Nature, 2010. **463**(7279): p. 360-3.
209. Morin, R.D., et al., *Somatic mutations altering EZH2 (Tyr641) in follicular and diffuse large B-cell lymphomas of germinal-center origin.* Nat Genet, 2010. **42**(2): p. 181-5.
210. Jones, S., et al., *Frequent mutations of chromatin remodeling gene ARID1A in ovarian clear cell carcinoma.* Science, 2010. **330**(6001): p. 228-31.
211. Wiegand, K.C., et al., *ARID1A mutations in endometriosis-associated ovarian carcinomas.* N Engl J Med, 2010. **363**(16): p. 1532-43.
212. Stratton, M.R., P.J. Campbell, and P.A. Futreal, *The cancer genome.* Nature, 2009. **458**(7239): p. 71924.
213. Vogelstein, B., et al., *Cancer genome landscapes.* Science, 2013. **339**(6127): p. 1546-58.
214. Sjoblom, T., et al., *The consensus coding sequences of human breast and colorectal cancers.* Science, 2006. **314**(5797): p. 268-74.
215. Kovac, M., et al., *Recurrent chromosomal gains and heterogeneous driver mutations characterise papillary renal cancer evolution.* Nat Commun, 2015. **6**: p. 6336.
216. Yoo, N.J., et al., *Somatic mutations of the KEAP1 gene in common solid cancers.* Histopathology, 2012. **60**(6): p. 943-52.
217. Kansanen, E., H.K. Jyrkkanen, and A.L. Levonen, *Activation of stress signaling pathways by electrophilic oxidized and nitrated lipids.* Free Radic Biol Med, 2012. **52**(6): p. 973-82.
218. Kim, Y.R., et al., *Oncogenic NRF2 mutations in squamous cell carcinomas of oesophagus and skin.* J Pathol, 2010. **220**(4): p. 446-51.
219. Shibata, T., et al., *NRF2 mutation confers malignant potential and resistance to chemoradiation therapy in advanced esophageal squamous cancer.* Neoplasia, 2011. **13**(9): p. 864-73.
220. Wang, R., et al., *Hypermethylation of the Keap1 gene in human lung cancer cell lines and lung cancer tissues.* Biochem Biophys Res Commun, 2008. **373**(1): p. 151-4.
221. Muscarella, L.A., et al., *Frequent epigenetics inactivation of KEAP1 gene in non-small cell lung cancer.* Epigenetics, 2011. **6**(6): p. 710-9.
222. Zhang, P., et al., *Loss of Kelch-like ECH-associated protein 1 function in prostate cancer cells causes chemoresistance and radioresistance and promotes tumor growth.* Mol Cancer Ther, 2010. **9**(2): p. 33646.
223. Hanada, N., et al., *Methylation of the KEAP1 gene promoter region in human colorectal cancer.* BMC Cancer, 2012. **12**: p. 66.
224. Lister, A., et al., *Nrf2 is overexpressed in pancreatic cancer: implications for cell proliferation and therapy.* Mol Cancer, 2011. **10**: p. 37.
225. Zhu, J., et al., *Targeting the NF-E2-related factor 2 pathway: a novel strategy for glioblastoma (review).* Oncol Rep, 2014. **32**(2): p. 443-50.

226. Mitsuishi, Y., et al., *Nrf2 redirects glucose and glutamine into anabolic pathways in metabolic reprogramming.* Cancer Cell, 2012. **22**(1): p. 66-79.
227. Singh, A., et al., *RNAi-mediated silencing of nuclear factor erythroid-2-related factor 2 gene expression in non-small cell lung cancer inhibits tumor growth and increases efficacy of chemotherapy.* Cancer Res, 2008. **68**(19): p. 7975-84.
228. Ji, X.J., et al., *Knockdown of NF-E2-related factor 2 inhibits the proliferation and growth of U251MG human glioma cells in a mouse xenograft model.* Oncol Rep, 2013. **30**(1): p. 157-64.
229. Reddy, N.M., et al., *Deficiency in Nrf2-GSH signaling impairs type II cell growth and enhances sensitivity to oxidants.* Am J Respir Cell Mol Biol, 2007. **37**(1): p. 3-8.
230. Taguchi, K., et al., *Genetic analysis of cytoprotective functions supported by graded expression of Keap1.* Mol Cell Biol, 2010. **30**(12): p. 3016-26.
231. Cui, X., et al., *NAD(P)H:quinone oxidoreductase-1 overexpression predicts poor prognosis in small cell lung cancer.* Oncol Rep, 2014. **32**(6): p. 2589-95.
232. Lin, L., et al., *Significance of NQO1 overexpression for prognostic evaluation of gastric adenocarcinoma.* Exp Mol Pathol, 2014. **96**(2): p. 200-5.
233. Ma, Y., et al., *NQO1 overexpression is associated with poor prognosis in squamous cell carcinoma of the uterine cervix.* BMC Cancer, 2014. **14**: p. 414.
234. Ren, D., et al., *Brusatol enhances the efficacy of chemotherapy by inhibiting the Nrf2-mediated defense mechanism.* Proc Natl Acad Sci U S A, 2011. **108**(4): p. 1433-8.
235. Feinberg, A.P., R. Ohlsson, and S. Henikoff, *The epigenetic progenitor origin of human cancer.* Nat Rev Genet, 2006. **7**(1): p. 21-33.
236. Jones, P.A. and S.B. Baylin, *The epigenomics of cancer.* Cell, 2007. **128**(4): p. 683-92.
237. Esteller, M., *CpG island hypermethylation and tumor suppressor genes: a booming present, a brighter future.* Oncogene, 2002. **21**(35): p. 5427-40.
238. Esteller, M., *Epigenetics provides a new generation of oncogenes and tumour-suppressor genes.* Br J Cancer, 2007. **96 Suppl**: p. R26-30.
239. Nojima, M., et al., *Frequent epigenetic inactivation of SFRP genes and constitutive activation of Wnt signaling in gastric cancer.* Oncogene, 2007. **26**(32): p. 4699-713.
240. Suzuki, H., et al., *Frequent epigenetic inactivation of Wnt antagonist genes in breast cancer.* Br J Cancer, 2008. **98**(6): p. 1147-56.
241. Suzuki, H., et al., *A genomic screen for genes upregulated by demethylation and histone deacetylase inhibition in human colorectal cancer.* Nat Genet, 2002. **31**(2): p. 141-9.
242. Takagi, H., et al., *Frequent epigenetic inactivation of SFRP genes in hepatocellular carcinoma.* J Gastroenterol, 2008. **43**(5): p. 378-89.
243. Dees, C., et al., *The Wnt antagonists DKK1 and SFRP1 are downregulated by promoter hypermethylation in systemic sclerosis.* Ann Rheum Dis, 2014. **73**(6): p. 1232-9.
244. Hanafusa, T., et al., *Reduced expression of insulin-like growth factor binding protein-3 and its promoter hypermethylation in human hepatocellular carcinoma.* Cancer Lett, 2002. **176**(2): p. 149-58.
245. Ibanez de Caceres, I., et al., *IGFBP-3 hypermethylation-derived deficiency mediates cisplatin resistance in non-small-cell lung cancer.* Oncogene, 2010. **29**(11): p. 1681-90.
246. Tomii, K., et al., *Aberrant promoter methylation of insulin-like growth factor binding protein-3 gene in human cancers.* Int J Cancer, 2007. **120**(3): p. 566-73.
247. Shahi, M.H., et al., *Human hedgehog interacting protein expression and promoter methylation in medulloblastoma cell lines and primary tumor samples.* J Neurooncol, 2011. **103**(2): p. 287-96.
248. Taniguchi, H., et al., *Transcriptional silencing of hedgehog-interacting protein by CpG hypermethylation and chromatic structure in human gastrointestinal cancer.* J Pathol, 2007. **213**(2): p. 131-9.
249. Tada, M., et al., *Down-regulation of hedgehog-interacting protein through genetic and epigenetic alterations in human hepatocellular carcinoma.* Clin Cancer Res, 2008. **14**(12): p. 3768-76.
250. Martin, S.T., et al., *Aberrant methylation of the Human Hedgehog interacting protein (HHIP) gene in pancreatic neoplasms.* Cancer Biol Ther, 2005. **4**(7): p. 728-33.
251. Suzuki, H., et al., *Epigenetic inactivation of SFRP genes allows constitutive WNT signaling in colorectal cancer.* Nat Genet, 2004. **36**(4): p. 417-22.
252. Fujimori, A., et al., *Cloning and mapping of Np95 gene which encodes a novel nuclear protein associated with cell proliferation.* Mamm Genome, 1998. **9**(12): p. 1032-5.
253. Antelo, M., et al., *A high degree of LINE-1 hypomethylation is a unique feature of early-onset colorectal cancer.* PLoS One, 2012. **7**(9): p. e45357.

254. Pavicic, W., et al., *LINE-1 hypomethylation in familial and sporadic cancer.* J Mol Med (Berl), 2012. **90**(7): p. 827-35.
255. Takai, D., et al., *Hypomethylation of LINE1 retrotransposon in human hepatocellular carcinomas, but not in surrounding liver cirrhosis.* Jpn J Clin Oncol, 2000. **30**(7): p. 306-9.
256. Cordaux, R. and M.A. Batzer, *The impact of retrotransposons on human genome evolution.* Nat Rev Genet, 2009. **10**(10): p. 691-703.
257. Gaudet, F., et al., *Induction of tumors in mice by genomic hypomethylation.* Science, 2003. **300**(5618): p. 489-92.
258. Ogino, S., et al., *LINE-1 hypomethylation is inversely associated with microsatellite instability and CpG island methylator phenotype in colorectal cancer.* Int J Cancer, 2008. **122**(12): p. 2767-73.
259. Yamada, Y., et al., *Opposing effects of DNA hypomethylation on intestinal and liver carcinogenesis.* Proc Natl Acad Sci U S A, 2005. **102**(38): p. 13580-5.
260. Jurgens, B., B.J. Schmitz-Drager, and W.A. Schulz, *Hypomethylation of L1 LINE sequences prevailing in human urothelial carcinoma.* Cancer Res, 1996. **56**(24): p. 5698-703.
261. Dante, R., et al., *Methylation patterns of long interspersed repeated DNA and alphoid repetitive DNA from human cell lines and tumors.* Anticancer Res, 1992. **12**(2): p. 559-63.
262. Santourlidis, S., et al., *High frequency of alterations in DNA methylation in adenocarcinoma of the prostate.* Prostate, 1999. **39**(3): p. 166-74.
263. Hervouet, E., F.M. Vallette, and P.F. Cartron, *Dnmt1/Transcription factor interactions: an alternative mechanism of DNA methylation inheritance.* Genes Cancer, 2010. **1**(5): p. 434-43.
264. Sabatino, L., et al., *UHRF1 coordinates peroxisome proliferator activated receptor gamma (PPARG) epigenetic silencing and mediates colorectal cancer progression.* Oncogene, 2012. **31**(49): p. 5061-72.
265. Momparler, R.L., *Pharmacology of 5-Aza-2'-deoxycytidine (decitabine).* Semin Hematol, 2005. **42**(3 Suppl 2): p. S9-16.
266. Yang, A.S., et al., *DNA methylation changes after 5-aza-2'-deoxycytidine therapy in patients with leukemia.* Cancer Res, 2006. **66**(10): p. 5495-503.
267. Kondo, Y., L. Shen, and J.P. Issa, *Critical role of histone methylation in tumor suppressor gene silencing in colorectal cancer.* Mol Cell Biol, 2003. **23**(1): p. 206-15.
268. Coombes, M.M., et al., *Resetting the histone code at CDKN2A in HNSCC by inhibition of DNA methylation.* Oncogene, 2003. **22**(55): p. 8902-11.
269. Takebayashi, S., et al., *5-Aza-2'-deoxycytidine induces histone hyperacetylation of mouse centromeric heterochromatin by a mechanism independent of DNA demethylation.* Biochem Biophys Res Commun, 2001. **288**(4): p. 921-6.
270. Qin, Y., et al., *UHRF1 depletion suppresses growth of gallbladder cancer cells through induction of apoptosis and cell cycle arrest.* Oncol Rep, 2014. **31**(6): p. 2635-43.
271. Mistry, H., et al., *UHRF1 is a genome caretaker that facilitates the DNA damage response to gammairradiation.* Genome Integr, 2010. **1**(1): p. 7.
272. Nady, N., et al., *Recognition of multivalent histone states associated with heterochromatin by UHRF1 protein.* J Biol Chem, 2011. **286**(27): p. 24300-11.
273. Babbio, F., et al., *The SRA protein UHRF1 promotes epigenetic crosstalks and is involved in prostate cancer progression.* Oncogene, 2012. **31**(46): p. 4878-87.
274. Kim, J.K., et al., *UHRF1 binds G9a and participates in p21 transcriptional regulation in mammalian cells.* Nucleic Acids Res, 2009. **37**(2): p. 493-505.
275. Trojer, P., et al., *Dynamic Histone H1 Isotype 4 Methylation and Demethylation by Histone Lysine Methyltransferase G9a/KMT1C and the Jumonji Domain-containing JMJD2/KDM4 Proteins.* J Biol Chem, 2009. **284**(13): p. 8395-405.
276. Weiss, T., et al., *Histone H1 variant-specific lysine methylation by G9a/KMT1C and Glp1/KMT1D.* Epigenetics Chromatin, 2010. **3**(1): p. 7.
277. Wu, H., et al., *Histone methyltransferase G9a contributes to H3K27 methylation in vivo.* Cell Res, 2011. **21**(2): p. 365-7.
278. O'Meara, M.M. and J.A. Simon, *Inner workings and regulatory inputs that control Polycomb repressive complex 2.* Chromosoma, 2012. **121**(3): p. 221-34.
279. Vire, E., et al., *The Polycomb group protein EZH2 directly controls DNA methylation.* Nature, 2006. **439**(7078): p. 871-4.
280. Jin, B., et al., *DNMT1 and DNMT3B modulate distinct polycomb-mediated histone modifications in colon cancer.* Cancer Res, 2009. **69**(18): p. 7412-21.
281. Brinkman, A.B., et al., *Sequential ChIP-bisulfite sequencing enables direct genome-scale investigation of chromatin and DNA methylation cross-talk.* Genome Res, 2012. **22**(6): p. 1128-38.

282. Shen, X., et al., *EZH1 mediates methylation on histone H3 lysine 27 and complements EZH2 in maintaining stem cell identity and executing pluripotency.* Mol Cell, 2008. **32**(4): p. 491-502.
283. Wu, X., et al., *Cooperation between EZH2, NSPc1-mediated histone H2A ubiquitination and Dnmt1 in HOX gene silencing.* Nucleic Acids Res, 2008. **36**(11): p. 3590-9.
284. Geng, Y., et al., *Diagnostic and prognostic value of plasma and tissue ubiquitin-like, containing PHD and RING finger domains 1 in breast cancer patients.* Cancer Sci, 2013. **104**(2): p. 194-9.
285. Jiang, T., et al., *High levels of Nrf2 determine chemoresistance in type II endometrial cancer.* Cancer Res, 2010. **70**(13): p. 5486-96.

# List of Figures and Tables

## Figures



## Tables

# Publications and Conferences

During my work as a PhD student I was able to contribute to the following publications/conferences.

**Publications**

1. Hubertus J, Zitzmann F, Trippel F, Müller-Höcker J, Stehr M, von Schweinitz D, Kappler R. **Selective methylation of CpGs at regulatory binding sites controls NNAT expression in Wilms tumors**. **PLoS One.** 2013 Jun 25;8(6):e67605. doi: 10.1371/journal.pone.0067605. Print 2013

2. Eichenmüller M*, Trippel F*, Kreuder M, Beck A, Schwarzmayr T, Häberle B, Cairo S, Leuschner I, von Schweinitz D, Strom TM, Kappler R. **The genomic landscape of hepatoblastoma and their progenies with HCC-like features.** J Hepatol. 2014 Aug 15. pii: S0168-8278(14)00548-0. doi: 10.1016/j.jhep.2014.08.009. *These authors contributed equally to this work.

3. Rettig I, Koeneke E, Trippel F, Mueller WC, Burhenne J, Kopp-Schneider A, Fabian J, Schober A, Fernekorn U, von Deimling A, Deubzer HE, Milde T, Witt O, Oehme I. **Selective inhibition of HDAC8 decreases neuroblastoma growth in vitro and in vivo and enhances retinoic acid-mediated differentiation.** Cell Death Dis. 2015 Feb 19;6:e1657. doi: 10.1038/cddis.2015.24

4. Gödeke J, Luxenburger E, Trippel F, Becker K, Häberle B, Müller-Höcker J, von Schweinitz D, Kappler R. **Low expression of N-myc downstream-regulated gene 2 (NDRG2) correlates with poor prognosis in hepatoblastoma.** Hepatol Int. 2015 Dec 8. [Epub ahead of print**]**

5. Trippel, F; Joppien, S; Schweinitz, D von; Längst, G; Kappler, R.
**UHRF1 regulates methylation of tumor suppressor genes relevant in hepatoblastoma** (in preparation

**Posters and talks at conferences**

**1.** Kauffmann, D; Trippel, F; Schweinitz, D von; Längst, G; Kappler, R: The role of the DNMT recruiting protein LSH in hepatoblastoma, Jahrestagung der Kind-Philipp-Stiftung für Leukämieforschung, Wilsede, 2012

**2.** Trippel, F; Joppien, S; Schweinitz, D von; Längst, G; Kappler, R: The role of the DNMT1/ UHRF1/USP7 complex in hepatoblastoma, Jahrestagung der Kind-Philipp-Stiftung für Leukämieforschung, Wilsede, 2012

**3.** Eichenmüller M, Trippel F, Leuschner I, von Schweinitz D, Strom TM, Kappler R: Deciphering the genetic origin of childhood liver cancer, Jahrestagung der Kind-Philipp-Stiftung für Leukämieforschung, Wilsede, 2012

**4.** Trippel, F; Joppien, S; Schweinitz, D von; Längst, G; Kappler, R: The role of the DNMT1/ UHRF1/USP7 complex in hepatoblastoma. *Proc. Amer. Assoc. Cancer Res. (AACR Annual Meeting 2012)*

**5.** Eichenmüller M, Trippel F, Kreuder M, Beck A, Leuschner I, von Schweinitz D, Strom TM, Kappler R: The genomic landscape of hepatoblastoma and their progenies with HCC-like features. *Proc. Amer. Assoc. Cancer Res. (AACR Annual Meeting 2014).*

# Acknowledgements

I would like to take the opportunity to express my gratitude to the people who supported me during the last 3 years. Firstly, I want to thank Prof. Dr. Dietrich von Schweinitz for allowing me to conduct my PhD thesis in the department of pediatric surgery in the Dr. von Hauner Children's Hospital. I am also very grateful for the expertise of my supervisor Prof. Dr. Roland Kappler who significantly contributed to my understanding of the topic, new ideas for the project and was patient enough to answer any of my questions profoundly. Special thanks go to Fatemeh Promoli for explaining the lab routines over and over again and helping me out with my experiments. Big thanks to my lab neighbors Diego Kaufmann, Laura Preis, Melanie Eichenmüller, Michaela Kreuder, Lena Münster Alexander Beck, Corinna Weber and Agnes Ganier for nice talks now and then; thank you for interrupting your work instantly whenever I asked for your help. I furthermore want to thank, Lena Brandlhuber, Friederike Rossmann, Ralf Zarbock, and Thomas Wittman for trouble-shooting and encouraging talks. Thanks to all the Kubus people for advices and laboratory equipment. A sincere 'thank you' to my whole family who has always had faith in everything I do. Finally, I would like to thank Philipp for the great support during the last three years, spending weekends in the lab, enduring my moods and giving pep-talks in between.